Performance of Pilot Scale Plug Flow Microbial Fuel Cell for Sustainable Wastewater Treatment and Energy Recovery

Ourania Dimou

Submitted for the degree of Doctor of Philosophy

Heriot-Watt University

Institute of Mechanical, Process and Energy Engineering

School of Engineering and Physical Sciences

March 2017

Abstract

Wastewater is increasingly considered a resource rather than a problem. This study investigates the rapidly developing Microbial Fuel Cell technology and its potential to be used in an industrial scale and environment in the context of the whisky industry and to be used as an alternative or complementary sustainable wastewater treatment process.

This study describes the development of a 122 litre multi-electrode open air cathode Microbial Fuel Cell. Throughout this study the reactor's performance is assessed on two levels; energy recovery and effluent quality.

During initial studies the principle of the MFC's ability to treat whisky distillation by-products was established. The reactor was operated directly on diluted spent wash in ambient Scottish temperatures. During successful start-up, no correlation was found to temperature. During long-term operation, a positive correlation was found between temperature and the positive energy balance achieved by the MFC while tCOD removal efficiency was maintained at approximately 83 %. The reactor was further optimised in regards to electrical connections, thus its electrical performance which was also validated through a bench scale study.

The successful initial experiments led to the integration of an operationally optimised pilot study in a local whisky distillery. The pilot set-up was successfully operated complementary to an anaerobic digester for over one year in the industrial environment achieving energy savings and a sustainable tCOD removal efficiency of over 80 %. Latterly, a simplified electrochemical model was examined to describe the performance of the MFC to be further developed.

This study concludes that the nature of industrial wastewater treatment is a complex subject and equally so is the multi-disciplinary MFC technology. The MFC developed for this study and the industrial experience gained contributes towards a more sustainable, energy saving and efficient treatment technology with the potential to be used complementary to existing technologies.

Acknowledgments

I have to admit that during the last 4 years that I have been working on my PhD one of the thoughts that kept me going was this very final moment. The moment I am writing the Acknowledgments section of my thesis. I have dreamed about this moment, yet the reality of it is even more overwhelming than expected. I wouldn't have made it to this day if it weren't for the help, guidance and sometimes unconditional support of others. There are so many people that I now have the opportunity and joy to thank.

First of all, the greatest acknowledgment should go to my supervisor Alan Harper for his help, guidance and advice. He was the one person that believed in me already during my masters' studies and I am very well aware that with his support, both academic and moral, and scientific insight I was able to make it to this point. I would also like to extend my acknowledgments to my other supervisors, Dr. John Andresen of Heriot-Watt University and Professor Igor Goryanin of University of Edinburgh, for their support and help during the last four years.

This PhD project was a collaboration between Heriot-Watt University, myself and an industrial partner. I would therefore like to express my gratitude to the Energy Technology Partnership (ETP) and MPower World Ltd for their financial, scientific and moral support. Especially, I would like to thank David J. Simpson and Vyacheslav (Slava) Fedorovich for the exchange of invaluable scientific knowledge and their help in moving everything from theory to practise. I would also like to extend a great thank you to the North British Distillery Ltd. in Edinburgh for providing raw material for my study and latterly, providing a home for my MFC and helping me take my research to the next level. Special thanks to Alistair Murphy and Brynjar Olafsson for their support to my project, and Steven Anderson for always providing a helping hand.

However, my first experiment back in my masters' days would have never happened and I would still be trying to figure out how a pipette works if it weren't for Eileen McEvoy, the heart and soul of the Heriot-Watt bio-laboratories. Eileen, I would like to thank you for your support and most importantly for your friendship and moral guidance during some of the most challenging times of my life, both personally and professionally. I would also like to thank all the technicians in the Mechanical Engineering laboratories of Heriot-Watt University for their help but, I would specifically like to thank Richard Kinsella for sharing so many rides back and forth to the North British Distillery with me and most importantly for his friendship and advice.

Dr. Amanda Hughes, Dr. Dalila Capão and Gregor Sneddon deserve a great thank you for introducing me to one of the greatest achievements of civilisation, the Krispy Kreme®. I would also like to thank Dr. Alan Faulkner-Jones, Dr. Marius Dewar and Chris Balmer (aka Justin) for their friendship and sharing an office and arguably some frustration during these 4 years. I would also like to thank Mirte for helping me in a very critical point in my life.

I would like to take this moment to thank my best and closest friends from the bottom of my heart for sticking with me through it all, and to officially apologise for the (slightly) horrible person that I (might) have been from time to time. Argiro, the woman of my life, Iliana, Todor (yes, this is how you will go down in history), Eli, Meriç, Kostas, Rosario, Alex, Isadora and Victoria. Thank you, so much, so greatly much for sharing your lives with me.

Last but not least, I would like to thank my family. My father Tolios, the most popular guy (I am sure he knows what I mean), my sister Nikolina whom I love so greatly much and finally my mother Tasoula (Dr. Anastasia Kambamanoli). I do not have the faintest idea how I would have ever made it without you. You are my rock and I hope you know how deeply grateful I am for your support.

Ourania Dimou

October 2016

"And once the storm is over you won't remember how you made it through, how you managed to survive. You won't even be sure, in fact, whether the storm is really over. But one thing is certain. When you come out of the storm you won't be the same person who walked in. That's what this storm's all about."

- Haruki Murakami, *Kafka on the shore, 2005*

ACADEMIC REGISTRY
Research Thesis Submission

Name*:*			
School:			
Version: *(i.e. First, Resubmission, Final)*		Degree Sought:	

Declaration

In accordance with the appropriate regulations I hereby submit my thesis and I declare that:

1) the thesis embodies the results of my own work and has been composed by myself
2) where appropriate, I have made acknowledgement of the work of others and have made reference to work carried out in collaboration with other persons
3) the thesis is the correct version of the thesis for submission and is the same version as any electronic versions submitted*.
4) my thesis for the award referred to, deposited in the Heriot-Watt University Library, should be made available for loan or photocopying and be available via the Institutional Repository, subject to such conditions as the Librarian may require
5) I understand that as a student of the University I am required to abide by the Regulations of the University and to conform to its discipline.
6) I confirm that the thesis has been verified against plagiarism via an approved plagiarism detection application e.g. Turnitin.

* *Please note that it is the responsibility of the candidate to ensure that the correct version of the thesis is submitted.*

Signature of Candidate*:*		Date:	

Submission

Submitted By *(name in capitals):*	
Signature of Individual Submitting:	
Date Submitted:	

For Completion in the Student Service Centre (SSC)

Received in the SSC by *(name in capitals):*			
1.1 Method of Submission *(Handed in to SSC; posted through internal/external mail):*			
1.2 E-thesis Submitted (**mandatory for final theses)**			
Signature:		Date:	

Nomenclature

AD	Anaerobic Digestion
ADLD	Anaerobic Digestion Liquid Digestate
AEM	Anion Exchange Membrane
BOD	Biochemical Oxygen Demand
CCV	Closed Circuit Voltage
CE	Coulombic Efficiency
CEM	Cation Exchange Membrane
COD	Chemical Oxygen Demand
EU	European Union
HRT	Hydraulic Retention Time
IEM	Ion Exchange Membrane
MEC	Microbial Electrolysis Cell
MET	Microbial Electrolysis Technologies
MFC	Microbial Fuel Cell
NER	Normalised Energy Recovery
NR	Neutral Red
OCV	Open Circuit Voltage
OLR	Organic Loading Rate
PFSA	Perfluorosulfonic Acid
PVC	Polyvinyl Chloride
tCOD	Total Chemical Oxygen Demand
tSS	Total Suspended Solids
TVS	Total Volatile Solids
UNEP	United Nations Environment Programme
UN	United Nations
VFA	Volatile Fatty Acid

Acknowledgment of contributions

Alan Harper provided guidance with experimental work and revision to all manuscripts.

Dr. John Andresen provided guidance with experimental tools and methods and interpretation of experimental results.

David J. Simpson provided assistance in MFC construction and guidance on theoretical background of MFC technology.

Ioannis Katsifarakis provided the 3-dimentional designs of the 122L prototype MFC presented in Chapter 3.2.

Tatyana Peshkur of Scottish Environmental Technology Network (SETN) of University of Strathclyde (later Strathclyde Eco Innovation Unit-SEIU) for assistance on wastewater quality methods and analysis performed in Chapter 5.3.8.

Table of Contents

List of figures

List of tables

Chapter 1 – Introduction

1.1 Background

The subject of increasing interest recently, a Microbial Fuel Cell can be defined as a bioreactor which has the ability to harness chemical energy and convert it directly into electrical. At its core an MFC is a fuel cell; however, its distinction lies the fact that, as implied by its name, a Microbial Fuel Cell utilises the metabolic reactions of electrochemically active microorganisms to harness the chemical energy contained in organic compounds.

1.1.1 *Timeline*

The ability of microorganisms to directly convert chemical energy into electrical is not a new concept in the scientific world. In 1911, M.C. Potter, a Professor of Botany at Durham University, UK, was the first to report on the occurrence of a difference of potential between electrodes immersed in bacterial or yeast cultures and in a sterile medium in a battery-type setup. Potter concluded that electric energy in the form of electrons can be liberated during the decomposition of organic compounds by microorganisms (Potter, 1911). Almost twenty years later, B. Cohen verified Potter's results by adding to his work, delivering a stacked configuration that achieved a voltage of 35 V at a 0.2 mA current; however, he also discussed the major disadvantage of a very low current which was also rapidly discharged (Cohen, 1930).

It was only during the 1960s that the idea was revisited, this time by the National Aeronautics and Space Administration (NASA) in the USA. The purpose of their investigation was to explore the feasibility of using microbial fuel cells for the recycling of human waste into electricity during the space flights and in space shuttles. The life of the investigation was short, mostly due to the rapid development of competing technologies, which were more efficient and better understood (Canfield, Goldner and Lutwack, 1963). The relative failure of this attempt along with low oil prices, underestimation of the issue of climate change, and the popularity of fossil fuels at the time, led to the abandonment of this field of study.

Microbial fuel cells were revived and brought back into focus mostly due to the work of R.M. Allen and H.P. Bennetto during the 1990s at King's College, London, UK, who developed a quite different, more socially-orientated approach to the topic. These authors

believed in the utilisation of MFC technology as a solution to sanitary issues in areas of the globe then known as the 'third world' (Allen and Bennetto, 1993). It was around that time that MFCs were also examined in the field of robotics, when Wilkinson introduced the 'Gastrobots', a self-sustaining (self-powered) robot (Wilkinson, 2000).

The breakthrough moment in the field should be considered to be the discovery of exoelectrogens, which are microorganisms that do not require the addition of a mediator but can transfer electrons themselves through various mechanisms (Kim et al., 1999). Until that discovery, MFC technology faced some major issues which minimised interest in further research mostly with regard to power output and thus scalability, but most importantly, a lack of applications; MFCs were considered an interesting feature of science and engineering, but a 'realistic' application had not yet been considered for them.

With the turn of the new century, however, the picture has completely shifted. Microbial fuel cells have gained considerably in interest, with possible applications varying from the original concept of electricity generation and the production of speciality chemicals, through to desalination and hydrogen generation. Most importantly in the context of the the present study, in 1991 the idea of utilising wastewater streams as the fuel in MFCs was first mentioned (Habermann and Pommer, 1991). The beginning of the 21st century is a time to take stock, which brings us to the next point: the motivation of the current study. Why are MFCs worth fighting for?

1.1.2 ***Motivation***

At the turn of the 21st century, the world faces a general water scarcity and quality crisis due to the cumulative effects of continuous population growth, urbanization, shifting land use priorities, industrialization, food production intensification, increased living standards, poor water use practices, and equally importantly, poor wastewater management strategies (UN Water, 2015). Over the past decade, a general shift in views on wastewater seems to have occurred, with a growing consensus that wastewater should not be considered an issue; on the contrary, it should be considered a valuable resource (Sutton et al., 2011). It is, therefore, essential that wastewater treatment and management is considered an integrated part of water's full life cycle. Currently, the systems available for wastewater treatment are highly energy intensive, typically taking up to 3 % of the overall electrical energy usage in developed countries, and are still considered by industry

as a regulatory obligation with increasing capital and operational costs (Mitchell and Gu, 2010).

At the same time, the energy crisis is one of the greatest issues faced in our time. According to the United Nations World Water Assessment Programme more than 1.3 billion people around the world still have no access to electricity (WWAP, 2014). As a general worldwide trend, energy and electricity consumption are likely to increase over the next 25 years. At this point, it is important to understand the complex nexus and mutual relationship which has developed between water and energy. It is to be expected that changes in one will have both direct and indirect consequences for the other. By the year 2035, energy consumption is projected to increase by 70 %, which in turn will increase the energy sector's water consumption by 85 % (WWAP, 2014).

Having noted the interconnection of water and energy and the opportunity to use industrial wastewaters as a source of potential gain rather than loss, it is the time to narrow down the picture. Looking specifically at the case of Scotland, the whisky industry is one of the most vital industries in the country which has a significant economic impact, dominating the food and beverage exports of the UK (Goodwin, Finlayson and Low, 2001). This industry produces 8-15 litres of bio-rich liquid per litre of whisky, which might contribute to pollution unless used as raw material for other processes, or otherwise processed (Mohana, Acharya and Madamwar, 2009). Microbial fuel cells have been identified as a natural solution to the complex nexus of energy, water scarcity and sustainability which has been briefly described here. By utilising the metabolic reactions of electrochemically active microorganisms, MFCs break down organic matter while simultaneously generating direct electricity, converting its chemical energy into electrical.

1.2 Aim and objectives

The primary aim of this research is to investigate the long-term performance of MFC technology as a sustainable alternative to conventional wastewater treatment systems through a multidisciplinary approach which combines both areas of technical interest, and areas that are in need of further research.

Research on the topic of microbial fuel cells has gained exponential interest since the present study has started. However, large scale systems that can respond to industrial and

real world requirements still require investigation in order for researchers to be able to match innovations to suitable real-worlds applications in industrial environments. The current study does not strive towards maximum power generation, but rather focuses on achieving the following objectives to further its aim:

- To address key performance parameters regarding electrical connectivity and effluent quality in a prototype MFC reactor;

- To develop an experimental pilot scale MFC reactor from start-up, through acclimatisation and operation on real wastewater substrates and ambient temperatures;

- To integrate the pilot installation into an existing treatment process in order to investigate the compatibility and potential of complementary and/or competitive operation with existing treatment methods; and

- To analyse and monitor performance over a long period, on a continuous operational mode, in a realistic, industrial environment.

All the objectives above were examined through a multi-disciplinary approach combining various operational optimisation methods while also developing a simplified electrochemical model with the objective of describing the performance of the multi-electrode MFC in greater depth.

1.3 Structure of the Thesis

This study is structured as follows:

Chapter 1 sets out the background motivations for the study and the timeline of developments in the MFC field to date. The aims and objectives are also set, as the main axis around which the following chapters develop.

Chapter 2 starts with a review of the progress made to date in the field of MFCs. The main part of the chapter clarifies the principles of MFC operation, then the components and materials making up an MFC are summarised, along with a discussion of the microbial and architectural considerations. The key developments to date in utilising

MFCs for wastewater treatment are presented along with an outline of the current industrial-scale experience. The chapter concludes with a critical review of these developments and the potential for integrating the technology into existing treatment systems.

Chapter 3 mainly describes the development of the pilot scale 122 litre prototype reactor used in this study and the 14 litre bench scale replica. The general materials and methods used both in relation to electrical performance and effluent quality assessment are also presented in detail. Some of the methods and operational conditions employed in specific parts of this study are explained separately in their respective chapters.

Chapter 4 investigates optimum electrical operations, in an experiment that should have proceeded the development of the large-scale prototype, but chronologically succeeded it. It focuses in on a 14 litre bench-scale MFC otherwise identical to the later developed large scale pilot, on which two electrodes are operated either independently or in parallel in order to establish the optimum electrical configuration which will then be implemented in the 122 litre reactor. The examination of these configurations is also in correlation to the quality of effluent treatment.

Chapter 5 establishes the potential for using the 122 L MFC prototype in the whisky by-products industrial context. The preliminary studies outlined in this chapter include a successful start-up, moving to the long-term examination of energy recovery and effluent treatment, while the effect of temperature is examined throughout this phase. Latterly, having established a proof of concept, a refurbishment protocol is also developed.

Chapter 6: Having established the treatability of whisky distillation process derivatives, this chapter moves a further step forward to the integration of a pilot scale-up in a local distillery and its existing treatment process. The long-term operation and performance of the pilot set-up consisting of two 122L reactors with regards to energy recovery and effluent treatment is examined in the main part of the chapter. During the last experimental phase of this integrated study, the possibility of further optimisation is examined through alternative anodic materials.

Chapter 7 takes this study a step further. A simplified electrochemical model is discussed based on each electrode's real voltage, as developed by subtracting the various

losses from the thermodynamically predicted voltage. Validation of the model is attempted through ohmic resistance, and the potential for utilising this model to describe the performance of the pilot scale prototype is examined.

Chapter 8 provides the detailed conclusions of this study.

Chapter 9 outlines possible directions and recommendations for future research based both on the work conducted in this research, and on some general insights.

Chapter 2 – Literature review

2.1 Progression of microbial fuel cell research

As the introduction to this thesis outlined through its timeline, interest in microbial fuel cells has developed relatively rapidly through the years since their modern introduction to the public eye in 1991 through the work of Allen and Bennetto (1993). Figure 2-1 (A) shows a Scopus search with the keyword 'microbial fuel cell' covering work from 1993 to today (using the two filters of document type: journal, and language: English). It can be seen that over the decade since 2006, the increase in published work on the field has been exponential. Additionally, the maximum power achieved in studies is also increasing over time (Logan et al., 2015).

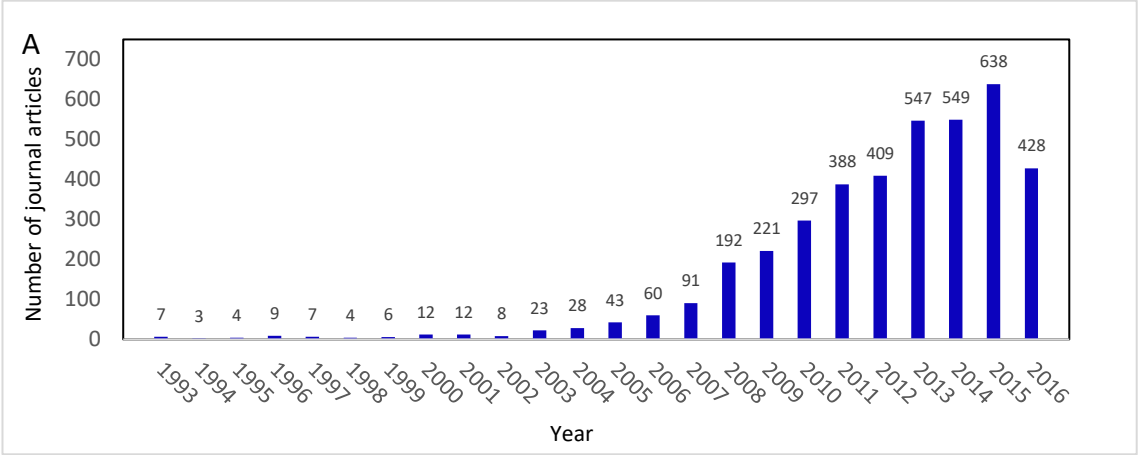

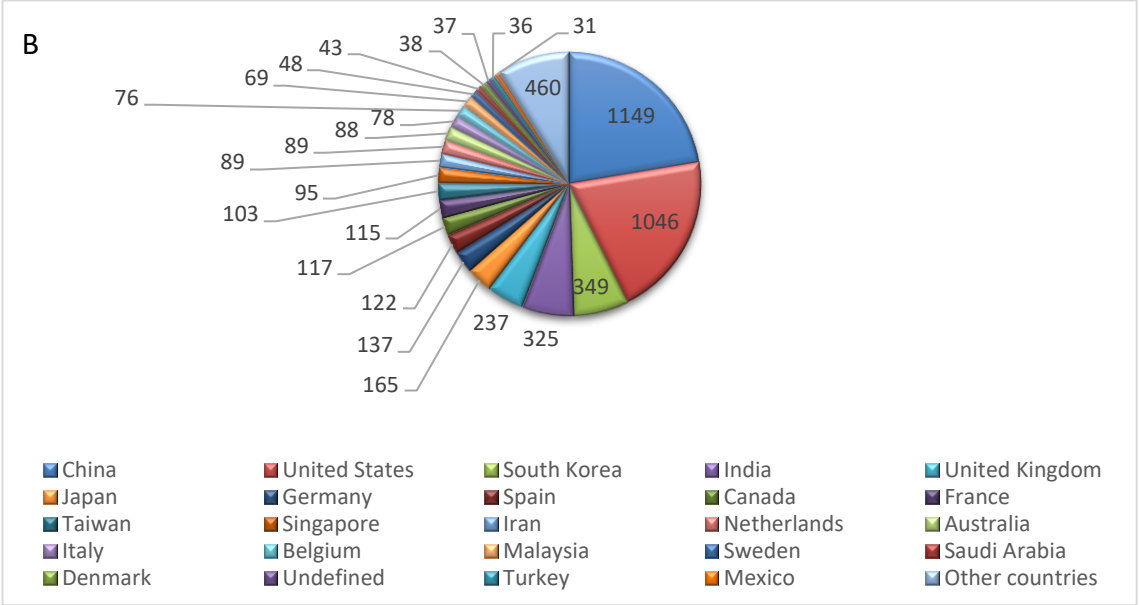

Figure 2-1: *(A) The number of published journal articles containing the keyword 'Microbial Fuel Cell' and (B) The distribution of MFC research according to the country of origin*
(Source: Scopus on 26/07/2016; document type: journal; language: English)

Figure 2-1 (B) shows the country-wise distribution of the relevant prior research in Scopus. Almost 50 % of the research on the field is shared between China, the USA and South Korea, with India and the UK following, meaning that these five countries are leading the research field. As an overview, though, from Figure 2-1 (B) it is obvious that interest is not dominated by the aforementioned countries, but is genuinely international and truly global, with interdisciplinary and international collaborations.

Along with the recent increase in publications on, and interdisciplinary approaches to, the subject came the diversification of MFCs by shifting them away from their original focus and spreading the concept to a variety of applications. Originally, MFCs were made to produce electricity, but the use of microorganisms on the anodes or cathodes or both has allowed modifications of the original device leading to a variety of diverse applications. All the other microbial electrochemical technologies (METs) will be described below in this section. They are typically known to use the MxC theme, where x denotes the specific application; for example, in the case of MFCs, the 'x' factor is 'Fuel' (Logan et al., 2015). Table 2-1, below, summarises the main microbial electrochemical technologies, thus demonstrating the current areas of interest in the field. It also describes each technology by indicating their main areas of difference.

One of the first modifications of an MFC was the Microbial Electrolysis Cell in 2005, a device in which additional voltage can be applied to drive the synthesis of hydrogen gas thus requiring lower energy input in comparison with electrolysis. The produced hydrogen can subsequently be used depending on its purity. This is an interesting feature since the additional voltage necessary to drive the process is considerably less than that needed for water electrolysis (Liu, Grot and Logan, 2005). Another particularly interesting adaptation is the Microbial Desalination Cell, which integrates the original MFC process and electrodialysis for wastewater treatment with simultaneous water desalination. During this process, the electricity generated from the anode to the cathode is used to drive the desalination process of water. MDCs can either be used as a stand-alone process or can be combined with other desalination processes, such as reverse osmosis, while at the same time treating wastewater streams (Saeed et al., 2015). The various METs are gaining considerable interest over time, mostly due to the increasing global needs for independent electricity generation and resource preservation, the

pressing need to eventually move away from fossil fuels, but most importantly due to their adaptability, their ability to be easily modified, and their wide range of applications.

Table 2-1: *Example of various Microbial Electrochemical Technologies (METs)*

MxC	Full name	Description
MDC	Microbial Desalination Cell	Can use electrodialysis stacks (MEDC, microbial electrodialysis cell), or forward osmosis (MOFC, microbial osmotic fuel cell) membranes.
MEC	Microbial Electrolysis Cell	Typically used for hydrogen production from the cathode, but also used for metal reduction.
MEDCC	Microbial Electrolysis Desalination Chemical production Cell	Includes bipolar membrane, so energy must be input for chemical production.
MES	Microbial Electrosynthesis Cell	An MEC is designed to produce soluble organics such as acetate.
MFC	Microbial Fuel Cell	Electrical power production.
MxB-MBR	MFC with a cathode membrane	The cathode serves a dual function, reduction and filtration of the water using either MFCs or MECs.
MMC	Microbial Methanogenesis Cell	Methane production from the cathode.
MREC	Microbial Reverse Electrodialysis Cell	Reverse electrodialysis stack inserted into an MEC.
MREEC	Microbial Reverse Electrodialysis Electrolysis and Chemical production Cell	An MEDCC that includes a RED stack and is used for production of acid and bases; can be used for carbon capture; can produce hydrogen gas; can also be used for desalination.
MRFC	Microbial Reverse Electrodialysis Fuel Cell	RED stack inserted into an MFC.
MSC	Microbial Struvite production Cell	Designed to precipitate struvite on the cathode.
sMFC	Sediment Microbial Fuel Cell	Also known as benthic MFC.

(Source: Logan et al., 2015, p.207)

2.2 Principles of microbial fuel cells

Logan et al. (2006) reopened and reshaped the current field of microbial fuel cells, shifting their use towards real-life applications. As the group redefined, MFCs are devices that use microorganisms as the catalysts to oxidize organic and inorganic compounds and generate electricity. In the MFCs, the electrons produced by microorganisms during their metabolic reactions in the substrates are transferred to the anode, the negatively charged

electrode terminal, and flow to the cathode, the positively charged electrode terminal, linked by a conductive material containing a resistor to complete an electrical circuit. The device should, therefore, operate on a substrate that is replenished in the anode after oxidation, either continuously or intermittently. Electrons can be transferred from the solution to the anodic electrode submerged in the anode through various processes, such as chemical mediators or shuttles. The electrons that reach the cathode combine with the protons that diffuse from the anode through a separator and with the oxygen provided from the air, with water being the resulting product. This constitutes the founding concept of the MFC device, with microbially catalysed electron liberation at the anode and subsequent electron consumption at the cathode, when both processes are sustainable.

The biological fuel cell that is an MFC is similar to the chemical fuel cell that utilises a hydrogen rich fuel. That is with a supply of fuel to the anode and a supply of oxidant to the cathode. In the anode, an organic fuel such as glucose is oxidised according to the reaction

$$C_6H_{12}O_6 + 6H_2O \rightarrow 6CO_2 + 24H^+ + 24e^-, \quad E_o = 0.014V$$

(2-1)

At the cathode, oxidant is reduced by the presence of a catalyst specific to the oxidant such as oxygen according to the reaction

$$6O_2 + 24H^+ + 24e^- \rightarrow 12H_2O, \quad E_o = 1.23V$$

(2-2)

The resultant electrochemical reaction creates a current as electrons and protons are produced, with the only difference to conventional fuel cells being the use of living organisms (Scott and Hao Yu, 2015).

Various distinct configurations are possible for an MFC (see Chapter 2.3.4), but during the first steps of the technology the typical design referred to as the H-shape MFC dominated the field. This consisted of two separate bottles in which the anodic and cathodic electrode were submerged, usually connected by a tube containing a separator which is typically a cation exchange membrane (CEM) (Figure 2-2 (A)) (Logan et al., 2006).

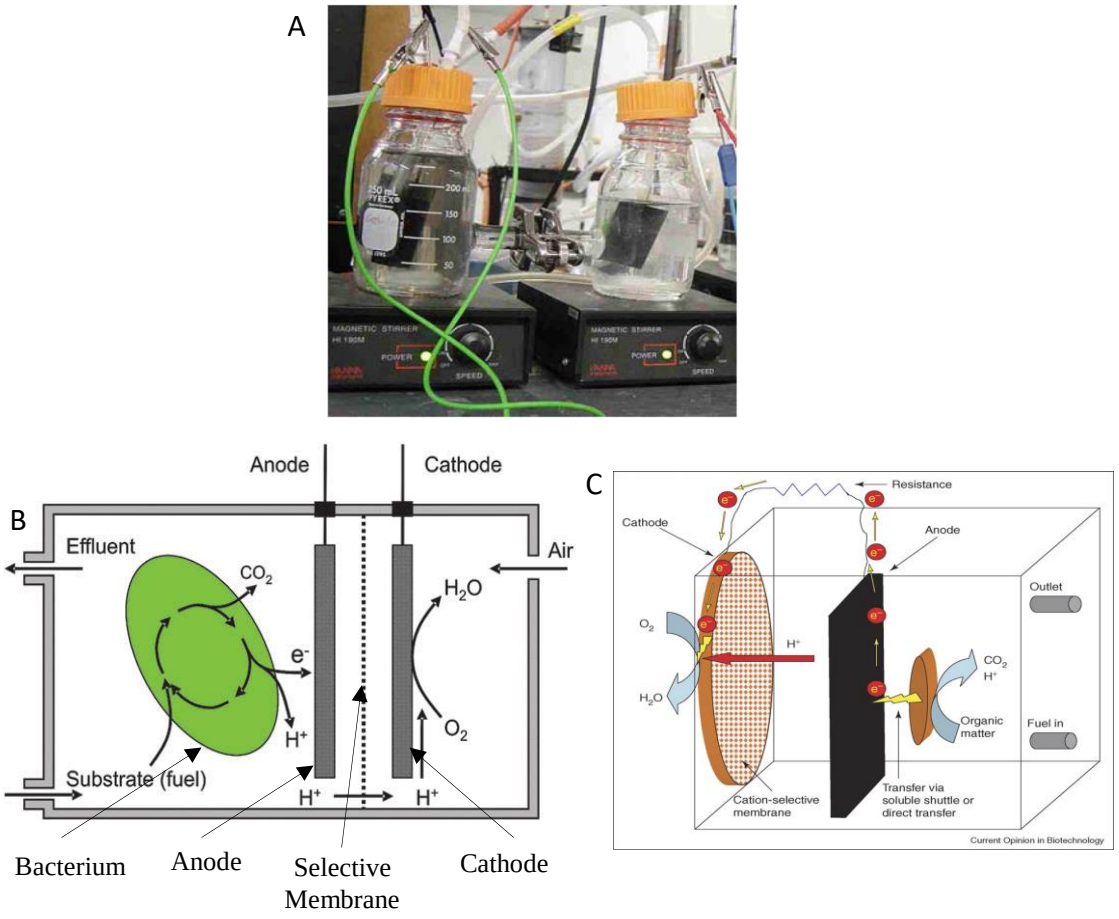

Figure 2-2: *Principle operations in an MFC (not to scale) in (A)an original H-shaped MFC, (B) a dual chamber MFC and (C) a single chamber open air cathode MFC*
(Source: (A):Logan et al., 2005, p.944, (B):partially adapted from Schroder, 2007, p.2619, (C): Lovley, 2006, p.328)

Figure 2-2 (B) depicts the principal operations occurring in a microbial fuel cell in the form into which the design was later developed: a dual chamber MFC where the anode and the cathode were incorporated within the same device and separated by the CEM. The microbial community in the anodic compartment transfers electrons obtained from an electron donor to the anodic electrode either through direct contact, nanowires, or mobile electron shuttles. During electron production, protons are also produced which then migrate through the CEM into the cathode chamber. The electrons flow from the anodic electrode through an external resistance (electrical circuit) to the cathode where they react with the final electron acceptor (oxygen). In this design, oxygen is usually provided through air which is pumped into the cathodic compartment (Rabaey and Verstraete, 2005; Logan et al., 2006).

The process described above is the founding process of the MFC. However, a vital recent moment has been the development of the single chamber open air cathode MFC. As can be seen in Figure 2-2 (C), the principal operation remains the same, with the key difference that no cathodic electrolyte is provided, and oxygen is not provided by artificial pumping. Instead, the cathode is exposed to open air, and oxygen is provided by natural circulation. Additionally, in this case, the membrane separator (if one is used) is coated on the cathode side, facing the anodic compartment (Lovley, 2006; Scott and Hao Yu, 2015).

2.3 Microbial fuel cell materials, components and reactor designs

Several materials have been used and developed over the years, either for conventional use in other treatment technologies or specifically developed for MFC applications. The selection of the appropriate electrode material with regard to both the anode and the cathode is critical for the performance of an MFC in terms of microbial adhesion, electron transfer, and electrochemical efficiency, and greatly affects its power generation and treatment efficiency (Wei, Liang and Huang, 2011).

Although the criteria in selecting materials for the anode and cathode are different on specific operations, at the first level of selection both should always possess certain specific properties. Firstly, the surface area and porosity of the electrode materials is of great importance since power generation is greatly constrained by it. Ohmic losses are directly proportional to the resistance of the electrode, and a method to decrease that is increasing the surface area while keeping the volume the same. Additionally, a higher surface area provides more sites for reactions and better adhesion of the microbial community. However, porosity will decrease the electrical conductivity of the material (Logan, 2008). The conductivity of the materials used is also of great importance. The electrons released during the metabolic reactions of the microorganisms have to travel through the anodic electrode to the external circuit in order to reach the cathodic electrode. Therefore, materials with as low an internal resistance as possible will make the flow of electrons easier (Scott and Hao Yu, 2015).

It is also necessary to ensure the biocompatibility, durability and stability of the electrodes. Regarding the microbial community, it is obvious that since the process of power generation is driven by microorganisms, the materials used should protect them

from poisoning, and should also be chemically stable in the bacterial culture, and corrosion resistant (Wei, Liang and Huang, 2011). Additionally, the long term operation and performance of reactors is of particular interest to the study and generally in the field over the past few years. Therefore, ensuring the durability of materials over time is necessary for successful applications.

Finally, the cost of materials is a factor, especially with regard to industrial-scale applications, and because the ultimate goal is for MFCs to be commercially deployed. In order for this to be achieved, the materials should be low cost, sustainable and easily available. Currently, two elements are prohibitive regarding material costs: membranes, and cathode catalysts. Some of the metals which are traditionally used as cathode catalysts, such as platinum, are neither cheap, nor durable or sustainable. Rozendal et al. (2008) studied the economics of MFCs as currently practised and according to their findings, capital costs per kg of COD treated were approximately 8 €, 38 % of which they attributed to the cathode, while 47 % of the cost was due to the membrane separator used in the majority of the studies. They also predicted that according to current trends, material costs would be reduced in the near future to approximately 0.4 € per kg of COD treated, with respective contribution of the cathode and membranes reduced down to 10 % and 20 %. This could be achieved in two-fold ways; firstly, membrane-less MFCs which make the use of a membrane obsolete are increasingly gaining interest and further research (You et al., 2007; Liu et al., 2008; Daud et al., 2015), and secondly, there has been development and use of non-precious catalysts in cathodic electrodes such as metal-based and carbon-based catalysts (Daud et al., 2015; HaoYu et al., 2007; Yuan et al., 2016), which will certainly contribute towards more economically viable MFCs.

2.3.1 *Anode materials*

The materials commonly used in laboratory developments usually include a large variety of carbon materials and several metal-based materials, whereas surface area is found to vary greatly. According to the considerations discussed previously concerning biocompatibility, chemical stability, high conductivity and relatively low cost, carbonaceous materials have been identified from the first steps of the development of MFCs as the most suitable for use, particularly with regard to the anode. In terms of structure, the aforementioned carbon-based electrodes can be separated into a plane structure, when a single material is used, a packed structure, when the electrode is a

'pocket' filled with a certain or a number of these materials, and a brush structure, where the electrode is developed in a brush form (Wei, Liang and Huang, 2011).

Figure 2-3, below, summarises the carbon-based materials most commonly used in both laboratory and pilot-scale studies. One of the materials used in very early studies was carbon paper, which is a very thin and relatively stiff material that has been found to be easily damaged (Logan, 2008). Graphite plates have been found to be much smoother, more robust, with a more compact structure, however, they have also been found to have relatively smaller surface area. Additionally, when used as an anodic electrode, roughened plates have been found to produce higher power outputs than the similar, smoother ones (ter Heijne et al., 2008). Carbon cloth and carbon mesh have also been used in the literature; the cloth is by nature more porous and could, therefore support a better microbial structure, but it is also more expensive. In a comparative study by (Wang et al., 2009a) between the two materials after going through a pre-treatment, the carbon mesh anode was found to produce a slightly higher power output. Graphite rods are another carbon material that has been used in literature; however, as with the graphite plate, these have a rather smooth surface area and when used have been reported to have been abraded with sand paper in order to enhance microbial attachment (Liu, Ramnarayanan and Logan, 2004). In a comparative study conducted by Chaudhuri and Lovley (2003) as cited by Wei, Liang and Huang (2011) a carbon felt and carbon rod anode were found to produce similar power outputs. Some studies have been conducted on reticulated vitrified carbon, a carbon-based material with a very high porosity of 97 % and conductivity, which is very rigid but also easily damaged (Scott et al., 2008; He, Minteer and Angenent, 2005). In a study by Ringeisen et al. in 2006 which made a comparison between a reticulated vitrified carbon anode and an anode with carbon felt, the first was found to have produced more than twice the power than the felt anode.

It is necessary to point out even at this early stage (as will also be discussed further later on), that a direct comparison between studies of microbial fuel cells and, thus, of their power outputs and COD removals, is particularly difficult, because an MFC by its nature is a technology synthesised by, and depending on, many different disciplines such as microbiology, chemistry and materials sciences. Therefore, many different parameters are involved even in the most basic, laboratory experiment. Additionally, regarding electrical units in particular, such as current and power, there are several ways of

representation which have only been unified in a way that is comparable in the last few years (see Normalised Energy Recovery, Chapter 3.3).

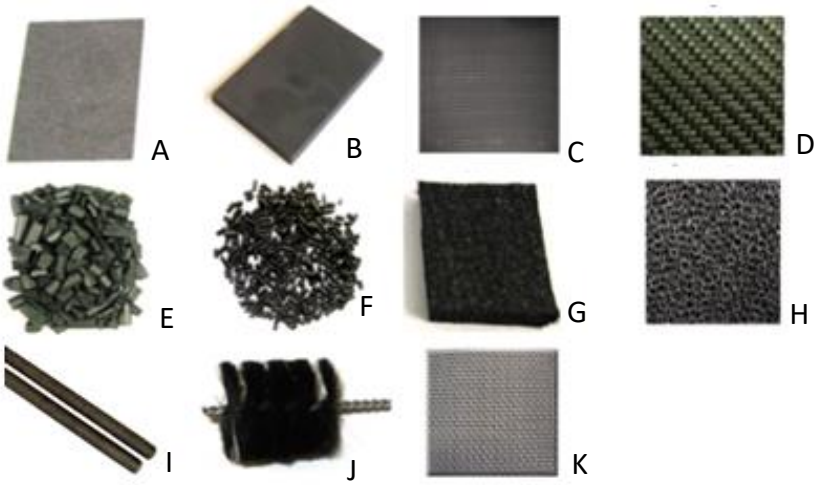

Figure 2-3: *Materials used in both anodes and cathodes; (A) carbon paper, (B) graphite plate, (C) carbon cloth, (D) carbon mesh, (E) granular graphite, (F) granular activated carbon, (G) carbon felt, (H) reticulated vitrified carbon, (I) graphite rods, (J) carbon brush and (K) stainless steel mesh (Source: partially adapted from Mustakeem, 2015, pp. 22; Wei, Liang and Huang, 2011, pp.9336)*

Moving on to packed structures, which are also considered the first 3-dimensional anodes (Aelterman et al., 2008), the use of granular graphite for the construction of an anode in a packed bed was first reported by Rabaey et al. in 2005, when the authors used this packed bed in a tubular open air cathode with the effluent entering from the bottom passing through the bed. The reason behind the use of both graphite granules and granular activated carbon was to increase the surface area available to the microbial community. The use of the aforementioned materials in packing forms for MFCs' anodes is becoming increasingly common (Jiang and Li, 2009; Aelterman et al., 2008; Rabaey et al., 2009; Kalathil, Lee and Cho, 2011). Similar to the biological filter, the anode chamber can either be filled with granular material in the form of bed, or can be in a shaped 'pocket' configuration. In these cases, having a high surface area is a great and desirable advantage, but in order to make the electrode effectively conductive, the granules must be tightly packed next to each other (Logan, 2008). However, it has also been found that in the long term, the clogging of MFCs is a potential issue (Rabaey et al., 2009).

Carbon brushes are currently becoming popular and are occasionally favoured in large scale applications due to their high surface area, high porosity and potential current collection (Ge et al., 2013; Zhang et al., 2013b, Zhang et al., 2011; Cheng and Logan,

2011). The brush was first introduced by Logan et al. in 2007, who used it with conductive and non-corrosive metal core in an open air single chamber laboratory scale MFC, achieving the maximum power output reported for a single chamber MFC at the time. Three studies further explored the concept of brushes in MFC anodes on a laboratory scale, this time examining the load/density of the brush and its effect on performance and electrical power output. Specifically, on the one hand, Lanas and Logan in 2013, and Lanas, Ahn and Logan in 2014 explored the use and position of multiple brushes within one anodic compartment, and found that multiple, smaller brushes could lead to higher power outputs than a single, bigger one. On the other hand, Hutchinson, Tokash and Logan in 2011 found that 65 % of the size of a single brush could be removed without current collected and thus power output reduced. Finally, in addition to the aforementioned indications of brushes being able of achieve higher power outputs, Feng et al. in 2010 found that additional acid and heat treatment of the brush anode could lead to up to a 34 % increase in its achievable power output. However, in order to make a realistic comparison, treatments of materials with various chemicals, such as ammonia, surface oxidation and heating, has been found to increase power outputs is almost every material, from plates and sheets to brushes and rods (Wei, Liang and Huang, 2011).

Metal materials and materials with metal coatings are much more conductive than carbon-based materials. However, their application in the MFC field remains relatively questionable. Additionally to being conductive, materials used for anodes and cathodes also need to be non-corrosive. Many metals have been ruled out because of the non-corrosive requirement, and up-to-date stainless steel and titanium have therefore qualified as relatively common metal materials for use in MFC anodes. It is also reasonable that microbial adhesion on such smooth surfaced materials is not favoured, especially when compared to carbon-based competitors. Dumas et al. (2007) found that the stainless steel anode produced lower power outputs than carbon-based ones, however, a metal-based cathode reported more promising results. Titanium was also examined in a comparative study by ter Heijne et al. (2008), who examined the performance of flat graphite, roughened graphite, Pt-coated titanium and uncoated titanium. According to their results, the best performance in terms of power output was achieved by the roughened graphite, followed by the Pt-coated titanium then the flat graphite, and the least power was generated by the untreated titanium anode. Biomass interactions were also a very important factor in the study. Ter Heijne et al. (2011) went on to use the titanium plate

and mesh with mixed metal oxide as an anode for the scale-up of a 5L prototype, and they reported a promising performance. The same anode construction of a titanium plate anode was also reported by Dekker et al. (2009), even though their work focused mostly on cathode limitations.

The combination of different materials has given rise to 3-dimensional, complex anodes and seems also to have enhanced electrical performance, particularly in comparison to traditional 2-dimensional anodes made up of materials such as carbon cloth (Chen et al., 2013; Yong et al., 2012). In this study, a 3-dimensional complex anode has been constructed in line with the principles discussed in this section. Increases in active surface area, conductivity, and biocompatibility, and the subsequent support of microbial communities have been the drivers for the development of the anodic electrodes that will be discussed in Chapter 3.2.2.

2.3.2 *Cathode materials*

As was discussed at the beginning of the section, and as will be explored in more detail here, the materials used for the cathodes in principle have the same qualities, as they are carbon-based, conductive and biocompatible, in the sense that they are not toxic towards bacteria. However, the supporting microbial biofilm formation is a different issue, as it could be argued that a smooth surface area as a cathode could lead to enhanced performance given that it will not suffer from biofouling, an issue commonly faced in cathodes.

Currently, the main limiting factor in MFCs is the cathode (Logan, 2008; Rismani-Yazdi et al., 2008), the design and the materials used in cathodes are therefore a challenging aspect of MFC research overall. The materials mentioned previously for anodes have been used in the three major different cathode designs: aqueous air cathodes, open air cathodes and bio-cathodes (Wei, Liang and Huang, 2011). Typically, in all cases, the main difference of the cathodes compared to the anodes, given that they are based on the same materials, is the use of a catalyst, even though it is not always necessary, to enhance oxygen reduction, which is the main reaction occurring in a cathode.

The first design which was widely deployed in laboratory experiments is the aqueous air cathode, in which the electrode is submerged in the cathodic compartment, and air is pumped into it and dissolved in catholyte. However, this design, which is also called the

dual chamber MFC, was more or less abandoned when the open air cathode design was deployed due to the fact that oxygen's solubility in water is 4.6×10^{-6} at 25°C but in air, it is 0.21 (Logan, 2008). Open air cathodes, either with or without catalysts (when they are the design of choice the MFC is usually called single chamber open air cathode MFC) are believed to be a more efficient design particularly in the context of wastewater treatment, due to lack of aeration and associated costs and inefficiencies, and also due to the higher power outputs achieved. The layout of an open air cathode typically comprises the carbon-based material on which the catalyst is impregnated (if existing), and is in contact with air, a conductive material, and a hydrophobic layer to avoid the diffusion of liquid from the anode to the cathode (Logan, 2008). If a selective membrane is present, as will be discussed further below, it is on that side of the cathode, facing the anode, as can be seen in Figure 2-2 (C) (Wei, Liang and Huang, 2011). The catalyst extensively used in early research was platinum (Pt), either impregnated on carbon-based materials such as carbon cloth, or coated on metal based cathodes (Logan et al., 2006; Cheng, Liu and Logan, 2006a; Cheng, Liu and Logan, 2006b). However, due to its high cost, toxicity and relatively rare availability as a resource, platinum was prohibitive for large scale applications. For this reason, non-precious metal catalysts were developed or otherwise catalysts would become obsolete.

A cost effective transition was therefore made towards iron, nickel and cobalt or to cathodes without any catalyst (Yuan et al., 2016). Zhao et al. in 2005 and then again in 2006 studied the application of iron phthalocyanin and other metal oxides as inexpensive alternatives to platinum, and found that the power outputs achieved were very similar to the respective outputs of cathodic materials catalysed with platinum. Iron phthalocyanin was the catalyst used in the current study, and recently, results of this catalyst achieving high power outputs in MFCs operating on real wastewater were verified (Burkitt, Whiffen and Yu, 2016). In non-catalysed applications of cathodes, activated carbon and granular carbon have been extensively used, and in studies comparing the two it has been found that activated carbon produces higher power outputs (Freguia et al., 2007; Tran et al., 2010).

Finally, bio-cathodes have gained considerable attention in the last few years due to their stability and multiple functions in an MFC, such as wastewater and biosynthesis. Currently, bio-cathode electrodes are mainly composed of, as like previous applications,

on carbon-based materials including graphite plate, carbon felt, granular graphite, and graphite brush, as well as stainless steel mesh. The main difference, as their name implies, is that bio-cathodes are also inoculated with either a single microorganism or a consortium of microorganisms, different than those in the anodic compartment (Wei, Liang and Huang, 2011). Algae in cathodes are currently gaining even more attention due to their potential in integrating MFC technology with photo-bioreactors, i.e. the reactors in which algae are traditionally grown (Wang et al., 2014; Gajda et al., 2015). However, as a field, bio-cathodes are still a relatively new modification of MFCs, and thus the materials used and their operation are still subject to ongoing research and development.

2.3.3 *Separators and membranes*

The third important factor concerning the materials used in MFCs is the ion exchange membrane (IEM) or separator. In typical fuel cell applications such as the hydrogen fuel cell, the membrane is a necessary component; however, that is not necessarily the case with MFCs. The reasons membranes are used in MFC applications are to allow the selective movement of ions from the anode to the cathode, and also to prevent the leaching of the anodic fluid in the cathode, whether that is in a dual MFC or an open air cathode (Logan et al., 2006).

The membranes and separators traditionally used in MFCs can be separated into three main categories; cation exchange membranes (CEMs), anion exchange membranes (AEMs) and uncharged porous membranes. The first two are the most expensive and were typically used in wider fuel cell applications before being adopted by MFC technology (Leong et al., 2013). Between the different kinds of membranes which are commercially available, CEMs, which are selectively permeable to cations, are the most commonly used. The structure of AEMs and CEMs is the same as the corresponding ion type which is not transferred, thus preventing its move from the anode to the cathode and back.

Perfluorosulfonic acid (PFSA) polymers are the most commonly used within the CEMs. These have three regions: a polytetrafluoroethylene backbone, a side chain of vinyl ethers, and a sulfonic acid group, and they have good proton conductivity precisely because the negatively charged hydrophilic sulfonate group is attached to the hydrophobic

fluorocarbon backbone, promoting proton transport through it (Scott and Hao Yu, 2015; Leong et al., 2013).

AEMs are solid polymer electrolyte membranes which usually contain positive ionic groups and mobile negatively charged anions. They have been found to provide a better management of liquid crossover, and tend to be a cheaper alternative (Scott and Hao Yu, 2015). A comparative study by Kim et al. (2007) utilising different membranes in an acetate-fed open air cathode MFC found that the AEM yielded a higher power density and had the lower oxygen and fuel permeability compared to the CEM.

Porous membranes, such as glass wools and microfiltration membranes, have gained some interest over the last few years as a low-cost alternative to AEMs and CEMs in MFCs. Single chamber MFCs with glass wool as separators instead of expensive membranes have been argued to be more cost effective in wastewater treatment and power generation. They have also been found to face similar issues to membrane-less MFCs, such as oxygen and substrate diffusion. Obviously, diffusion rates for both are lower in MFCs with no membrane separator, but higher than in the cases of AEMs and CEMs. The crossover also facilitates faster biofouling, leading to a general reduction of performance in the cell, and therefore, their use in MFC technology is not yet favourable (Mohan, Raghavulu and Sarma, 2008; Sun et al., 2009; Leong et al., 2013).

The main disadvantage associated with membranes is the cost, which is possibly the highest in terms of materials, attributing as it does 47 % to the total cost (Rozendal et al., 2008). Additionally, they can add to the internal resistance and can be susceptible to biofouling, reducing the overall performance of the cell (Logan, 2008). Relatively recently, membrane-less MFCs have been examined in order to try to eliminate the aforementioned disadvantages (Du et al., 2008; Ghangrekar and Shinde, 2007; Liu and Logan, 2004). However, in the long term, particularly in long term operational MFCs, it has been proven that oxygen and substrate diffusion pose a particular issue by reducing the cells efficiency. Having a closer look at the large scale applications which have been published to date, it can be seen that the majority utilised an ion exchange membrane (Janicek, Fan and Liu, 2014). For the time being, the advantages of a membrane particularly in such large scale applications have not yet been overturned, but as discussed

at the beginning of the chapter, with cost as the main driver, developments in membrane-less MFCs are increasing.

2.3.4 *Microbial fuel cell reactor configurations*

Various configurations have been reviewed by Du, Li and Gu (2007) and Zhou et al. (2013), who looked at different designs in the field of MFCs as well as microbial electrolysis cells, and more recently configurations have been reviewed by Hernández-Fernández et al. (2015) and Gude (2016). MFCs are a very dynamic technology, as has become clear through this literature and research review, and there has been an almost exponential increase in MFC studies in recent years. However, in this section, an examination of the basic MFC architectures will be attempted. The descriptions of MFC reactors that follow are far from exhaustive as different designs are configured almost every year, but the major applications and better defined MFC reactors are described presently.

One of the reasons why so much research is currently taking place with MFCs as the main feature is their multi-disciplinary nature. Therefore, a categorisation of designs according to one criterion would be too generic. Figure 2-4, below, gives a classification of designs, some of which have been mentioned up to this point, based on five criteria: configuration, structure, the separator or membrane used, flow type, and cathode type.

According to the relative position of the anode and cathode, MFCs can be divided into dual chamber, single chamber (also usually referred to as open air cathode MFCs) and multi-chamber. The dual chamber MFC was the design developed in the early years of research; here, the anode was separated from the cathode (in two separate bottles in the case of the H-shaped MFC) typically using a salt bridge or a membrane, as shown in Figure 2-2 (A) (Logan et al., 2006). The electrons generated from in the anode from the cathodes were transferred externally through a wire to the cathode and protons were transferred to the cathode through the membrane. This design, however, was relatively complex and impractical for further scale-up, mostly due to the costs associated with the need for aeration to the cathode to provide oxygen. For this reason, it was abandoned early on, particularly for scaling-up (Hernández-Fernández et al., 2015b).

Regarding different configurations of MFCs, single chamber open air MFCs have been introduced as an answer to the mechanical aeration issue faced by dual chamber MFCs.

The anode is exposed to air and oxygen is reduced from free air. In single chamber MFCs the anodic compartment is separated from the cathodic compartment by a membrane, preventing liquid crossover, or in some cases the membrane is completely absent (membrane-less single chamber open air cathode MFCs). In one of the first comparative studies in the field of MFCs, Liu and Logan (2004) presented a cube-shaped reactor where they examined the effect of the presence against the effect of the absence of a cation exchange membrane. The researchers found that the MFC without the cation exchange membrane produced a little less than twice the power the same MFC produced with the membrane in place. Similarly, the tubular MFCs currently used in most scaled-up studies are single chamber open air cathode MFCs with differences in their structures but not in their principle of operation according to which the cathode is exposed to air (Liu, Ramnarayanan and Logan, 2004; Janicek, Fan and Liu, 2014). Also, in terms of configuration, multi-chamber MFCs have recently been introduced with the intention of further scaling-up. Samsudeen et al. (2015) designed an MFC with four anodes electrically connected in parallel, forming one joint anode which was then connected by an external circuit to one cathode and was separated by a proton exchange membrane. This was operated with distillery wastewater, achieving a maximum power of 135.4 mW/m^2.

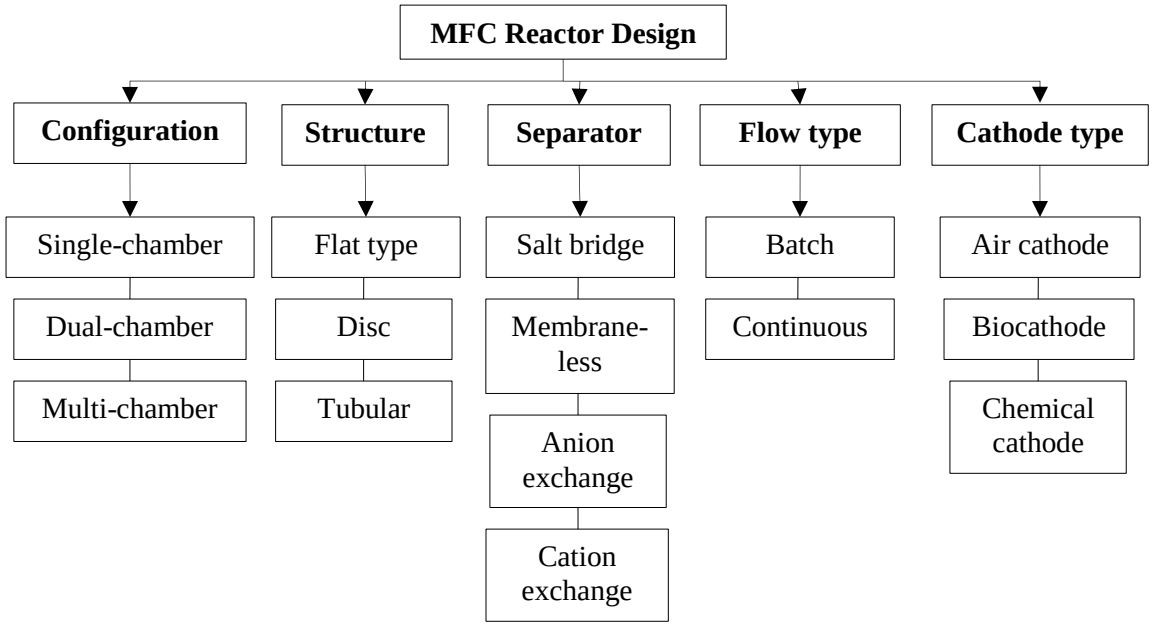

***Figure 2-4**: MFC reactors classification according to various criteria*
(Source: partially adapted from Zhou et al., 2013)

Regarding structure, four main designs have been widely reported. Currently, the most popular design as discussed in scaled-up studies is the tubular MFC, on which the cathode either surrounds the anode and is exposed to air (Ge et al., 2013), or the cell is shaped as a tube with the cathode in the middle creating a void space (exposed to air), and the anode surrounding it (Liu, Ramnarayanan and Logan, 2004). Cheng, Ho and Cord-Ruwisch (2012) designed a rotatable bio-electrochemical contactor in which the anodic and the cathodic electrodes did not have a distinct function, but instead consisted of an array of rotating electrode disks, each of which had its upper semi-circle exposed to air and its lower side submerged in water. Continuous rotation allowed each half to act as an anode and a cathode alternately, thus achieving a promising COD reduction, 40 % of which contributed to the current generation and was not due to aeration. Finally, in terms of structure, the flat plate MFC (which is the design used in this study) has also been used in scaled-up studies, albeit less widely than the tubular design. The concept of a baffled reactor is incorporated in this design. Li et al. (2008) designed a baffled reactor as early as 2008 in which the cathodes were exposed to air and were able to achieve 88 % COD removal with an HRT of 91h, and a maximum power output of 133 mW/m^2. A similar concept of a baffled reactor but which in this case was horizontally placed was more recently developed by Dong et al. (2015) achieving a COD reduction of 87.6 % while harvesting 0.034 kW/m^3. The overall volume of this reactor was 90 L, and it can be considered to have a serpentine circulation as the reactor developed in this study has.

The categorisation of MFCs according to the cathode design and the membrane separator (or the absence of one) were developed earlier in Chapters 2.2 and 2.3.3 respectively. Therefore, the last categorisation is according to flow type: more specifically, continuous and in batch mode. During the first steps in the context of field effluents, either artificial or real wastewater were examined in batch mode in order to examine the extent to which the MFC can be powered by a single batch of organic matter, but as the field progressed, the need to examine long term, continuous flows became obvious (Logan, 2008). There has been a debate in the research community on the most effective method in relation to the processing regime for effluent, and currently both types are being used in scale-up studies (Janicek, Fan and Liu, 2014).

2.4 Biological aspect of microbial fuel cells

2.4.1 *Microbial electron transfer and inocula*

The microbial community in an MFC is clearly responsible for the transport of electrons to the anode and through the cathode, and thus for the generation of electrical current. The transfer process of electrons resulting from the metabolic reactions of the microbial community can be classified into two categories. Firstly, there is the mediated electron transfer during which a mediator, either produced by the microorganism itself or mechanically added to the system, is used to move the electrons to the surface of the electrode, and secondly, there is mediator-less electron transfer, during which electrons are either transferred through direct contact with the anodic electrode or by nanowires developed between the microorganisms and the electrode (Logan, 2008).

MFCs using mediators involve microorganisms that can transfer electrons only to soluble compounds which are either natural, such as nitrate, sulphate, and sulphide, or synthetic soluble mediators such as thionine, methylene blue and neutral red (Ieropoulos et al., 2005; Park and Zeikus, 2000). Originally, mediators were used in order to enhance the transport of electrons to the anode, and thus increase current generation. Ideal mediators should be able to cross the cell membrane easily, have good solubility in the anolyte, and be non-biodegradable and non-toxic to the microorganisms. If large scale applications are targeted, then they should also be particularly low in cost. It was also found that in some cases bacteria such as *Shewanella oneidensis* can generate their own mediators (Du, Li and Gu, 2007; Park and Zeikus, 2000). When added in the anode, artificial mediators had to be continuously replenished or they otherwise had to be impregnated into the anode material using physicochemical methods. However, even in the case that they are impregnated in the anode material, mediators can still be deactivated due to drop out, or degraded during long-term operation (Wei, Liang and Huang, 2011).

The defining moment in the field though came when Kim et al. (1999) found that certain bacteria are capable of directing electrons outside their cells by themselves. Mediator-free MFCs utilise microorganisms such as *Geobacter sulferreducens* (Bond and Lovley, 2003), *Geobacter metallireducens* (Min, Cheng and Logan, 2005) and *Rhodoferax ferrireducens* (Chaudhuri and Lovley, 2003), all of which are bioelectrochemically active and able to form a biofilm on the anode surface, and to transfer electrons directly by conductance through the membrane. When they are used, the anode acts as the final

electron acceptor in the dissimilatory respiratory chain of the microbes in the biofilm (Bond and Lovley, 2003; Chaudhuri and Lovley, 2003). Certain microorganisms have also been found to connect to the anodic electrode through extracellular appendages, called nanowires (Logan, 2008).

The use of mediators carries both advantages and disadvantages. Their main advantage is that they allow the microorganisms in the bulk liquid in an anode outside the biofilm to be involved in the process. If the electron transfer is solely based on contact with the anodic electrode, then microorganisms which are either incapable of the direct transfer, such as many anaerobes, or are placed far from the electrode, especially in a large reactor, would be unable to contribute to the generation of current. On the other hand, mediators are expensive to produce in terms of carbon and energy requirements, and are non-selective, which means that they can be used by competing microbes and upon transport away from a suspended microbial cell toward the anodic electrode acceptor, might not come back to the microorganism, thus creating a loss for the microorganism (Scott and Hao Yu, 2015).

Regarding the specific microbial strain and communities used, MFCs have operated in both mixed consortia and pure cultures, and it has generally been found in prior research that MFCs operating using mixed cultures are capable of achieving substantially greater power densities than those with pure isolated cultures (Logan et al., 2006). However, it should be kept in mind that in order to accurately attribute electrical power output performance solely to one parameter, in this case the microbial community, the remaining experimental parameters should remain unchanged and a benchmark should be established. In the majority of prior research studies it can be seen that, even in comparative research, more than one parameter has been changed within the experiments, rendering direct comparisons very difficult. Additionally, in most studies it could be argued that the achievement of higher power outputs might possibly be attributed more to the reactor's architectural features, electrode spacing and material, rather than solely to the bacterium used (Franks, Malvankar and Nevin, 2010).

In using the source of inoculum as a criterion for the classification of MFC studies, four major, generic categories can be formed: pure cultures as inocula, mixed cultures,

pre-acclimated bacteria from already operating MFCs, and the utilisation of the bacteria already existing in real wastewater effluent streams with no additional bacterial input.

Pure cultures used in the majority of MFC studies are typically microorganisms with electrogenic potential, such as *Geobacter* and *Shewanella* (Min, Cheng and Logan, 2005; Bond and Lovley, 2003; Dewan, Beyenal and Lewandowski, 2008), generating a power output in the range of 0.005-0.05 mA/cm^2. Dumas, Basséguy and Bergel (2008) used a pure culture of *Geobacter sulfurreducens* in a stainless steel cathode half-cell and achieved a considerably higher power output of 2.05 mA/cm^2.

Studies using mixed consortia have achieved a much wider range of power outputs. Given that MFCs are an anaerobic or anoxic biological treatment, the most commonly used consortia referred to in the literature are the mixed anaerobic microorganisms usually procured from wastewater treatment facilities (Ha, Tae and Chang, 2008; Kargi and Eker, 2007; Wen et al., 2009; Sharma et al., 2014). For example, Aldrovandi et al. (2009) used a granular anaerobic sludge inoculum from an upflow anaerobic sludge blanket in a mediator-less and membrane-less MFC operating in synthetic wastewater. The average COD removal ranged from 66 to 91 %, whereas the average power production achieved was at 70 mW/m^2 for ten months. The same inoculum was used in the present study. Several studies have also used a combination of aerobic and anaerobic inocula under MFC anaerobic conditions (Pant et al., 2010). Interestingly, in a comparative study of aerobic and anaerobic mixed consortia Gao et al. (2014) used a single chamber open air cathode MFC operated on an artificial medium and found that the anaerobically pre-treated aerobic community produced a higher power output of 5.79 W/m^3 compared to the anaerobic consortia, which generated 3.66 W/m^3.

From a very early stage, the bacteria used in previous MFC studies have been used as inocula in new studies. This method of serial transfusions has a few advantages, the most important of which is the acclimatisation of the community. The biomass has adapted to electrogenic metabolic processes, which subsequently leads to faster start-up periods and higher power outputs (Catal et al., 2008; Logan et al., 2007; Cheng, Liu and Logan, 2006a). However, the additional inoculum used in an MFC, whether as a fresh inoculum or serially transfused, could be attributed to the need for the microbial factor for the catalysis and break-down of organic matter, and this was obviously necessary in early

laboratory research into artificial substrates. Over the last few years, it has been recognised that in real wastewaters a plethora of microorganisms native to the effluents are readily available, and there has therefore been a trend of utilising either different effluents as the initial inoculum, or more importantly, no additional microbial inoculum (Sharma et al., 2014).

It has been argued that if MFCs are to be utilised in wastewater treatment, mixed consortia are capable of providing several advantages, such as robustness in the context of adverse environments. Mixed bacterial communities are also capable of sustaining fluctuations in influent organic load (Franks, Malvankar and Nevin, 2010). Additionally, it has been found that bacteria enriched by an MFC operation demonstrating successful COD removals and power outputs could not be grown as pure cultures. This is most likely due to the syntrophic interaction between species in mixed consortia, the absence of which inhibits the growth and optimum behaviour of the extracted bacteria (Kim et al., 2004; Parameswaran et al., 2009), thus highlighting the need for better understanding of microbial interactions in order to further scale-up the MFC technology. On the other hand, genetic modification to create a 'super bug' has also been suggested as a necessary breakthrough if MFCs are to generate the high electrical outputs that will allow their further scale-up (Zhou et al., 2013).

2.4.2 *Electrogenesis and methanogenesis*

Methane is the natural end product in most anaerobic environments, and methanogenesis is therefore an important biological process, particularly when anaerobic consortia are used in MFCs as inocula. Methanogens have been found to compete with the electrochemically active microorganisms for the organic compounds found in wastewater. Therefore, unless the methane which is formed can be re-oxidized and subsequently reused for electrical current generation, methanogenic activity is expected to reduce electron recovery. Prior research using pure artificial mediums has shown that although electrochemically active microorganisms at an anode can outcompete methanogens for acetate as an electron donor, the use of glucose leads to notable amounts of methane production (Rozendal et al., 2008; Lee et al., 2008).

Methane production in an MFC might not be the principally desirable output of the process, however, if energy recovery is considered in a wider perspective then the

methane production in an MFC should not be regarded a loss. The focus of many MFC studies, including the present one, is wastewater treatment. Methanogenesis undoubtedly contributes towards COD reduction in the same way an anaerobic digester does. However, methanogenesis possibly poses an issue with specific regard to power generation. In case methane is generated in an MFC, an interesting experiment would be to calculate energy recovery from both processes, and then supress methanogenesis and examine if electrogenesis, thus electrical power output increases and if so, if the energy recovered only from electrogenesis is higher than in the case of both electrogenesis and methanogenesis being present. Ge et al. (2013) calculated the energy production from a tubular MFC operating on sewage sludge both from direct electricity generation and from the biogas produced from the MFC. According to their findings, the total energy produced by the MFC was 22.79 kWh/m^3 (operational value), whereas typical production from an AD was estimated at the average of 10.73-38.06 kWh/m^3. These findings partially support the previous argument. Finally, Xiao et al. (2014a) found in a study similar to the previously mentioned one on sewage sludge that methane production in the anode chamber could enhance the electricity production from it, and the output voltage of the MFC in methane production was higher than that of the MFC without it. The above demonstrates that if methane generation occurs in an MFC, it should be further examined in order to be able to optimise its operation, energy recovery and treatment efficiency.

2.4.3 *Microbial fuel cells and temperature*

Last but certainly not least, temperature should be considered in relation to the performance of an MFC given that the core of its operation is based on microorganisms. Since the field of biological fuel cells was re-opened, the majority of research has been conducted in temperatures of around 30^{o}C in controlled laboratory conditions (Logan, 2008). However, it is acknowledged that real field applications of MFCs would differ from that environment, with the variations in conditions including temperatures. As Figure 2-1 (B) indicates, MFC research is currently being conducted worldwide; therefore, it is necessary for the influence of temperature to be examined in field applications. In the present study, MFC deployment is examined for the case of Scotland, an area of the UK with considerable adverse conditions regarding temperatures, which can vary seasonally from -5^{o}C to 22^{o}C, often even with significant variations within a single day (Met Office, 2016).

The majority of studies on temperature and its effect on biofilms seem to arrive at the same conclusions. Temperature affects the growth of the microbial community, thus MFCs operated at different temperatures but with the same original inoculum have different biofilm formations, and the profile of the microbial community is also different (Michie et al., 2011; Min, Román and Angelidaki, 2008; Catal et al., 2011). Results from studies by Liu, Cheng and Logan (2005) and Min, Román and Angelidaki (2008) are in accordance with this, and have demonstrated that beyond the start-up period, the power densities achieved at 30^{o}C and 32^{o}C were reduced when the operational temperature was reduced to 22^{o}C, by a factor of 9 % and 12 % respectively. Ahn and Logan (2010) conducted a temperature-phased experiment during which domestic wastewater was passed first from a mesophilic single chamber open air cathode MFC to an ambient MFC, and found that the maximum power density was achieved during the first stage of the treatment. For temperatures lower than 20^{o}C, which are realistic for field trials in many areas around the globe including Scotland, a study by Larrosa-Guerrero et al. (2010) involving the operation of an MFC using a mixture of domestic and brewery wastewater from 4^{o}C up to 35^{o}C found a decline for both COD removal (from 94 % to 58 % respectively), and power density.

Interestingly, in contrast to the research groups described above, Michie et al. (2011) found that whilst start-up time was longer when the MFC was operated at 10^{o}C than when it was operated at 20^{o}C and 35^{o}C, less biomass accumulated in the reactor after the biofilms were mature. Additionally, due to the low temperature, the level of methanogenesis was lower at 20^{o}C, whereas power outputs were highest at 10^{o}C and lowest at 35^{o}C. It could therefore be argued that lower ambient temperatures might be beneficial to the electrical performance of biofilms, especially since methanogenesis is inhibited or at least is slowed at temperatures of around 10^{o}C. This argument is also supported by Jadhav and Ghangrekar (2009), who operated an MFC at two distinct temperature ranges, 8-22^{o}C and 20-35^{o}C and found that coulombic efficiencies were higher for the first range of temperatures, leading them to argue that the suppression of methanogenesis, a competitive process, led to an increase in electrogenic activity, even though a precise microbial analysis was not conducted.

It is therefore concluded that temperature can have contradictory effects on MFCs since the technology is clearly based on bioelectrochemical principles. In bacterial systems,

the rates of reactions approximately double with every 10^{o}C rise in operational temperature (Rittmann and McCarty, 2001). However, the literature has shown that the issue is more complicated, especially in the case of mixed consortia and complex substrates such as real wastewater, and particularly when considering processes competing with electrogenesis, such as methanogenesis. Therefore, examining the effects of temperature changes, especially in ambient temperatures in field trials, is of key interest in building better understanding which will support the commercial development of MFC technology.

2.5 Microbial fuel cells for wastewater treatment

According to a UNEP report by Corcoran et al. (2010), two million tons of sewage, industrial and agriculture waste is discharged into the world's waterways every year. Whether one looks at the situation in developing countries, where an estimated 90 % of wastewater is discharged untreated directly back to the environment, or at the most densely populated central cities of the world, half of which suffer from inadequate infrastructure and lack the resources to deal with the wastewater generated, the message is clear: unless urgent action is taken, the situation will only get worse by 2050, when the global population will exceed nine billion.

Biological wastewater treatment is one of the most developed, established and efficient methods of wastewater treatment practiced around the globe, and it utilises a broad range of technologies which can in principle be categorised as aerobic or anaerobic (von Sperling, 2007). The former is the most common biological method with which to treat both municipal and industrial wastewaters, but it has an extremely intensive energy demand since it requires a continuous feed of oxygen through the wastewater for it to be used by the microbial community. Specifically, according to a report issued by the Environmental Knowledge Transfer Network (2008) activated sludge aeration, one of the most common aerobic technologies, contributes to almost up to 56 % of the energy cost in sewage systems. The water and wastewater treatment market was projected to be worth £10.30 billion by 2015 (Caffoor, 2008). Therefore, there is a clear market drive and opportunity on the one hand for current technologies to be optimised, and on the other hand for new innovative technologies to be developed that can also provide more attractive options with regard to capital and operating costs (Caffoor, 2008).

2.5.1 *Conventional wastewater treatment methods and the current situation*

In the UK, wastewater treatment requires approximately 6.34 GWh of electricity on a daily basis, which makes up almost for 1 % of the average daily electricity consumption in England and Wales (Gude, 2016). Depending on the chosen process and the composition of the wastewater, treatment requires about 0.5-2 kWh/m^3 but at the same time it contains about 3 to 10 times the energy required for its treatment which is locked within it in various forms. Part of that energy is chemical, which is the form that physical, chemical and microbial treatment utilises, in the form of carbon and nutrients, which accounts for approximately 26 % of the overall energy available, the remaining being thermal energy (Gude, Kokabian and Gadhamshetty, 2013; Gude, 2015).

Biological wastewater treatment methods are required to remove carbon and nutrients in order to minimise impacts when returning the water back to the environment. These impacts range from chronic ecosystem damage due to oxygen depletion of the receiving waters from the biodegradation of organic matter to ecosystem damage via the eutrophication of waters resulting from the excessive inputs of nutrients present in waste water, and further, to potential health risks emanating from water-borne pathogens (DEFRA, 2012). However, as mentioned earlier, conventional treatment systems, especially aerobic treatments, are very energy-intensive; specifically, for 1 kg of COD to be treated, 1.48 kWh are required, while for nitrogen the demand would be 13.44 kWh and for phosphorus the energy need would be 6.44 kWh. However, if these chemicals were recovered through the use of various other processes, the respective maximum potential energy savings could be 3.86 kWh/kg COD, 19.3 kWh/kg N and 2.11 kWh/kg P (McCarty, Bae and Kim, 2011).

Originally, the main purpose of those technologies in the field was to meet discharge limits set by EU Directives and possibly stabilise the final effluent in order for it to be further applied on land. Since compliance was the target and main drive, energy needs were given on a secondary priority. However, from the very early stages, the shortage of resources and the development of sustainability concepts indicated that there was a need for a shift of focus. It became clear that there was a need to achieve the necessary treatment quality with greater energy efficiency, or at least to achieve energy recovery at the same time. Research in the field at the time demonstrated, as mentioned earlier, that the energy potential locked in wastewaters was 3 to 10 times higher than the energy

required to treat them. For example, a study by Shizas and Bagley (2004), as quoted by Gude (2016), found that the energy content in the methane produced by an anaerobic digester operating on sludges of municipal primary and secondary wastewater treatment generated 3.5 times the energy required for the operation of the plant, and this does not even include the energy contained in agricultural and industrial wastewaters, as has been demonstrated by another recent study of Heidrich, Curtis and Dolfing (2015).

Anaerobic digestion was soon identified as a potential way to address the issue of high energy requirements, and through the years it became established as one of the most efficient energy recovery systems, of particular interest to the waste treatment sector. Anaerobic digestion involves a series of four processes leading to methane generation as its last step. Complex organic compounds such as proteins, carbohydrates and fats are converted to amino acids, fatty acids and sugars by the process of hydrolysis, which are then converted to volatile fatty acids by acidogenesis. These are then further degraded during acetogenesis to acetic acid, hydrogen and carbon dioxide. Finally, methanogenesis takes place during which methane is produced (Appels et al., 2008). Research has shown that AD with biogas utilisation can produce up to 350 kWh of electricity for each million gallons of wastewater treated in a plant, depending on the type of specific technology utilised (Gude, 2016).

2.5.2 *Wastewater substrates in microbial fuel cells*

The substrate consumed by any biological process is of vital importance since it serves as carbon, nutrient and energy source. The chemical composition and the concentrations of the substrate that can be converted in MFCs are therefore of key interest. Its influences are not only integral, and possibly determinant of the composition of the bacterial community in the anode biofilm, but it also affects the MFC performance including the power density and coulombic efficiency, as was studied at an early stage by Chae et al. (2009). In their research, the authors found that both coulombic efficiency and power outputs varied with the different composition of substrates, but increased similarly in response to the initial concentration of each substrate. Some substrates were found to be preferable for electricity generation, whereas others seemed mostly to affect the biodiversity of the biofilm, the diversity of which subsequently led to more efficient substrate utilisation. Therefore, it was concluded that different substrates affect the overall performance of an MFC in different ways.

Throughout the development of the field a variety of substrates has been used, the majority of which, at the beginning at least, were acetate and glucose, pure compounds or generally artificial substrates, because made-up substrates are well defined and their composition can be strictly controlled (Pant et al., 2010). However, the suggestion of using wastewater as a valuable substrate was then introduced in the early stages of research (Allen and Bennetto, 1993). The direct conversion of waste into electricity or high-value chemicals, which forms the basis of a bioelectrochemical system has since been recognised as a better option and possibly as an answer to energy efficiency issues by Logan (2008). Additionally, MFCs have considerable advantages over conventional systems with regard to their use in wastewater treatment. They can indeed offer additional energy savings due to anaerobic conditions and the elimination of technical aeration, considering their open air cathode design (which will be further examined) and their potential for both decentralised and centralised technology which is able to adjust to specific needs. Since an MFC is an anaerobic or anoxic biological process, its bacterial biomass production will be lower than that of an aerobic system. In its early stages, the potential of reducing odours has also been considered as an advantage given that aeration of wastewater is eliminated. With regard to the environment, MFCs can contribute to water reclamation depending on the desired quality, have a low carbon footprint, and as mentioned earlier, eliminate issues related to excess of sludge disposal. MFCs also provide economic benefits with potential revenues through electricity generation, unlike aerobic treatments which are solely targeting treatment, through the reclamation of high-value chemicals such as in the case of struvite, and have low operational costs. However, the main constraint still remains the use of expensive membranes, an issue in large scale applications but currently being researched through investigations of membrane-less MFCs. Finally, on an operational level, MFCs have been shown to be able to withstand environmental stress through the robustness of their microbial communities, and they are self-sustaining systems by conception (Rabaey and Verstraete, 2005; Scott, 2014; Pham et al., 2006).

Pant et al. (2010) published a comprehensive review of the substrates used in MFCs, including pure mediums, synthetic effluents, and real wastewaters. In the review, glucose, acetate, lignocellulosic biomass, ethanol and a variety of real wastewaters ranging from brewery and food wastewater to urban and domestic wastewaters was presented, with the main outcome being that artificial mediums were preferred,

particularly at earlier days of the research field. Additionally, they found that brewery wastewater has been a favourite context among researchers, due to its appropriate strength, and the fact that the food-derived nature of the organic matter involved and the lack of high concentrations of inhibitory substances, such as ammonia and ammonium nitrogen, which is a common issue with animal-derived waste, made it a suitable candidate for electricity generation. With the development of the field, an emerging trend is that substrates are beginning to be more complex with higher organic load. The review, however, had two more interesting outcomes. It managed to demonstrate the diversity of inocula used as the microbial catalysts, which on the one hand shows the potential of the MFC for diversification, and one the other hand shows the potential of taking different approaches to the subject rather than there being a single right path. Finally, the study pointed out an issue which only recently has begun to be addressed, which is that as a technology in its development stage, a direct comparison between studies in the prior literature is very difficult due to the use of different electrodes, substrates, inocula, etc. Also, the reporting of power outputs can be done in several ways, which was why normalised energy recovery was introduced, a concept which has been mentioned already and will be further discussed in the experimental methods (He, 2013).

Regarding real wastewaters as substrates of MFCs, Table 2-2 below, as partially adapted from Pant et al. (2010) and Scott and Hao Yu (2015), summarises the research to date according to the category of wastewater and the reactor configuration, as will be discussed in more detail below. It can be seen that over the last few years, the field of MFCs in wastewater treatment has further diversified. The food and beverage industry still plays a considerable role, since the effluents derived from that industry are rich in nutrients and carbon sources yet not contaminated with heavy metals or potentially toxic elements (Feng et al., 2008). Alcohol distillation process wastewater is similar in composition to brewery, however, there has only been one study up to 2012 on this specific effluent. Ha et al. (2012) studied the treatment of distillery wastewater with a thermophilic MFC and were able to achieve higher power outputs than the levels recorded in literature at that time, while achieving a coulombic efficiency of up to 89 %, maximum COD removal efficiency of 76±3 % and maximum sulphate removal of 60.7±1.3 %.

It is noticeable that until 2010 when the review on MFC substrates by Pant et al. (2010) was published, little research had been conducted in areas other than pure wastewater

streams. At the beginning of the field MFCs were looked at against anaerobic digestion, as a competitive technology to eventually replace the established AD (Pham et al., 2006). However, in the same year Aelterman et al. (2006) introduced the potential of using microbial fuel cells before the AD process, but must importantly, downstream. According to this study's findings, the power output of the dual MFC operating on influent of the AD of potato processing factory effluent maintained an average of 58±2 W/m^3, whereas when operating on the AD effluent, the same value was 42±8 W/m^3. This identified the suitability of AD effluent as an MFC substrate but most interestingly, the substrate removal rate in the second case was 2.99 kg of COD/m^3.day, which was 1.76 kg of COD/m^3.day higher than the removal rate of AD influent. Coulombic efficiency reached 29 %, as against 20 % achieved on the AD influent. This study introduced the early concepts underpinning the integration of MFCs and complementary potential, which will be further discussed below.

Table 2-2: *Various real wastewater substrates used in MFC studies and the respective reactor designs*

Wastewater Source	MFC reactor design
Domestic wastewater	Single/dual
Primary effluent	Dual
Dairy process wastewater	Single/dual
Brewery wastewater	Single
Distillery/alcohol wastewater	Single/Dual
Farm/agriculture/forest wastewater/waste	Single/Dual
Food waste/wastewater	Single/Dual
Hospital wastewater	Dual
Human faeces/urine	Single/dual
Landfill leachate	Single/Dual
Palm oil effluent	Dual
Paper process wastewater	Single
Protein-rich wastewater	Dual
Urban wastewater	Dual
Rhizodeposits (wetland)	Single
Sewage sludge	Tubular
Starch processing wastewater	Single
Swine wastewater	Single
Wine wastewater	Dual
AD influent/effluent	Dual

(Source: partially adapted from Pant et al., 2010 and Scott and Hao Yu, 2015)

2.5.3 *Whisky distillation process by-products*

Distilling is practiced around the world and is one of the most profitable industry sectors. For Scotland and the UK in general whisky distillation is a significant part of the food and beverage industry. In Scotland, the whisky distillation industry provides almost 10,000 jobs, and in 2015, revenues from whisky exports generated £3.95 billion for the UK balance of trade (Scotch Whisky Association, 2015). Heriot-Watt University is highly involved in the sector and research to date has been targeted towards several opportunities and applications of whisky by-products treatment. The industry in Scotland is one of the country's most vital, dominating the food and beverage exports of the UK with 115 distilleries licenced to produce Scotch whisky located within the territory (Scotch Whisky Association, 2015). The basic process has not changed for centuries, and according to legislation water, yeast, malted barley and other cereals can only be used, Scotch whisky must undergo a maturation process in oak casks for at least 3 years and finally, it has to be produced and bottled in Scotland using traditional methods, and no additives other than caramel are allowed (Piggott and Connor, 2003).

The main waste stream of the whisky distillation process consists of liquid residues. One of these, spent wash, is the residual liquid produced by the grain distillation process. A typical production rate is 8-15 litres of pot ale per litre of alcohol produced in the case of malt whisky, and 16-21 litres of spent wash in the case of grain whisky (Mallick, Akunna and Walker, 2010). The effluent generated from distillation without any treatment has a temperature of around 70^{o}C to 80^{o}C, with a brown colour, high acidity and a concentration of organic compounds and suspended solids. It is also very high in nutrients such as phosphate, nitrogen compounds, and sulphate (Mohana, Acharya and Madamwar, 2009).

Various environmental issues are posed when effluent is discharged directly to the environment, most of which are connected with direct de-oxygenation and eutrophication (excess bloom, and an increase in phytoplankton in water bodies due to increased nutrients), or that due to its caramel-dark colour it can block sunlight from water bodies, thus reducing oxygen and inhibiting photosynthesis. Therefore, it is indisputable that spent wash cannot be directly discharged, and must receive further treatment (Goodwin and Stuart, 1994; Mallick, Akunna and Walker, 2010; Mohana, Acharya and Madamwar, 2009).

2.5.4 *Anaerobic digestion and whisky distillation by-products*

Several treatment methods have been identified over the years for treating distillery derived effluents and, as described earlier, a moderate amount of research has been performed on the utilisation of MFCs for this purpose. However, other biological processes have become well established. Mohana, Acharya and Madamwar (2009) published an extensive assessment of the potential treatment technologies suitable to deal with spent wash. Physicochemical technologies have also been identified, such as oxidation, adsorption, coagulation and flocculation; however, these are all associated with the excessive use of chemicals, sludge production, and the further need for the disposal of separated by-products. As with other industrial effluents, aerobic treatments have been used; however, as well as high operational costs, there have been issues related to acidity, high oxygen demand, and sludge bulking (Mallick, Akunna and Walker, 2010). In contrast, anaerobic digestion has been identified and recognised from very early on as a technology suitable for efficient and economic treatment (Goodwin, Finlayson and Low, 2001; Goodwin and Stuart, 1994; Mohana, Acharya and Madamwar, 2009).

The typical composition of whisky distillery effluent varies greatly and depends on the process of distillation. COD, one of the key quality indicators of water and wastewater, for distillery effluent, can vary from as high as between 30,000 mg/l to 50,000 mg/l, to as low as between 1,000 mg/l to 2,000 mg/l. Due to this wide range of variance, the different anaerobic technologies, with methane fermentation and subsequent energy recovery, are suitable for the treatment of spent wash. Table 2-3 summarises and provides averages for the key quality indicators of distillery effluent, both as a raw material and after anaerobic digestion treatment. It can be seen that the values of both AD influent and effluent greatly vary. According to the table, BOD is heavily reduced by more than 83 %, and COD is considerably reduced during the process too by up to 72 %. TVS, sulphates and nitrogen have the same fate, with reductions of more than 40 %, 60 % and 40 % respectively. However, phosphate reduction is more moderate in AD, whereas the table also highlights the issue of solids which is faced by most anaerobic processes.

Table 2-3: *Characteristics of untreated and anaerobically treated distillery effluent*

Parameters (unit)	Values of distillery effluent	Values of anaerobically treated effluent
pH	3.0-4.5	7.5-8.0
BOD_5 (mg/l)	50,000-60,000	8,000-10,000
COD (mg/l)	110,000-190,000	45,000-52,000
Total Solid TS (mg/l)	110,000-190,000	70,000-75,000
Total volatile solids TVS (mg/l)	80,000-120,000	68,000-70,000
Total suspended solids tSS (mg/l)	13,000-15,000	38,000-42,000
Total dissolved solids TDS (mg/l)	90,000-150,000	30,000-32,000
Sulphate (mg/l)	7,500-9,000	3,000-5,000
Phosphate (mg/l)	2,500-2,700	1,500-1,700
Total nitrogen (mg/l)	5,000-7,000	4,000-4,200

(Source: partially adapted from Mohana, Acharya and Madamwar, 2009)

In every case, AD has been certainly recognised as an energy recovering, efficient method for distillery wastewater treatment. However, as highlighted by the table above, there is clearly a need and potential for further treatment of anaerobically digested whisky wastewater. As discussed at the beginning of the chapter, when the MFC technology was at its infancy and up to 2010, it was considered to be a competitor to AD technology. However, the discussion up to this point has demonstrated the potential of using MFC technology downstream of AD, as described in brief by Aelterman et al. (2006) instead of being viewed as a technology competitive to AD. This could also be considered a first step towards the integration of the technology within existing wastewater treatment systems, which, again, will be further discussed later in this thesis.

Additionally, MFCs have focused on the recovery of energy, however, effective COD removal is often a stronger industrial concern and drive. Particularly, in the UK context, levels of COD and suspended solids are used as key costing factors when calculating wastewater treatment costs. The Mogden formula is used for calculating costs and as can be seen below;

$$C = R + (V + B_v + V_m + M) + [B \times (O_t/O_s)] + [S \times S_t/S_s] \quad \textbf{(2-3)}$$

where R is a reception and conveyance charge (p/m^3), V is a primary treatment (volumetric) charge (p/m^3), B_v is an additional volume charge if there is biological

treatment (p/m^3), M is a treatment and disposal charge where effluent goes to sea outfall (p/m^3), *B* is a biological oxidation of settled sewage charge (p/kg), O_t is the Chemical Oxygen Demand (COD) of the effluent after one hour of quiescent settlement at pH 7, O_s is the Chemical Oxygen Demand (COD) of crude sewage after one hour of quiescent settlement, *S* is a treatment and disposal of primary sewage sludge charge (p/kg), S_t represents the Total Suspended Solids of the effluent at pH 7 (mg/l), and S_s is the amount of Total Suspended Solids of crude sewage (mg/l) (Wrap, 2016). It is therefore suggested that MFCs can work in a complementary way to existing technologies in polishing off industrial wastewaters prior to their final discharge to a commercial wastewater treatment plant, in order to achieve lower charges and guarantee compliance with local regulators.

2.6 Microbial fuel cell scale-up and pilot scale studies

Research on the topic of MFCs might be sharply increasing, especially in a laboratory setting, but the need for more practical feedback from field applications has been identified since the first large scale applications encountered difficulties (Logan, 2010). The purpose of this study, as set out above, is to investigate the potential of an industrial scale MFC in the Scottish whisky industry, thus a review of work on similar scale, along with relevant field trials and key lessons learned, will provide insight into the current status of pilot scale field trials.

Table 2-4 summarises the various studies carried out to date in which real wastewaters have been used as substrates in pilot scale MFCs. The information presented provides a holistic overview of scaling-up attempts to date, including reactor configurations, the wastewater substrates used, the chosen operation temperature, and electrical and effluent quality performance. The following table is a summary only of microbial fuel cell studies, excluding microbial electrolysis cells or any other kind of MET, due to the sense that these have very distinct functions, that have been conducted in reactors bigger that 1 L and are thus considered large scale, and finally, studies that have been operated in real wastewaters. Several other studies of similar scale have been carried out in artificial substrates, or within the large scale classification and with real wastewaters, but which were treated by hydrogen producing cells (microbial electrolysis cells) or by the recently popular constructed wetland fuel cells. These will not be examined at this point, in order to specifically define the area of interest and niche.

As can be seen in Table 2-4, the total reactor volume in scale-up field studies varies considerably from a minimum of 1 L up to 250 L, with the majority being less than 20 L. Currently, the largest reactor in terms of volume was reported by Feng et al. (2014), who constructed a 250 L horizontal flat plate MFC that operated for 130 days on municipal wastewater, however it had a very long hydraulic retention time (HRT) of 6 days. Even though a variety of designs is reported in the literature as seen in Table 2-4 (Zhou et al., 2013; Hernández-Fernández et al., 2015a), the majority of large scale field trials have focused on mostly tubular MFCs or flat-plate trays, with the majority of MFCs bigger than 20 L being stackable plug-flow flat-plate designs. As will be described in more detail later, this was the chosen design for the development of the present study. To date, different scaling-up scenarios in regards to reactor designs have been examined around the world without any study conclusively proving the superiority of one design over the others.

As was mentioned earlier, one of the interests of the current study is the temperature during the period of operation, a factor which has therefore been included in the table below. The majority of studies in Table 2-4 were conducted either at room temperature, which by definition is around 20^{o}C or higher, with 30^{o}C being a common operational temperature reported (at least ten out of the 18, with three not reporting their operational temperature). These temperatures are usually very well suited to mesophilic microorganisms, for which optimum temperatures are between 30^{o}C to 35^{o}C, as it is also the typical temperature in mesophilic anaerobic digestion (Gerardi, 2003). In relation to the studies referred to below, which are from exhaustive, very few were conducted in ambient temperatures. However, those that did demonstrated a similarly successful operational efficiency both with regard to wastewater treatment and to power output. Even though MFCs are the sole focus in this section, it should be mentioned that other fuel cells such as MECs have also shown successful results in ambient environments, but they are out of the scope of the current study (Heidrich et al., 2014). Overall, the need for further experience in ambient temperatures in field trials is highlighted in Table 2-4.

As in most cases in the field of MFCs, and was pointed out earlier in the review, direct comparisons of the electrical performance of MFCs are impossible due to the fact that power can be normalised either over surface area, of the anode or cathode (if not specified, the convention is the anode surface area), or over the volume of the reactor. For this

reason, over the last few years Normalised Energy Recovery has been used as the standard way to report energy recovery (see Chapter 3.3). In the studies discussed here, regarding volumetric normalisation, Ge and He (2016) only very recently achieved the highest power output of 1,000 mW/m^3 operating a modularised stack consisting of 96 tubular sub-reactors operating on primary effluent for almost 360 days at an HRT of 18 h and ambient temperatures. This can be regarded as a particularly successful trial as it also achieved an average of 76.8 % COD removal efficiency, therefore certainly expanding the collective knowledge on the field.

Regarding effluent quality, an up to date assessment of past studies is certainly much simpler. COD removal efficiency (which typically refers to total COD removal efficiency, unless stated otherwise) is used as the major key performance indicator. Yu et al. (2012) achieved a maximum of 95.7 % COD removal efficiency in domestic wastewater treated in a baffled reactor operating at room temperature. However, according to their findings, this removal was achieved at the lowest organic load rate and further declined as the organic load increased. Most of the research studies presented here follow this very closely regarding treatment efficiency, which clearly highlights the potential of MFCs in the wastewater treatment field.

As an overview, it can be concluded that none of the above studies claimed to have optimised performance. Additionally, different regimes have been attempted for all the parameters included above, from substrates to reactor architecture. However, only Hiegemann et al. (2016) have examined the potential of directly integrating a large scale MFC into an existing treatment process. The need for further research and field experience on flat plate MFCs is also highlighted, since they are considered a valid candidate for the further scaling-up of the technology. Therefore, the examination of a plug-flow, flat plate MFC downstream of an AD has the potential to shed more light into the field of industrial MFC applications for wastewater treatment.

Table 2-4: *Summary of volume, substrate and operational conditions for large scale reactors operating on real wastewater as reported in the literature*

Vol (L)	Substrate	Reactor design	Operational temperature (°C)	HRT[2]	Total operational period	Power density	COD[3] removal (%)	Reference
1	Domestic WW[1]	Tubular	30	N/A	N/A	4.3 mW/m^3	N/A	Cheng and Logan, 2011
1.5	Swine WW	Tubular	30	1.21 and 4.84days	N/A	11 mW/m^3	77.10	Zhuang et al., 2012b
2	Primary effluent	Tubular	Not reported	11.1h	400days	0.37±0.31 mW/m^3	<53	Zhang et al., 2013a
2.5	Manure slurry	Spiral/ tubular	Room temperature	N/A	N/A	0.03 mW/m^2	N/A	Scott et al., 2007
2.7	Landfill leachate	Tubular	Not reported	4 (4.68) days	28days	0.0018 mW/m^2	79 (31)	Gálvez et al., 2009
3	Domestic with sodium acetate	Vertical plug-flow Complete mixing MFC	25	10h	12weeks	281.74±7.71 and 239.56±10.4 mW/m^2	70±13 and 81±09	Karra et al., 2013
3.6	Sludge	Tubular	35	14days	<500days	9.6 mW/m^3	60	Ge et al., 2013
4	Primary effluent	U-shape/ tubular	-10-36	11h	450days	N/A	>90	Zhang et al., 2013b
5.7	Domestic WW	Baffled reactor	Room temperature (22±4)	12h	150days	874.1 mW/m^2	95.7	Yu et al., 2012
10	Brewery	Tubular	30	2days	180days	6 mW/m^3	86.40	Zhuang et al., 2012a
20	Primary effluent	Flat-plate	Room temperature	5-20h	15weeks	0.2 mW/m^3	60-84	Jiang et al., 2011
45	Non-thickened primary sludge	Not reported in detail	Ambient temperature	44-12h	82days	73-82 mW/m^2_{cat} (average)	67-13.5	Hiegemann et al., 2016
50	Diesel contaminated soil	Horizontal flat-plate	Room temperature	Not reported	120days	3.4±0.1 mW/m^2	89.7 (THP[4])	Lu et al., 2014
90	Brewery WW	Horizontal Flat-plate	Ambient temperature	3 and 6 days	6 months	181±21 mW/m^2	84.7	Dong et al., 2015
200	Primary effluent	Tubular modularised stack	Ambient temperature	18h	<360days	1,000 mW/m^3	76.8	Ge and He, 2016
250	Municipal WW	Horizontal Flat-plate	Not reported	6days	130days	116mW	76.3	Feng et al., 2014

[1] WW: Wastewater
[2] HRT: Hydraulic Retention Time
[3] COD: Chemical Oxygen Demand
[4] THP: Total Petroleum Hydrocarbon
N/A: Non Applicable

(Source: partially adapted from Janicek, Fan and Liu, 2014)

2.7 Integration of microbial fuel cells in wastewater treatment systems

It has been long argued that in order for MFCs to be an industrially and economically viable technology, certain issues have to be addressed to allow their further scale-up and commercialisation. Cost is certainly one of these issues, with current capital and operational costs of MFCs at prohibitive levels (Rozendal et al., 2008). When the field

was becoming established, MFCs were viewed as a technology which could be competitive with anaerobic digestion. It has, however, been estimated that a unit price of £2-£42 per 10 L of tubular reactor would be necessary in order to make the technology competitive against AD in wastewater treatment (Scott and Hao Yu, 2015).

Current practice in the wastewater treatment field demonstrates that successful processing plants do not utilise a single technology to achieve the full treatment of effluents (McCarty, Bae and Kim, 2011). For this reason, it has been suggested that the integration of MFC technology into biohydrogen and biomethane anaerobic treatment processes could lead to improved energy recovery and sustainability of both the MFCs and the processes which they are deployed with (Aelterman et al., 2006; Premier et al., 2013; Kelly and He, 2014).

On a theoretical level, Sheets et al. (2015) examined the potential of reusing anaerobically digested effluent derived from agricultural and food waste, which is currently used primarily for land application and crop nutrition. The research raised the concern that as AD has already stabilised the waste stream, there isn't much readily biodegradable COD available in an already digested effluent. Inconclusive research is cited with regard to this topic but overall, the group suggests that the specific composition of the waste could potentially allow MFCs to be used sequentially to AD; therefore, the concept of integration should be further examined. Tugtas, Cavdar and Calli (2013) examined the potential of further polishing-up anaerobically treated landfill leachate with a dual chamber MFC. The young leachate underwent anaerobic digestion and was passed through the MFC, achieving a maximum current density of 109 mW/m^2, with 90 % simultaneous total volatile fatty acids (VFAs) removal efficiency. A comparative study involving raw and digested pig slurry showed that, as expected, higher COD efficiencies were achieved when raw slurry was utilised in an MFC, due to COD influent values representing readily biodegradable COD, but ammonium reduction was greater in the AD-MFC model rather than when raw slurry was used (Cerrillo et al., 2016). Similar results were obtained by Kim et al. (2015), who examined the treatment of COD and ammonia in an MFC from digested swine waste, also highlighting the inefficiency of AD in successfully managing nitrogen rich effluents, unlike the MFC anode-cathode system that created a COD/total ammonia nitrogen ratio which was more useful for further COD reduction. Finally, a more collective integration was attempted by Hou et al. (2016), who

utilised algae in the anode of a tubular MFC to treat anaerobically digested kitchen waste, achieving the integration of a photobioreactor and MFC technology downstream of an AD. The study achieved a maximum power density of 6255 mW/m^3 although the ratio of nitrogen and phosphorus due to the algal treatment seemed to affect COD removal, leading to a low rate of COD reduction efficiency.

In this section, studies using AD as a clearly separate previous step were described, with prototypes of AD-MFC integrated technology within one reactor excluded from the discussion. Additionally, studies on AD and microbial electrolysis cells were not included in the current examination due to the focus of this study being on microbial fuel cells rather than on all microbial electrochemical technologies. All the research presented up to this point demonstrates the clear potential of utilising MFCs downstream of AD, rather than considering the former solely as a competitor of the latter. This study will examine the potential of utilising both dilute spent wash and anaerobically digested spent wash derived from the grain whisky distillation process, in order to demonstrate the beneficial use of MFCs in this traditional Scottish industrial sector.

2.8 Modelling of microbial fuel cells and losses

Modelling is a powerful tool used across different disciplines, in order to study the behaviour of processes and reactions in depth, for instance in both chemical and biological terms. Specifically, in the case of MFCs, there have been several research papers on experimental observation, but less research has been focused on developing a model that would attempt to describe and predict the performance of an MFC based on certain laws and equations that define MFC performance generally (Ortiz-Martínez et al., 2015). The advantages of modelling followed by experimental verification are that a deeper understanding can be gained of where the inefficiencies lie, and areas for potential improvement can be identified in order to further optimise the system, bringing us a step closer to scaling-up to an industrial-size system.

In order for a model to be developed, there is a need to identify the key losses occurring in an MFC. The potential measured when no current is passing through the MFC's electrical circuit (point of infinite resistance), referred to as Open Circuit Voltage (OCV), is in the order of 750–800 mV. When the circuit is connected to an external resistance, the voltage measured, referred to as Closed Circuit Voltage (CCV), decreases

significantly due to three kinds of overpotentials: activation overpotentials, ohmic losses, and concentration polarization, each of which are due to internal cell resistance and electron transfer (see Figure 2-5) (Rabaey and Verstraete, 2005).

Activation polarization relates to the energy lost due to oxidising the organic matter or reducing the electron acceptor, resulting in lower cell potential. Activation losses are observed at low currents and are increase with the growth of current, resulting in lower working potential. Increasing the electrode surface area, temperature and oxidant concentration can offer lower activation losses in the system, therefore materials offering greater reaction interface area, such as graphite granules, are preferred. Ohmic losses are considered to be the most important losses; they can be observed in MFCs due to the internal resistance of the reactor, and essentially relate to the voltage that is required to drive the electron and proton transport processes. Reducing the distance between electrodes using an exchange membrane with low resistance, and increasing the concentration of ions, would reduce the amount of ohmic losses. Finally, mass transfer losses can be observed when the flow of the reactants to the anode or the cathode is limited. These losses often appeared at high current densities and are mainly related to the architecture of the reactor; therefore, in order to be reduced, both a reactor design enabling better transport of reactants towards the anode and the cathode, and a better electrode design to facilitate collection, are necessary (Rismani-Yazdi et al., 2008; Rabaey and Verstraete, 2005).

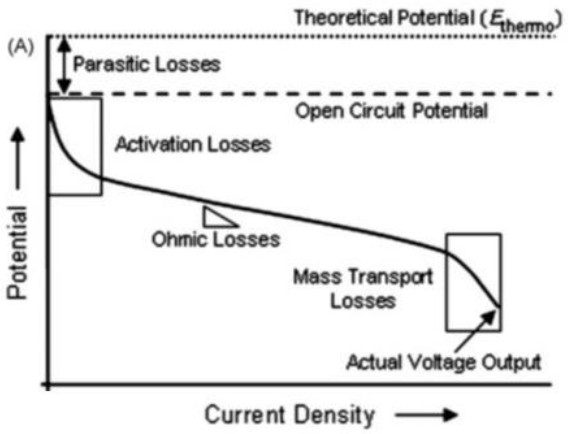

Figure 2-5: *Schematic of losses occurring in an MFC from the theoretical potential, down to OCV and working potential*
(Source: partially adapted from Rismani-Yazdi et al., 2008)

How complicated the proposed model could be depends on a variety of factors including the dimensions selected, certain assumptions made, and most importantly on the level of detail used to describe the complexity of the process taking place in an MFC. By its nature, an MFC is a cross-disciplinary subject which as a process includes mass transfer, different phases of matter, microbial growth, and the electrochemical behaviour of the overall system. In a recent review by Ortiz-Martínez et al. (2015), MFC models were divided into two major categories depending on the approach they followed: (a) global models studying the overall behaviour of MFCs, and (b) specific models describing key components, variables and processes in MFCs. The majority of the first group specialise in specific facets of the MFC process such as biochemical and biofilm study, based mostly on the Monod equation and Nernst equation, with complicated modelling processes.

In the first case, the models attempting to describe the behaviour of the overall system adopted two main directions. At first, research evolved around the anode, addressing the interactions occurring solely on the half cell. The first model attempted by Zhang and Halme (1995) was a one-dimensional model based on a dual chamber MFC operating on fermented marine sediment, with a buffer solution and an electron mediator. The model addressed mass balance and substrate oxidation in the anode, current generation in the cell, and the basic electrochemical behaviour involved in the mediated electron transfer. More complex models were later developed solely focusing on the biofilm interactions on the anode of an MFC (Marcus, Torres and Rittmann, 2007; Picioreanu et al., 2007). However, since the cathode has been identified as the limiting factor, the second direction observed for global models included the reactions occurring both in the anode and the cathode. These models were considerably more complicated yet also holistic, and thus can possibly be regarded as more realistic in describing an MFC process (Zeng et al., 2010; Oliveira et al., 2013).

With regard to the second category of specific models, a basic, simpler electrochemical model that attempts to describe the overall performance of an MFC was described in the early studies by Wen et al. (2009), chronologically the second to have attempted to describe the MFC process. The model is based on the equation describing the real voltage output of a fuel cell, as the thermodynamically predicted voltage minus the various overvoltage losses that occur in all fuel cells; chemical and microbial (Larminie and Dicks, 2003). The equation describing the principles of the electrochemical performance

of a fuel cell is used to quantify parameters that are then verified against experimental results. The group found that this model is capable of describing the performance of a 180 mL single chamber open air cathode MFC operating on beer brewery wastewater. It is the work based on this simple model that will be further adapted in the present study in order to attempt to describe the performance of the multi-electrode plug-flow MFC operating on AD liquid digestate derived from the whisky distillation process.

2.9 Chapter conclusions

This chapter, as the beginning of the present study's detailed examination of MFC technology, has presented the theoretical and technical background upon which the current study is based. It started with a review of the progression of the field in recent years, after the field was revived by Allen and Bennetto in 1993, moving on to give an overview of the work performed to date. The principal operations were described, and the basic components were examined, from the anode, cathode and membrane separator to the architectural layouts formed by those components and various designs. Materials are an integral part of this technology, so a review of the most typically used materials was necessary for each component. Additionally, the microbial aspect is obviously a central point of interest, and as such it was examined during this survey, from the mechanisms of electron transfer and inocula to the effects of temperature.

Moving on from general principles and applications, the chapter further focused on the use of microbial fuel cells for wastewater treatment through revisiting traditional treatment technologies, and latterly it summarised the various wastewater substrates with an industrial focus. At this point of the literature research, whisky distillation process by-products were introduced both at a raw level and subsequent to anaerobic treatment.

The chapter then focused on pilot scale applications of microbial fuel cells for the treatment of industrial wastewaters, thus setting out the main focus of the later experimental work: the implementation and integration of MFC technology in the whisky distillation by-products industry. The chapter finally introduced the basic theoretical background of microbial fuel cell electrochemistry and modelling.

Due to their nature and as deduced from the above literature review, microbial fuel cells are a multi-disciplinary technology combining various scientific areas, from materials to electrochemistry, biology, and process deployment. Therefore, it is strongly believed that

this literature survey has examined every basic facet of the technology as thoroughly as possible, focusing on the industrial deployment of MFCs in the wastewater treatment sector and their integration with existing treatment technologies, which is the main focus and objective of this study, as will be further developed in the following chapters.

Chapter 3- Materials, designs and general methods

3.1 Introduction

In this chapter, the different facets of the experimental design and process are presented. The materials used in the development of a microbial fuel cell will be described in detail, along with the methods of preparation of the different components of the system. A detailed design will follow, demonstrating the set-up of the physical unit. The methods used and the relevant calculations regarding the electrical performance of each electrode and of the overall unit will be described. Finally, the methods and relevant calculations used in the determination of the effluent quality will be set out.

3.2 Multi-electrode microbial fuel cell

The reactor constructed for the purposes of this study can be characterised as a plug-flow, multi-electrode bioelectrochemical reactor based on the initial description and studies by Fedorovich et al. (2009). In terms of liquid flow, the influent follows a serial serpentine circulation, while different electrical connections are attempted during the study.

With regard to electrode design, the same cathode design was used throughout the study, but for the anodic electrode, various designs were attempted, as will be further described. From an overall perspective, the reactor comprises eight anodes and eight cathodes, so regardless of the electrical connections between these, the system is considered a multi-electrode reactor.

3.2.1 *Reactor design*

Independently of the anode design used in specific experimental stages, the eight anodes and eight cathodes were placed in the cell as can be seen below in Figure 3-1. The overall horizontal reactor had an external dimension of 98 cm x 98 cm x 16 cm, and was made of polyvinyl chloride (PVC) panels which were soldered in place, with an overall volume of 122 L. The cathodes (2) were fixed in place with an extra inactive adhesive layer for leakage protection. The anodes (1) were fixed in an upright position in the reactor, standing on the bottom, held in place by their tight fit and a metal pin connected to the outer side of the cell wall, from where the electrical circuits were connected. A final electrically inactive compartment (95 cm x 6.5 cm x 13.5 cm) was used as the effluent collecting path. The aforementioned construction led to an active anodic volume of 57 L.

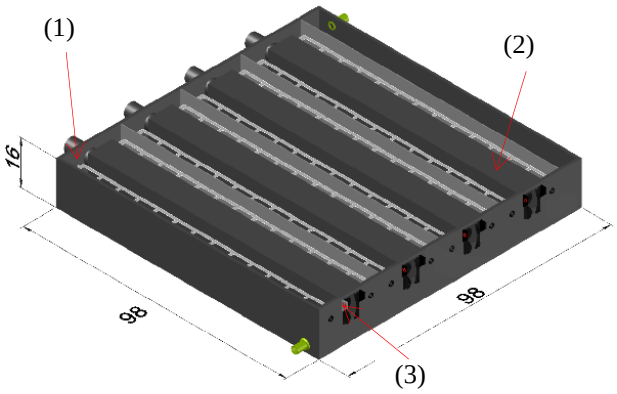

Figure 3-1: *3-Dimensional design of 122L prototype reactor (all dimensions are in cm); (1) Anodic electrode (x8), (2) Cathodic electrode (x8) and (3) cathodic area exposed to open air*[1]

The pattern in which the anodes and cathodes were physically arranged was as follows: an anode faced a cathode exposed to air, and a second cathode exposed to air faced an anode and a separator, allowing the liquid flow to pass to the next compartment, which was of identical construction. The overall reactor consisted of four of these sequences separated by PVC panels and self-adhesive sealant tape in order to prevent liquid transfer from one compartment to the other, with a square diode for internal communication.

The flow, as described in Figure 3-2 as the red-coloured sequence, it can be characterised as plug-flow with a serpentine circulation; the influent entered at the bottom, front rear, passed through the first anodic compartment to the back rear, flowed into the second towards the front and entered the next compartment from the diode on the bottom of the PVC panel separator. The liquid flowed throughout the unit in a similar way, entering the last compartment, and exiting from the top, back rear of the unit. Therefore, it can be considered that the internal liquid connection is serial.

Influent and effluent samples were collected from points (1) and (2) as shown in Figure 3-2. On both sampling points, a T-shaped connection was added in order in order to collect the influent sample precisely prior to entering the reactor.

[1] 3-Dimensional designs of the 122 L reactors were made by Ioannis Katsifarakis, an MSc student within the School of Engineering and Physical Sciences at Heriot-Watt University

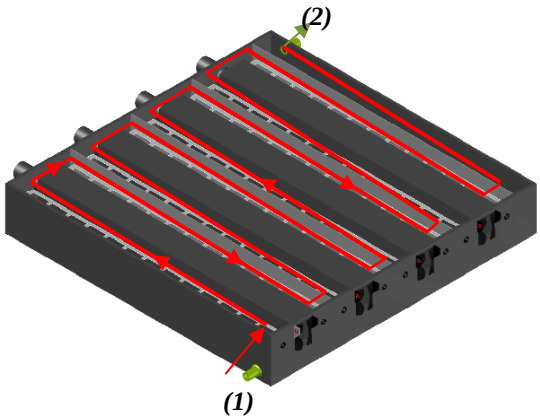

***Figure 3-2**: 3-Dimensional design of 122L prototype reactor; the red arrows indicate the serpentine liquid circulation within the reactor; (1) is the influent collection point, and (2) is the final effluent collection point*

A transparent lid made of acrylic material (100 cm x 100 cm x 1.0 cm) was bolted to the top of the reactor and additionally sealed with self-adhesive PVC foam sealant tape (35.0 mm wide, 5.0 mm thick) in order to prevent any leaking and to ensure anoxic conditions. Additional sampling ports on the back rear of the reactor for each anode were created, projected through the lid to allow for gas collection (if present) and anode potential readings.

In the later experimental part the original reactor was retro-fitted by being divided into two identical sub-reactors in order to strengthen the performance of the electrodes and, most importantly, to demonstrate reproducibility. As shown in Figure 3-3, the diode allowing the internal liquid flow in the middle part of the reactor was sealed (5) and new effluent sample ports were introduced in order to allow the collection of representative samples. In terms of the overall liquid flow, the untreated influent entered the reactor at the same point as before (1) and the treated effluent exited the left sub-reactor through an external tube, where a sampling port was introduced (2), leading to the back blank compartment. Similarly, in the right sub-reactor a new influent port was introduced (3) so the effluent exited internally (4) to the blank compartment where both streams are joined and exited the overall construction at the previous point (5). Additionally, the gas collection points were moved towards the middle of the reactor on the lid, based on the findings from the preliminary experiments.

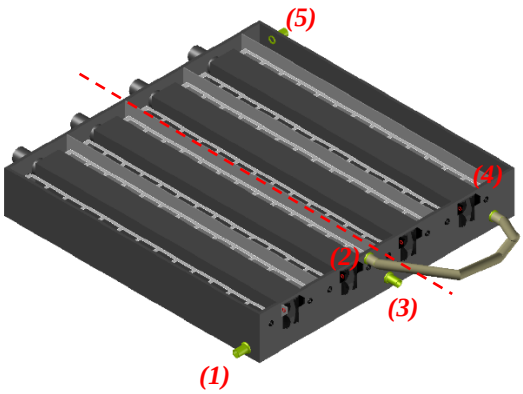

Figure 3-3: *Modified 122 L prototype reactor consisting of two identical sub-reactors isolated across the red dotted axis; (1) is the front rear sub-reactor influent point, (2) is the corresponding effluent collection point, (3) is the back rear sub-reactor influent point, (4) is the corresponding internal collection point and (5) is the final exit point*

In order to more closely examine the electrical behaviour on parallel or independent circuits, as will later be described, a reactor identical in layout and materials reactor was constructed in scale. Anodes and cathodes were placed in the reactor identically to the design set out above with the only difference being that the reactor was designed to look at only two independent, or one paired connection, thus consisting only of two anodes and two cathodes with identical placement, and a serpentine internal liquid flow connection. The external size of the reactor was 16 cm x 40 cm x 22 cm, resulting in an active reactor volume of 8 L.

3.2.2 *Anode designs*

Two experimental anodic electrode designs were attempted in the study at different stages. The specific designs and relevant positions in the reactor will be described in the respective chapters. At this point, both the designs which were used will be described. The nature of the anodic electrodes in MFCs is relatively complex as it involves both bio-catalytic and electro-catalytic processes, thus an ideal electrode has to be highly conductive in order to reduce ohmic losses, biocompatible with the microbial community to prevent microbes from poisoning, chemically stable in the bacterial culture, corrosion resistant, inexpensive, with a high specific surface area, highly porous and preferably, easily manufactured and suitable for scaling-up (Logan, 2008). For the aforementioned reasons, two complex three-dimensional structures with a combination of different materials were developed in order to gain higher power densities and ensure the long term stability of the reactor. However, in such structures, defining the surface area can be

particularly challenging; thus, the anodic volume is preferred in terms of normalising power generation (as will be examined later in the chapter).

In every case, the basic skeleton on which the electrodes are to be developed was made, in a similar manner to the outer cell, consisting of two PVC frames with dimensions of 96 cm x 9 cm fixed opposite to each other with PVC connectors at a distance of 6 cm (the dimensions and construction of which are shown in Figure 3-4). The anodic electrodes were developed across the two sides, resulting in a three-dimensional structure. The materials used were carbon fibre (Zoltek PX35, Toray Group, USA), carbon cloth (Plain Carbon Cloth untreated, Fuel Cell Store, USA), activated carbon granules (AquaSorb HS, Jacobi, UK), and in-house made conductive glue (based on graphite powder and polystyrene binder).

Design 1 (Figure 3-4 (A)) incorporated a mesh made solely of carbon fibre woven onto each side of the basic skeleton with a distance between each mesh of 6 cm. *Design 2* (Figure 3-4 (B)) which was used throughout the majority of the study, as will be described in later chapters, consisted of two pieces of carbon cloth covering the two lengths of the skeleton with the internally-facing side coated with conductive glue in order for a layer of activated carbon granules to be held in place, with a projected surface area of 0.2994 m^2. The graphite granules were impregnated with neutral red (NR) (Sigma Aldrich, UK) but only upon initial construction. The NR was dissolved to saturation, the granules were impregnated, and the excess was washed off with deionised water. This process was repeated until a red colour remained and the granules were left to dry in ambient air.

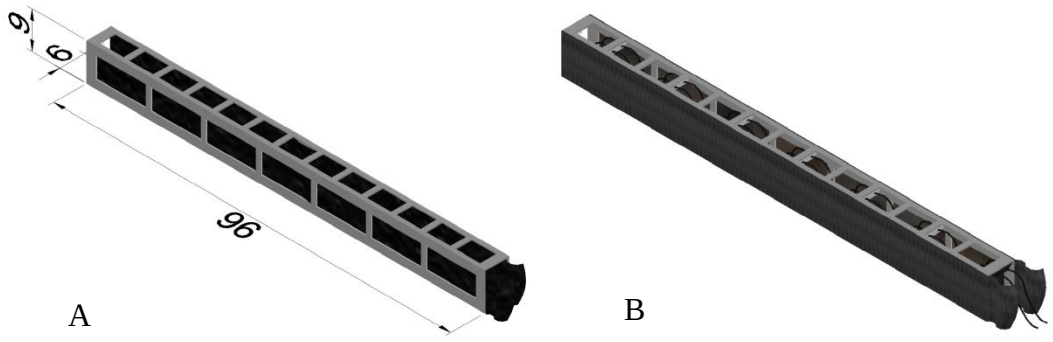

Figure 3-4: *3-Dimensional anode design**;** (A) Design 1: carbon fibre and (B) Design 2: carbon cloth coated with conductive glue and a layer of activated carbon granules*

With regard to the 14 L reactor, the anodes used were according to *Design 2* with the sole difference being in length, resulting in an anodic electrode of 35 cm x 9 cm x 6 cm.

3.2.3 *Cathode designs*

The structure of the cathode was based on the basic design patent by Fedorovich (2012). The concept supporting the construction of the cathode was to provide a cathodic electrode that would be characterised as open air, thus providing a better supply of oxygen to the cathode for oxygen reduction, while simultaneously providing the potential of an electrolyte in order to enhance the reaction.

Each cathodic electrode used in the MFC unit was of identical design and materials, and consisted of eight windows which were electrically and physically connected by a carbon cloth exiting the construction at the front rear connecting the electrode to the outer cell through a metal pin where the electrical circuit was connected. The frame was made of PVC material. Figure 3-5 is a schematic of a top section of the basic window.

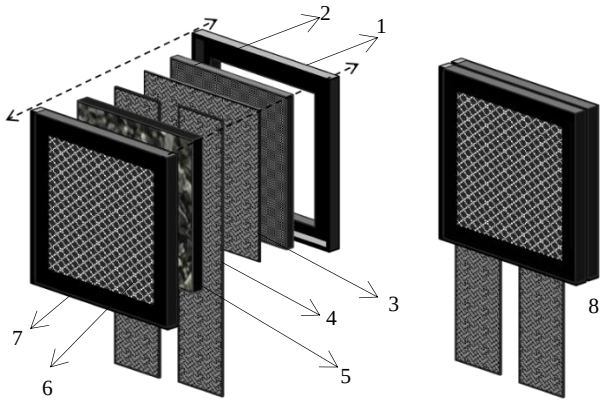

Figure 3-5*: Schematic diagram of basic cathode window; starting from the left (1) is the PVC skeleton, (2) is the graphite plate, (3) is the carbon cloth, (4) are carbon cloth strips, (5) are activated carbon granules, (6) is a plastic net, (7) is the PVC holding frame, and (8) is a basic cathode window*

Each window's size was 8 cm x 6 cm, and a graphite plate of 3 mm thickness (Xinghe County Muzi Carbon Co. Ltd, China) was fixed onto the PVC panel with epoxy resin, the sizing and construction of which can be seen in Figure 3-6. The construction of each individual window can be seen in Figure 3-5. The side facing the anodic compartment was coated (using a spray gun) with approximately 10 ml of liquid PFSA, 5 % wt in aqueous solution (FumaTech, Fumion FLA-1005) and allowed to air-dry at an ambient temperature for 24 hours (2). A layer of carbon cloth connecting the eight windows lay

directly in contact with the plate, in parallel to the working surface area, exiting the construction on the front rear in order to be used as the electrical contact area connected through a pin to the outer part of the MFC cell (as mentioned earlier) (3). Two additional strips of carbon cloth (6.0 cm x 22 cm) (4) were placed in direct contact, extending from the top of the window through the frame downwards in order to tap in an electrolyte solution (if it existed). Activated carbon granules (from the same supplier as the granules used in the anodic electrode) impregnated with iron (II) phtalocyanin as a catalyst were added at 50 ml per window (5). All the aforementioned components were pressed together with a rigid net aperture (6) and fixed in place on a PVC frame (7).

For the preparation of the activated carbon granules as previously described by Fedorovich et al. (2009), a 5 % solution of iron (II) phtalocyanin in N-methylpyrrolidone was deposited on the granules. The solvent was then removed by heating in a furnace at 300^{o}C in an atmosphere of nitrogen.

Two of the overall cathode electrodes were fixed together in place at a 4 cm distance, facing each other in order for air to freely circulate through them. Figure 3-6 shows the two cathode block placed in the MFC cell with external dimensions of 92.5 cm x 6 cm x 13 cm.

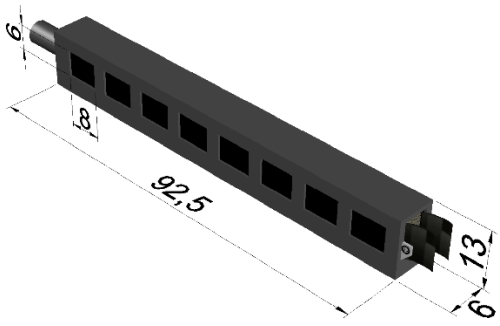

Figure 3-6: *3-Dimensional design of two-cathode block as positioned in the reactor*

With regard to the 14 L reactor, an identical, two cathode block was deployed with the only difference, similar to the length of the anode, being the length of the cathode resulting to a cathodic electrode block with dimensions of 35.5 cm x 6 cm x 13 cm.

3.2.4 *External electrical circuit design*

In order for the electricity to be observed and harvested, an external circuit had to be put in place to connect the two electrodes; the negatively charged anode, and the positively charged cathode, to an external resistor. As was mentioned earlier, the electrodes were projected to the outer cell through a metal pin on which the electrical circuit was attached. As can be seen in both Figure 3-7 (A) and (B), (1) corresponds to the anode and (2) to the cathode, while the circuit consisted of copper wire, a switch (RS Components, UK) allowing the circuit to be controlled and operated in open or in closed mode, and finally either a variable resistor (1 Ω-1 kΩ) or a standard value resistor (RS Components, UK).

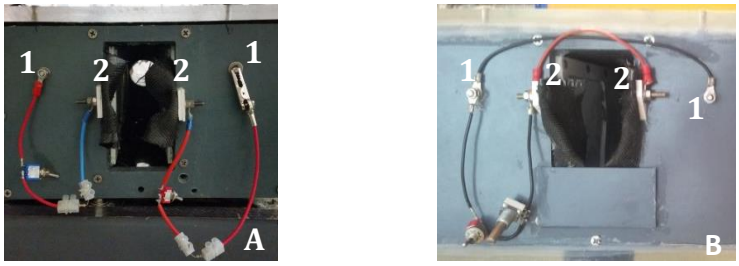

Figure 3-7: *Electrical connections; (1) denotes to an anode and (2) to a cathode; while (A)shows the independent connection (x8 electrode pairs) and (B) shows the parallel connection (x4 coupled electrode pairs)*

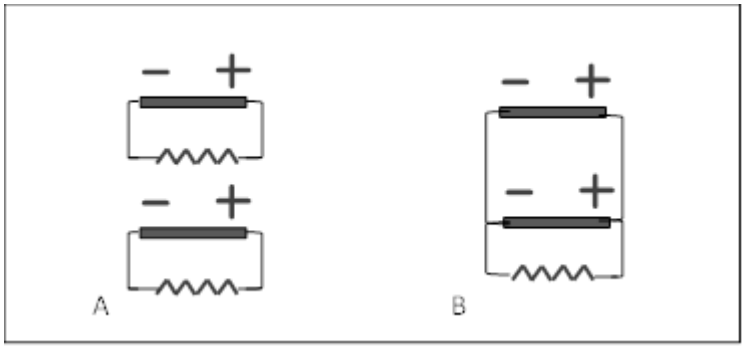

Figure 3-8*: Schematic diagram of equivalent electrical circuits; (A) independent electrode circuits (x8 electrode pairs) and (B) in parallel connected circuits (x4 electrode pairs)*

Throughout the study, two different electrical connections were applied. The first, a plain configuration, consisted of connecting one anode to one cathode with an external circuit and therefore, eight independent pairs of electrodes operated in the multi-electrode reactor (Figure 3-7 (A) and Figure 3-8 (A)) and are named here as R_1, R_2, R_3, R_4, R_5, R_6, R_7 and R_8 starting from the influent point and then moving to the effluent exit point. However, after acclimatisation and during the majority of the study, every two neighbouring anode and cathode electrodes as shown in Figure 3-7 (A) and Figure 3-7 (B) were connected in

parallel: a copper wire connected two anodes to one another (Figure 3-7 (B), (1) and (1) connected with black wire) and similarly, two facing cathodes were connected to one another (Figure 3-7 (B), (2) and (2) connected with red wire). The newly-coupled electrodes were then connected to an external circuit (Figure 3-7 (B) the circuit is completed with a switch and a resistor connected with black wire), resulting in four coupled electrode pairs, yet independent to one another per reactor, meaning that the previously named R_1 and R_2 were jointly in a parallel connection which from then onwards was called R_1 and similarly, R_3 and R_4 resulted in R_2, R_5 and R_6 resulted in R_3, and R_7 and R_8 resulted in R_4.

With regard to the 14 L reactor, the same concept was used resulting in the circuit connections described in Figure 3-8 (A) and (B). The circuit was connected in parallel during inoculation and start-up, and was operated like that for a certain period, while an independent connection was evaluated after the parallel operation has been established.

3.2.5 *Inoculation procedures*

In laboratory tests, the transfer of adapted inoculum from an operating MFC to another MFC has proved efficient and successful in relation to the start-up of new reactors (Logan, 2008; Pant et al., 2010). However, an inoculum sufficient enough for a 57 L active volume reactor was not available, so anaerobic granular biomass was harvested from the anaerobic digester operated in the North British Distillery Company, Edinburgh, UK (55°56' N, 3°14' W) as part of its wastewater treatment process. According to various prior studies, mixed cultures used as inocula in MFC studies have demonstrated more efficient effluent treatment than pure cultures, since the latter have been proven to be more sensitive to changes in the wastewater influent (Logan et al., 2006). Therefore, for the purposes of this study, the aforementioned anaerobic granular sludge was harvested. Originally, 60 L of biomass were harvested and after being allowed to settle over 24 hours, the supernatant was removed and the remaining biomass was inoculated to the reactor.

Throughout this study, maintenance of the reactors was carried out and as will be described in more detail later on, the reactors were re-deployed at the North British Distillery. During maintenance intervals, the adapted MFC biomass was harvested back

from the reactors, re-inoculated, and occasionally enriched with new anaerobic granular biomass from the same digester operating in the wastewater treatment facility.

3.2.6 *Experimental set-up*

Following the construction phase, the bioreactor was inoculated, and operation commenced. Figure 3-9 presents the core of operation of the MFC reactor used throughout the study as the main process.

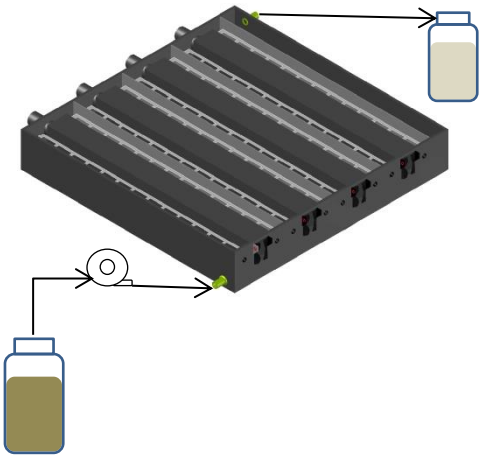

Figure 3-9: *Schematic diagram of the 122 L reactor experimental set-up*

Influent was collected either manually or through direct piping to an influent tank where additional conditioning could be delivered and subsequently pumped into the reactor for treatment with a peristaltic pump (Masterflex HV-07528-10, Cole-Parmer, UK), connected with silicon tubing of various sizes (Masterflex L/S, Fisher Scientific). The effluent exiting the reactor was collected in a second tank and appropriately discharged. Hydraulic retention time (HRT) (hours) expressing the time an effluent is held within the reactor is calculated as the active volume in which case is the anodic volume V_{an} (m^3) divided by the influent flow rate Q (m^3/h):

$$HRT = {V_{an}}/{Q} \quad (3\text{-}1)$$

3.3 Electrical methods and analytical procedures

The MFC reactor is a multi-electrode system; therefore, in terms of performance every electrode pair can be considered independently, but the reactor will also be examined as a whole. Throughout the study, the electrical circuit was operated on two different electrical modes. The first electrical mode applied was a two-day transition cycle from open circuit (no resistance applied to the electrode pair) to closed circuit (resistance applied to the electrode pair) with a 24-hour interval to allow for the performance of each electrode pair to reach a pseudo-steady state (Logan, 2008). During this period of operation, the voltage across the resistor was recorded for each independent electrode pair, either on the eight independent electrodes mode or the four coupled electrodes mode, using a multimeter (UNI-T, UT30B, Maplin, UK) at a 24-hour intervals. During the second electrical mode, the circuit connections used were the parallel ones, resulting in four pairs, and each and every circuit was continuously operated under a load, with no interruption of no load, while voltage was recorded on a data acquisition system (Midilogger GL820, Graphtech Corporation, Japan) at 1-hour intervals. For every case (Logan, 2008), current *I* (A-Amps) was calculated via Ohm's Law as:

$$I = {}^{V}/_{R_{ext}} \qquad (3\text{-}2)$$

Where *V* is the measured voltage across the resistor (V-Volts), and R_{ext} is the external resistance (Ω-Ohms).

The electrochemical performance of the MFC was examined through various values, the most elemental expression of which is the amount of power produced, which can be expressed as:

$$P = I\,V \qquad (3\text{-}3)$$

Where *P* is the power produced (W-Watts), *I* is the current calculated (A-Amps) and *V* is the voltage (V-Volts) measured across the resistor. Power can therefore be alternatively expressed as:

$$P = {}^{V^2}/_{R_{ext}} \qquad (3\text{-}4)$$

Knowing how much power is generated across an electrode is a first step in evaluating performance; however, it is not sufficient on its own. Thus, it is common practice to normalise power over the anodic electrode surface area, A_{an} (m^2). Power density P_d (W/m^2), allows for different systems to be comparable.

$$P_d = {}^{P}/_{A_{an}} \quad \textbf{(3-5)}$$

Estimating the surface area can be a complicated process; therefore, power density P_d (W/m^3) can alternatively be derived by normalising power to the anodic volume V_{an} (m^3), a practise also preferred in environmental engineering.

$$P_d = {}^{P}/_{V_{an}} \quad \textbf{(3-6)}$$

In a similar way to power, current can be normalised to the electrode surface area and volume.

$$I_d = {}^{I}/_{A_{an}} \quad \textbf{(3-7)}$$

$$I_d = {}^{I}/_{V_{an}} \quad \textbf{(3-8)}$$

Where, I_d is current density (A/m^2) in equation 3-7 and (A/m^3) in equation 3-8.

The three fundamental parameters, voltage, resistance and current, are measured and calculated for each independent electrode pair for the multi-electrode MFC. However, in relation to normalising power over anodic volume, the system will be examined as an overall entity (see Appendix A).

Polarisation curves are an additional tool typically used in electrochemistry to evaluate the performance of an electrode under different loads, and can therefore, also provide information on the maximum performance of an electrode. Such tests were conducted manually with the constant resistance discharge method on each electrode, as described in a previous study by (Logan et al., 2006). In order to obtain the polarization data, each electrode pair was initially kept in an open circuit mode (with an absence of external load) and was allowed to acclimate. After the voltage was observed to reach its maximum value and maintained in a pseudo-steady state without major deviations, the external

resistors were connected to each independent circuit allowing for a 20min interval to reach a pseudo-steady state condition, where the voltage across the resistors remained constant. A total number of 20 resistors were used for all electrodes, varying from 4.7 kΩ to 12 Ω. In some cases, when the curve lacked accuracy or a particular phenomenon was not observed, more resistors were used.

Current and power plots and polarisation curves are tools used to present the performance of an anode and cathode pair, but they cannot provide information on the respective contributions of the anode and the cathode to that performance. For this reason, and in order to determine the performance of two different anodic electrode constructions under various current loads, anode potential was measured against an Ag/AgCl reference electrode (Radiometer Analytical XR300 Reference Electrode, HACH, USA).

Coulombic efficiency (*CE*) is also used as a value to describe the performance of an MFC, as it can express the amount of substrate that is converted into electricity and is estimated from the ratio of the output charge by a microbial fuel cell or other battery to the input of charge and is obtained in percentage form. It can also be described as:

$$\boldsymbol{CE = \frac{C_T}{C_{Th}} \times 100\%} \qquad \textbf{(3-9)}$$

where *CT* is estimated by integrating the calculated current over a period of a complete cycle (t), expressed as:

$$\boldsymbol{C_T = \int_0^t I dt} \qquad \textbf{(3-10)}$$

Thus, C_{Th} is estimated in relation to the COD removed, and is expressed as:

$$\boldsymbol{C_{Th} = \frac{FbV_{an}\Delta COD}{M}} \qquad \textbf{(3-11)}$$

Where *F* is Faraday's constant, *b* represents the amount of electrons exchanged per mole of electron acceptor, V_{an} is the volumetric capacity of the anodic compartment, ΔCOD is the concentration change of COD, and *M* is the molecular weight of the electron acceptor (Logan et al., 2006; Logan, 2008). However, Equation 3-11 is only applicable to fed-batch systems, so because the system developed in the current study operates on a continuous flow, the volumetric flowrate, *Q*, must be considered. This can be done by

replacing the concentration change, ΔCOD, in Equation 3-12 with the COD consumption rate, $COD_{consumed}$.

$$\boldsymbol{COD_{consumed} = Q \cdot \left(COD_{Influent} - COD_{Effluent}\right) = Q \cdot \Delta COD} \quad \textbf{(3-12)}$$

Therefore, the Coulombic Efficiency (*CE*) for continuous flow systems can be expressed as:

$$\boldsymbol{CE = \frac{MI}{FbCOD_{consumed}}} \quad \textbf{(3-13)}$$

Where *I* represents the steady state current (A). For the calculation of coulombic efficiency in the case of a multi-electrode, an assumption is made. The COD consumption per electrode is necessary; however, the COD was measured in all cases at the end of the reactor, thus the consumption value corresponds to the four coupled pairs of electrodes. The assumption made is that reduction is equally distributed within the reactor; therefore, in the previously mentioned case, the consumption considered for the calculation of the one electrode pair coulombic efficiency is one quarter of the overall reactor consumption. The relevant prior research suggests that the distribution of consumption within a multi-electrode reactor is not uniform, so for a more accurate calculation of coulombic efficiency per electrode pair, the COD should be measured for each compartment (Fedorovich et al., 2009). However, doing so would create considerable cost, so for the purposes of the present study the equal distribution assumption was used.

An important argument can be made at this point that neither power nor coulombic efficiency are an energy parameter. Energy is expressed in the form of the kilowatt hour (kWh), which can be calculated by introducing time into a fed-batch system, whereas for a system operating continuously, volumetric flow rate should be taken into consideration, so energy density in kWh/m^3 can therefore be expressed as the energy per volume of wastewater treated (He, 2013; Xiao et al., 2014b). By estimating this parameter we will be a step closer to understanding the actual performance of an MFC, as it will allow for an initial energy balance to be reached. However, this approach incorporates two basic assumptions; firstly, that electrical power is the only energy produced in an MFC, and secondly, in terms of the balance, it is assumed that all the energy which is generated can be transferred at 100 % efficiency to the powering system (a pump in most cases). Therefore, in cases where other energy forms are produced, such as methane (especially

in cases where anaerobic microorganisms are used as inoculum), the energy recovery occurring through them should be estimated. Also, the conversion efficiency of the electricity generated, when potentially channelled to a pump, should be considered. In all cases, for the purposes of this study energy recovery is estimated and an energy balance attempted by taking into account the only source of electricity demand, the peristaltic pump used to pump the influent in the MFC, and the energy recovered through the electricity generation. Therefore, according to Xiao et al., (2014b) and Ge et al. (2014), normalised energy recovery (NER) can be expressed in kilowatt hours per cubic meter, based on the volume treated or the power divided by the influent flow rate:

$$\boldsymbol{NER = power \times time\ t / [wastewater\ volume\ (treated\ within\ time\ t)] = (power)/(wastewater\ flow\ rate)} \quad \textbf{(3-14)}$$

Similarly, in a reactor power density calculation, the value of power used for the calculation of the NER is the sum of the independent electrode power normalised over the reactor's active volume.

In order to establish an energy balance for the system, its energy consumption and production need to be evaluated. As was mentioned above, assuming that electricity is the only form of energy generated, the generated energy can be calculated through NER, and expressed in kilowatt hours. In the system developed for the current study, the main energy consumption was accounted for by the pumping system feeding the reactor with wastewater, thus its calculation should be included in balancing the MFC performance. Equation 3-15 estimates the electrical consumption of the peristaltic pump used in this study:

$$\boldsymbol{P_{pumping} = \frac{Q \times \gamma \times E}{1000}} \quad \textbf{(3-15)}$$

Where P is the power requirement (kW), Q is the flow rate (m^3/s), γ is 9800N/m^3, and E is the hydraulic pressure head (m). By dividing the value by the flow rate (in m^3/h), the pump's energy consumption (kWh/m^3) can be calculated (Dong et al., 2015).

3.4 Methods and calculations for determination of effluent quality

The influent and effluent samples collected through the sampling points mentioned earlier were used in the evaluation of the wastewater treatment provided by the MFC reactor,

and were analysed as soon as possible or otherwise stored according to standard methods (APHA, 1998). Influent and effluent quality was determined through a variety of parameters, with those used throughout the study being total Chemical Oxygen Demand (*tCOD*), total Suspended Solids (*tSS*), and pH. tCOD was measured with a spectrophotometer (DR2800, HACH Company, UK) and according to the manufacturer's method (method 8000, HACH Company, UK). tSS were filtered with 1.2μm pore size filter (Whatman Glass Microfibre Filters, GF/C 7.0cm, previously treated) and heated at 110^{o}C for 1 hour (APHA, 1998). Meanwhile, pH values were established using a multi-probe (HI 9812-5, HANNA Instruments, RS Components, UK) (APHA, 1998).

Conductivity (*EC*) was measured using a method similar to that employed for pH (HI 9812-5, HANNA Instruments, RS Components, UK). Nitrogen as nitrates (NO_3^--*N*), phosphates (PO_4^{3-}), and sulphates (SO_4^{2-}) were estimated (when mentioned) colorimetrically with a spectrophotometer (DR4000U, HACH Company, UK) according to the manufacturer's methods (method 8039, method 8048, and method 8051 respectively). Temperature was recorded manually throughout the study with a thermometer (Mini-Digital Thermometer, Maplin, UK).

In addition to the absolute values of the aforementioned parameters, the removal efficiency is defined for both *tCOD* and *tSS* as follows, in order to describe the efficiency of the reactor:

$$E_{tCOD} = \frac{COD_{in} - COD_{out}}{COD_{in}} \times 100\% \quad \textit{(3-16)}$$

$$E_{tSS} = \frac{SS_{in} - SS_{out}}{SS_{in}} \times 100\% \quad \textit{(3-17)}$$

Removal efficiencies for nitrates, phosphates and sulphates were similarly calculated.

3.5 Chapter conclusions

This chapter has described the design of the prototype 122 L reactor, which is characterised as a plug-flow, multi-electrode MFC, with an internal serpentine circulation. The materials and construction of two different anodes were presented in detail, outlining their composition from granular graphite, carbon cloth, conductive glue and carbon fibre, with the second design being the one used in the majority of the study, unless stated otherwise. The construction of the cathode and a detailed schematic was described, as had been set out by Fedorovich (2012). The chapter went on to explain the

electrical circuits, both independent and connected in parallel, which form an integral part of the examination that follows in the next chapter, for the purposes of which a 14 L scaled-down reactor was deployed, also described in this chapter.

In addition to the designs of the prototype reactors, the inoculation protocol was described which, as will be seen in the following chapters, was used throughout this study. The basic experimental set-up as used throughout this study (unless stated otherwise) was also described.

The chapter concluded with a description of the electrical performance indicators as established in the field of microbial fuel cells. It also provided the wastewater quality parameters, set according to international standards. Overall, the chapter aimed to establish the general designs and methods used throughout the study, with other specific methods to be described in each following chapter when necessary.

Chapter 4- Independent or parallel?

4.1 Introduction

The main examination body of this study conceptually begins with this chapter. The prototype MFC reactor studied throughout this project was a plug-flow, multi-electrode configuration, and an initial approach to better understanding its optimum operational parameters was therefore to examine whether an independent or a parallel electrical connection in the otherwise internally hydraulically connected in series reactor, was more beneficial in relation to various key performance parameters. For these purposes, in this chapter, a scaled-down 14 L reactor identical to the prototype was examined. The effect of the independent operation of the two electrodes against a parallel connection was examined in this chapter, with power output used as the main comparative electrical parameter. The tCOD and tSS removal efficiencies were also examined throughout the various phases in order to establish an effective wastewater treatment.

4.2 Materials and experimental set-up

The 14 L reactor with an active volume of 8 L was set up according to the same principles by which the 122L reactors were deployed, as a plug-flow multi-electrode reactor, as previously described. It consisted of two anodes and two cathodes which were constructed according to the standard design (Figure 3-4 (B) and Figure 3-6 respectively) and materials. The reactor design and internal flow followed the path of circulation described in Figure 3-2, so the only difference in the reactor was the length of the anode and cathode and the overall reactor cell (as described in Chapter 3.2.1). In terms of electrical performance, equivalent circuit connection, polarisation methods and constant resistance discharge were used.

Anaerobic granular biomass was harvested from the AD reactors operating at the North British Distillery, and was used as inoculum. The influent used in this study was anaerobic digestion liquid digestate (ADLD) from the same reactors, and was fed continuously into the reactor by a peristaltic pump. The influent feeding rate was set at 5.5 ml/min, resulting in an HRT of approximately 1 day, in order to simulate the operational conditions to be achieved from the large-scale reactors. For the same purpose, no electrolyte was used meaning that the reactor was operated solely as an open air cathode.

The reactor was operated at open circuit for the start-up period of almost 24 days. Following that period, a polarisation test was conducted to evaluate the performance of the reactor. The coupled electrodes were then switched to closed circuit and were operated at constant discharge mode at a fixed R_{ext} of 1000 Ω for a short period, and were then switched to maximum power point resistance according to the results of the polarisation test. Since the objective of this study was to evaluate whether a parallel or an independent connection for two hydraulically connected electrodes is preferable, the electrical parameters under consideration were the current and the power output.

Voltage output was monitored using a data acquisition system with a sampling interval of five minutes. In terms of effluent quality, the tCOD, pH and tSS were monitored on a daily basis (with triplicate samples). Influent samples were collected throughout the study, however one effluent sample was collected from the exiting point of the reactor for both operational modes, thus no information on specific electrode performance on the multi-electrode mode is available, but quality is instead regarded in terms of the overall reactor.

4.3 Results

4.3.1 *Start-up and acclimatisation*

Prior research has shown that uniform biofilms facilitate both the process of electrogenesis and the transfer of electrons from biofilms to electrodes (Mardanpour et al., 2012; Wen et al., 2009). Higher levels of external resistances contribute to the formation of a uniform biofilm in anodic compartments, thus it was decided to operate the reactor in open circuit which (which is infinite resistance), for the start-up process.

Voltage was produced upon inoculation, with a gradual increase up to a maximum point of 0.537 V which was maintained only for a short period of time. This voltage increase is related to increased electrogenic microbial behaviour due to its resemblance to a slower growth curve. The OCV stabilised for the latter part at a slightly lower level of 0.499±0.012 V. The slight decrease and eventual stabilisation lead to the notion that the reactor had reached its maximum potential, with the start-up period lasting for a little more than 23 days. According to the similar start-up and adaptation methods of otherwise laboratory scale MFCs operating in similar effluents (Wen et al., 2009), the current time is longer than has usually been observed. However, as can be seen in Figure 4-1, that

period could have been shortened by a few days since a steady performance was observed well before the 23rd day. Thereafter, a polarisation test was conducted following the connection of external resistance of 1000 Ω to the coupled circuit, in order both to examine ideal performance, and to establish a steady performance at a constant discharge (closed circuit) operation.

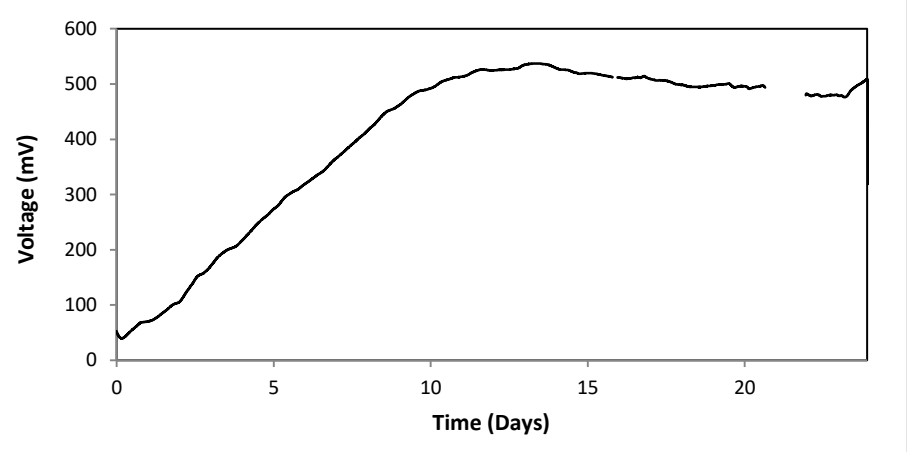

Figure 4-1:*Open circuit voltage during start-up of the 14L prototype reactor*

4.3.2 *Performance profiles of parallel circuit*

The polarisation test was performed according to the method described in the previous chapter by varying the external resistance from 5600 Ω down to 12 Ω, allowing for a 'pseudo-steady' voltage output at each resistance. The plot of voltage over current revealed two of the three regions of losses. An initial activation loss connected to reaction kinetics was observed, leading to a relatively faster voltage loss, followed by the linear ohmic loss stage where ionic and electronic resistance was dominant. The third stage of concentration losses was not obvious through this test, although it could be argued that it could possibly be observed at the last point of the curve. The curve of power over current also revealed the maximum power point of 1.053 mW, which occurred at R_{ext} of 15 Ω.

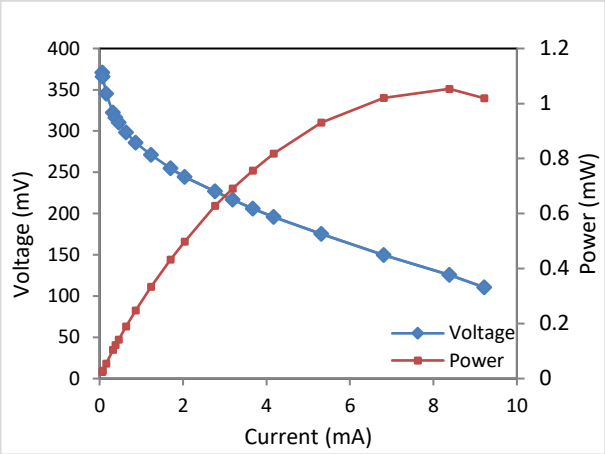

Figure 4-2: *Polarisation curve for 14 L prototype reactor*

The coupled electrode pair was subsequently operated at R_{ext}=1000 Ω for ten days at first, and then at the maximum power point at R_{ext}=15 Ω, and Figure 4-3 and 4-4 depict current and power performance respectively. The maximum levels reached were 9.127 mA and 1.249 mW respectively after a short sharp increase, while performance throughout a little over 26 days was steady at an average of 6.965±0.554 mA and 0.732±0.118 mW. A slightly increasing trend during the last three days could be observed, which was possibly due to the adaptation and the increase of performance of the microbial community to the latest R_{ext} imposed on the electrode. However, further investigation would be necessary to confirm that, which lies beyond the scope of this experiment. Even though there has been variation over time, it can be argued that the power output during this stage is also steady, with relatively little variance.

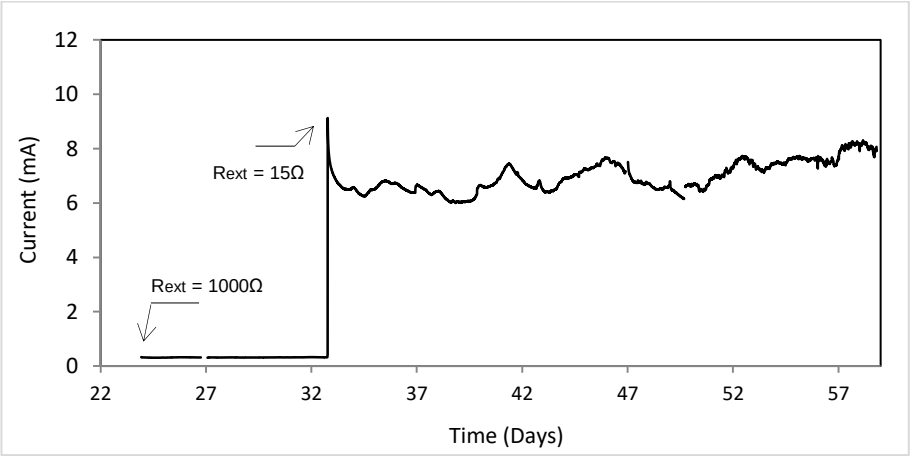

Figure 4-3: *Current generation under various external resistances on parallel electrical connection*

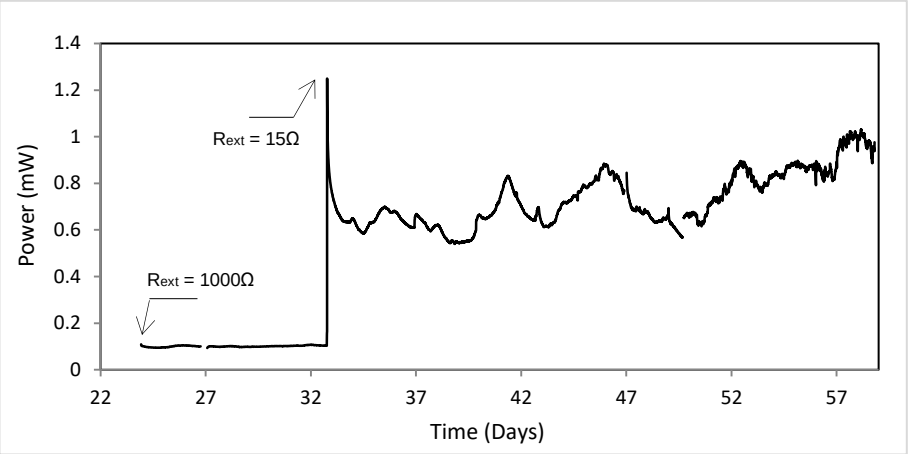

Figure 4-4: *Power generation under various external resistances on parallel electrical connection*

By comparing either current or power output in the long-term performance profile to the polarisation test, it can be observed that both parameters were slightly lower during long term recording. This supports the notion that in order to achieve an in depth understanding of the realistic application of MFCs over the long term in an industrial environment, polarisation curves provide a very useful insight into optimum performance, but monitoring electrical performance over time is also essential. This is because constant discharge can show the long term performance revealing effects which will not be apparent form the relatively instant measurement represented by polarisation tests, such as biofouling and material degradation.

4.3.3 *Performance profiles of independent circuits*

Following operation on a continuous, parallel mode, the reactor electrodes were split into independent circuits as described in Figure 3-7 (A), with each anode-cathode pair connected to a distinct external resistance, thus transforming the reactor into a multi-electrode reactor with the anodic chambers hydraulically connected internally. Polarisation tests revealed a maximum power point of 0.473 mW for $R_{(10)1}$ at R_{ext}=33 Ω and 0.288 mW for $R_{(10)2}$ at R_{ext}=68 Ω. Since the maximum power point is the point at which the external resistance matches the internal, both independent electrodes demonstrated a higher R_{int} compared to the electrode connected in parallel, which is reasonable considering the obvious reduction of electrode surface area. In terms of the voltage over current curve, a clear activation area is obvious, followed by ohmic losses represented by the linear part of the curve. In $R_{(10)2}$ there is no obvious area of concentration losses whereas in $R_{(10)1}$, this area seems to be defined by the last two points. The open circuit voltage reached 0.5 V for $R_{(10)1}$, followed by a slightly lower level of

0.468 V for $R_{(10)2}$. The reactor was then operated at constant discharge mode at R_{ext}=15 Ω for both circuits.

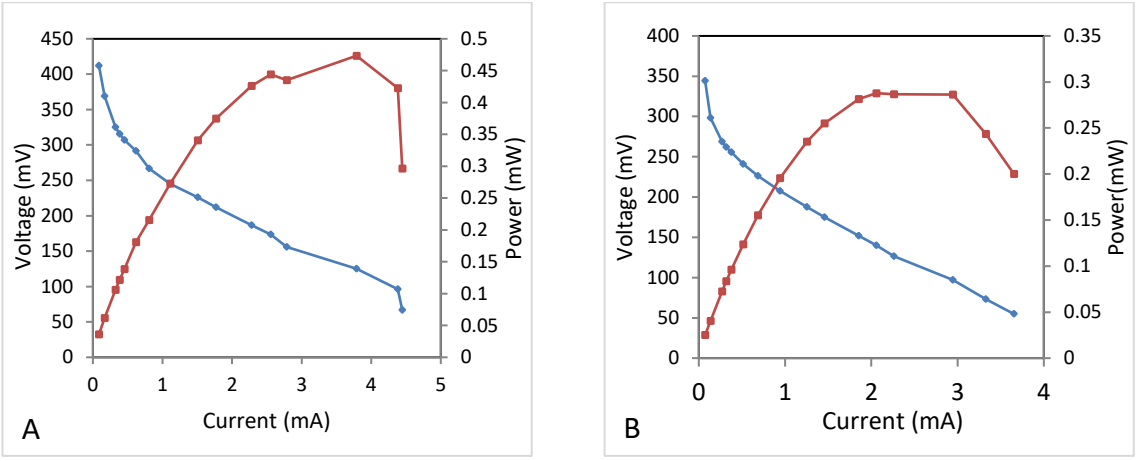

Figure 4-5: *Polarisation curves for independent electrode connections of 14 L for (A) electrode $R_{(10)1}$ and (B)electrode $R_{(10)2}$*

Figure 4-6 shows the performance of the independent electrodes, which was found to be steady over the nine-days period of examination. A relatively declining behaviour can be observed for the first electrode, as average current and power generation were 4.555±0.528 mA and 0.315±0.082 mW respectively. The corresponding performance for the second electrode in the flow direction was 3.041±0.311 mA and 0.140±0.047 mW. Therefore, it can be deduced that performance reduced to more than half in power output, as the flow forwarded, which can be explained by the decreasing feeding source for the microbial community as the flow progressed from the influent to the exiting point.

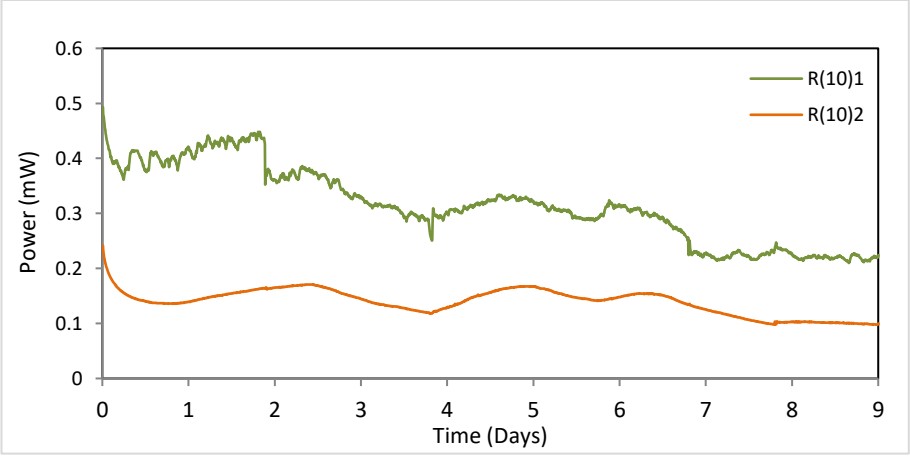

Figure 4-6: *Power generation of independent electrode connections $R_{(10)1}$ and $R_{(10)2}$*

With regard to 'long term' realistic performance compared to the results obtained from the polarisation curves, discharge over the nine days was slightly higher than that expected from the latter. However, it should be borne in mind that the resistance used was 15 Ω, which does not correspond at the maximum power point resistance. Therefore, in terms of comparing the performance of the two modes, multiple methods should be considered.

4.3.4 *Comparison of independent and parallel performance profiles*

External resistance which is clearly significantly affecting the performance of an MFC should be very carefully chosen in order to make a valid comparison between performance in parallel and independent modes. Therefore, the primary comparison between the two different modes should as a first stage be done through the polarisation curves, which provide information on maximum power output. Figure 4-7 (A) provides a direct comparison between the two distinct modes in regards to power output, which for the two independent circuits added was 0.761 mW, while the parallel connection reached 1.053 mW, 27.2 % higher for the latter.

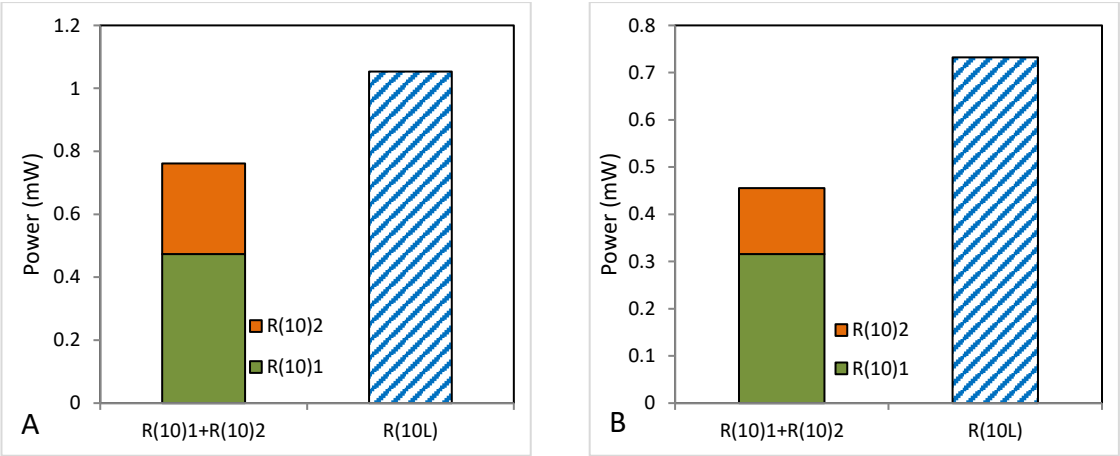

Figure 4-7: *Comparison of power generation between the independent and the parallel electrode connection according to (A) the maximum values obtained by polarisation curves and (B) the average operational values*

In order to gain a complete view of performance, Figure 4-7 (B) also provides a comparison between the two distinct modes in terms of their average long term power outputs. According to average operations power outputs, the sum of the power output of the multi-electrode mode reached 0.455 mW while for the parallel connection, the reactor exhibited a 37.8 % higher output of 0.732 mW, thus rendering the parallel connection a

preferable operational choice according to both comparative approaches, at least with regard to electrical reactor performance.

4.3.5 *Effluent quality performance*

Even though the major examination point in the scope of this experiment is to examine the electrical performance of a prototype mid-scale MFC reactor, effluent quality, which later on becomes the main focus of the study, should also most certainly be examined, at least in order to contrast it with electrical performance.

Table 4-1 offers a detailed presentation of the average performance in relation to all the effluent quality parameters, categorised according to the electrical connection mode. For R_{ext}=1000 Ω when the electrodes were operated in parallel, in terms of tCOD the influent value was 1871±458 mg/l, reduced by 81.9±6.2 % down to 318±71 mg/l. tSS performance in the same mode achieved an average reduction of 61.53±20.82 %. Performance at R_{ext}=15 Ω with the same electrical configuration maintained the average of 80.54±6.18 % in terms of tCOD reduction, with the effluent value increasing relatively to the previous operation to 356±86 mg/l. tSS demonstrated a slightly different pattern with an increase in reduction efficiency of 65.8±14.34 %. In the latter part of operation at R_{ext}=15 Ω but in the independent circuits mode, now for the multi-electrode system, the tCOD reduction efficiency slightly decreased to 79.8±8.74 % with a slightly higher effluent output of 425±66 mg/l, which can however be explained by the increase in the influent value relatively to the levels earlier on in the experiment, whereas the tSS reduction efficiency slightly increased to 69.75±7.5 %. pH throughout the study was steady at around approximately 7.4 for the influent and 7.6 for the effluent in every case. Overall, the removal efficiency of both tCOD and tSS seemed to have reached a 'standardised' level of performance after which changes in R_{ext} did not seem to affect it. The pH values at the first level suggest that no toxic build up occurred in the reactor.

Table 4-1: *Summary of effluent quality parameters during the two operational regimes*

	tCOD (mg/l)	E_{tCOD} (%)	tSS (mg/l)	E_{tSS} (%)	pH
Influent	1871±458		887±352		7.4±0.1
$R_{(10)}$ at 1000Ω	318±71	81.9±6.2	292±84	61.5±20.8	7.6±0.1
Influent	1924±433		1140±550		7.5±0.2
$R_{(10)}$ at 15Ω	356±86	80.5±6.2	272±83	65.8±14.3	7.6±0.2
Influent	2249±772		1101±401		7.4±0.1
$R_{(10)1+2}$ at 15Ω	425±66	79.8±8.7	338±79	69.8±7.5	7.6±0.4

Figure 4-8 depicts the variations in the performance of influent and effluent tCOD values as well as in reduction efficiency. As all the information is visually depicted, unlike the averaged values in the previous table, considerable variation in the influent level is evident, whereas effluent output was kept relatively steady apart from a small increase in the output level at the time of the multi-electrode, independent circuit mode, the numeric values for which are mentioned above.

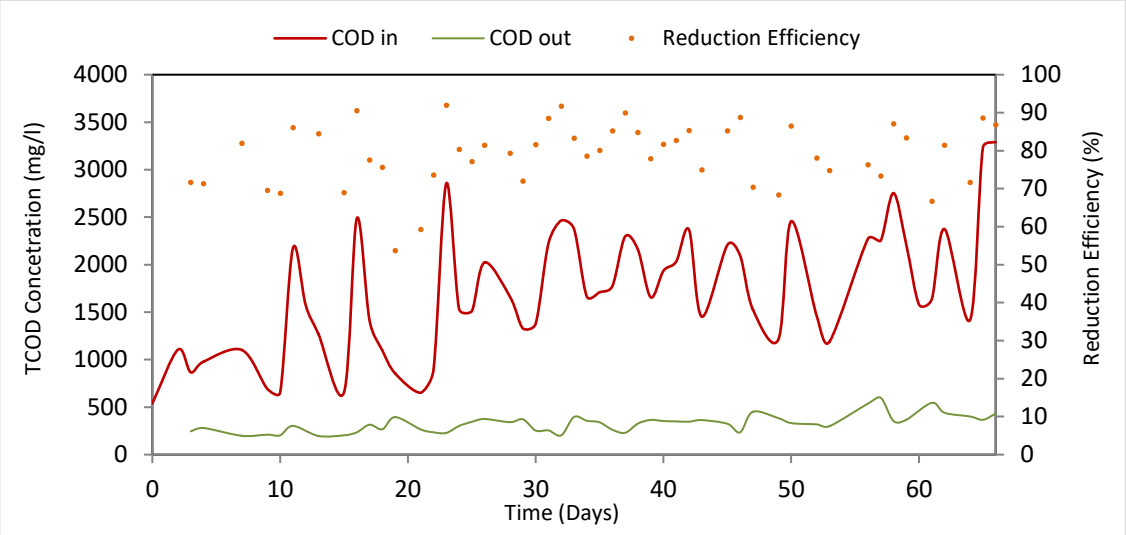

Figure 4-8: *tCOD influent and effluent values and percentage of removal efficiency of 14 L prototype*

4.4 Discussion

The 'small scale' experiment, during which two electrodes were internally hydraulically connected within one reactor, revealed several important aspects of MFC operation. On the first level, operating the MFC on open circuit during the initial stage provided start-up insight. The maximum OCV potential was clearly identified, and consequently the

reactor demonstrated a steady state performance for the remainder of the experimental period.

The use of different electrical methods such as polarisation tests and constant discharge verified that the former is as important tool in electrode characterisation. Assuming that the maximum power for the in parallel connected electrode occurred at R_{ext}=15 Ω, the same resistance was applied during long term operation at the two independent electrodes. If that were the only test conducted, then the power output during independent operation would have been considerably underestimated. A comparison between Figure 4-7 (A) and 4-7 (B) reveals that during the aforementioned external resistance, the summed power output of the combined independent electrodes only reached 0.455 mW. However, during the polarisation test it was revealed that the maximum potential of the summed independent electrodes was 0.761 mW, meaning that the previous result was an underestimation of the electrodes' potential. As the polarisation curves revealed, the reduction of surface area by operating the electrodes independently led to higher internal resistance, therefore, maximum output occurred at higher external resistances.

With regard to the main objective of this chapter, it has been proven that in the context of the specific plug-flow multi-electrode MFC, a parallel connection between the two adjacent anodes and cathodes results in a higher power output. As has been demonstrated, regardless of whether the electrodes were examined at a specific level of external resistance during long term operation, or via optimum performance through polarisation curves, the parallel connection produced a considerably higher power output.

The final finding of this investigation is that during independent operation, the first electrode (first in regards to the inlet point) demonstrated a considerably higher power output than the second electrode, according to both polarisation curves and constant discharge method. This could be attributed to the fact that the majority, or the more complex, organic compounds were consumed closer to the influent point by the first electrode. Therefore, less readily degradable matter was available for the microbial community in the second compartment to consume, so less power was generated from it. In a larger plug-flow multi-electrode reactor with an internally hydraulically connected flow, it is expected that the power profile would demonstrate similar behaviour, with the

first electrode generating higher outputs which are then reduced as we move closer to the exit point.

4.5 Chapter conclusions

The purpose of this chapter has been to examine and establish the optimum electrical connection between two neighbouring electrodes in a multi-electrode reactor, with regard both to electrical performance, for which power was used as the main parameter, and to effluent treatment, for which various parameters have been examined.

From an overall perspective and in relation to the aims set as in the beginning of this experiment, a parallel connection between two adjacent electrodes in a plug-flow multi-electrode MFC appears to be preferable concerning optimum power output. The parallel connected electrical circuit achieved a maximum power of 0.732 mW during constant discharge as against the sum of the independent circuits, which achieved 0.455 mW. Additionally, it was demonstrated that the polarisation test overestimated the maximum power achievable in comparison to the constant discharge method, confirming the necessity of both tests in order to be able to accurately describe the electrical performance of a reactor. In terms of effluent quality, this chapter has demonstrated the fundamental ability of the reactors to treat whisky distillation by-products, considerably reducing quality parameters, such as tCOD by an average of almost 82 % and tSS by an average of almost 70 %.

This chapter and the bench scale experiment described within it has successfully defined an optimum electrical connection for two neighbouring electrodes and the treatability of anaerobic digestion liquid digestate. Finally, these results are adopted by, and further implemented and examined in, the next part of this study, which concerns the commissioning of a 122 L pilot scale multi-electrode MFC reactor.

Chapter 5 – Preliminary studies of prototype 122 L reactor

5.1 Introduction

The main focus of this chapter is the preliminary experiments which aimed to establish the potential of the prototype 122 L reactor to sustainably treat whisky distillation by-products and generate a positive energy balance in ambient temperature in a Scottish environment. During this phase of development, a successful start-up period was examined, followed by regular operation for an overall duration of almost 250 days. The key characteristics of the large scale reactor were established, and its performance was examined against various key performance indicators both in relation to its electrical potential and its effluent quality, including its open circuit voltage, current and power as well as the tCOD, tSS, pH and a variety of nutrients. The energy balance was also examined under different phases and parameters.

5.2 Materials, methods and experimental set-up

A 122 L prototype MFC reactor was deployed according to the designs and specification described in Chapter 3, using the standard cathode design shown in Figure 3-6 and Figure 3-4 (B) for the anode, consisting of activated carbon granules impregnated with NR upon construction fixed upon carbon cloth with conductive glue. In terms of characteristics, therefore, regardless of the electrical connections and influent/effluent sampling points involved, the reactor, with an active volume of 57 L, consisted of eight anodes and eight cathodes and is characterised as a plug-flow reactor with a serpentine circulation as described in Figure 3-2. The inoculation of the reactor upon first deployment was carried out according to the procedure described in Chapter 3. The experimental set-up also follows the layout shown in Figure 3-10.

For the purposes of this chapter, it can be said that four distinct phases of experimentation were implemented. During *phase 1A*, the liquid flow in the reactor was undivided as described in Figure 3-1 and for electrode connection, eight independent circuits consisting of one anode connected to one cathode through an external circuit as described in Figure 3-8 (A) were monitored for open circuit voltage. This operation was followed by *phase 1B*, during which the electrical connections were changed to four coupled anode-cathode pairs as described in Figure 3-8 (B), and both open and closed circuit voltage were recorded. The common ground during the two first phases is that the carbon cloth strips in the cathode as described previously in Figure 3-5 (4), extended outside and under the

reactor to tap in an electrolyte bath of 0.1M hydrochloric acid solution thus, following the concept described by Fedorovich (2012) by operating as a reactor with an open air cathode with a simultaneous use of catholyte for the enhancement of the cathode oxygen reduction. Electrically, the reactor was operated on switching from open to closed circuit (where R_{ext}=1Ω was used) on a 24-hour basis as described in Chapter 3.3; however, closed circuit data were only collected during *phase 1B* when the neighbouring electrodes were coupled.

In both phases, a spent wash derived effluent diluted with distilled water collected from the water treatment plant operating at North British Distillery (Edinburgh, UK) was pumped into the reactor at a feeding rate of 9 ml/min, resulting in a hydraulic retention time of four days. Influent samples from the influent container were collected, and effluent samples were collected at the exiting point of the reactor, and both were monitored for tCOD. Temperature and pH values, according to the methods described in Chapter 3.4 were measured at four points. The minimum difference in values was monitored, so the levels presented are the averages throughout the reactor. Figure 5-1, below, presents every point of sampling used during *phases 1A* and *1B*.

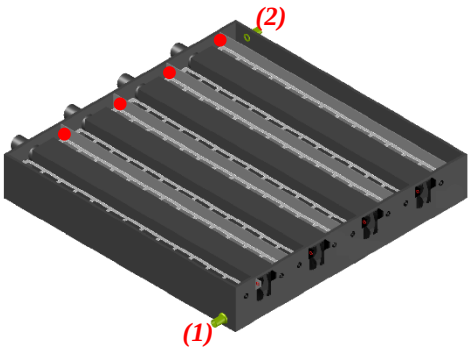

Figure 5-1: *Sampling points for phases 1A and 1B; (1) influent sample, (2) effluent sample (both monitored for tCOD) and red bullet points for temperature and pH*

Phase 2 consisted of the refurbishment of the reactor and the retro-fit as described in Figure 3-3 in Chapter 3.2.1. The reactor was monitored in relation to electrical performance and specifically for open circuit voltage, in order to establish a successful start-up and re-utilisation.

During *phase 3*, the reactor was operated by dividing it into the two sub-reactors, with two coupled electrode pairs each. Anaerobic digestion liquid digestate (ADLD), which originated from spent wash that had undergone anaerobic digestion, was provided by the digester operating in the water treatment plant at the North British Distillery (Edinburgh, UK), and was used as influent and fed to each sub-reactor. Table 5-1 below represents the variations in the two main experimental parameters throughout this phase, which had a duration of which was 60 days; hydraulic retention time and external resistance.

Table 5-1: *Experimental parameters during phase 3 for sub-reactors MFC_{R1+R2} and MFC_{R3+R4}*

HRT (Days)	Day	R_{ext} (Ω)
	0-10	100
4	11-20	50
	21-30	25
	31-40	100
1	41-50	50
	51-60	25

In terms of effluent quality, the tCOD and pH where measured as before, while the tSS, nitrates, phosphates, sulphates and EC were introduced according to the methods described in Chapter 3.4. The optimisation of the prototype and a study of its operation in industrial conditions are two key objectives of the current study, so the following section aims to explore how to minimise the flow rate while achieving sufficient and efficient performance both in electrical terms, and as effluent treatment.

5.3 Results and discussion

5.3.1 *Start-up and acclimatisation of the 122 L reactor (phase 1A)*

The 122 L prototype reactor was started upon inoculation, and OCV was used as the parameter by which to monitor the start-up process. Electrical potential was generated from the first moment at values of around 0.15 V for every one of the 8 electrodes. The performance had already sharply increased by the third day, after which a decrease was noticed for all the electrodes, with R_4 and R_1 most severely affected, an event which can be attributed to the unsteady conditions in the reactor and the adaptation of the microorganisms to the electrogenic metabolic paths. The OCV kept steadily increasing, reaching the maximum recorded values on the 83rd day at a similar level for all eight electrodes of the system, which were 0.788 V, 0.816 V, 0.817 V, 0.830 V, 0.816 V,

0.819 V, 0.823 V, and 0.814 V for R_1, R_2, R_3, R_4, R_5, R_6, R_7 and R_8 respectively. The voltage output decreased after that point at a scale of approximately 0.2 V for every electrode apart from the two electrodes in the middle, R_4 and R_5, which dramatically decreased to 0.256 V and 0.328 V respectively. The overall start-up under the current regime lasted for 75 days; however, that could have been reduced to between 43 and 57 days, when maximum performance is noticed.

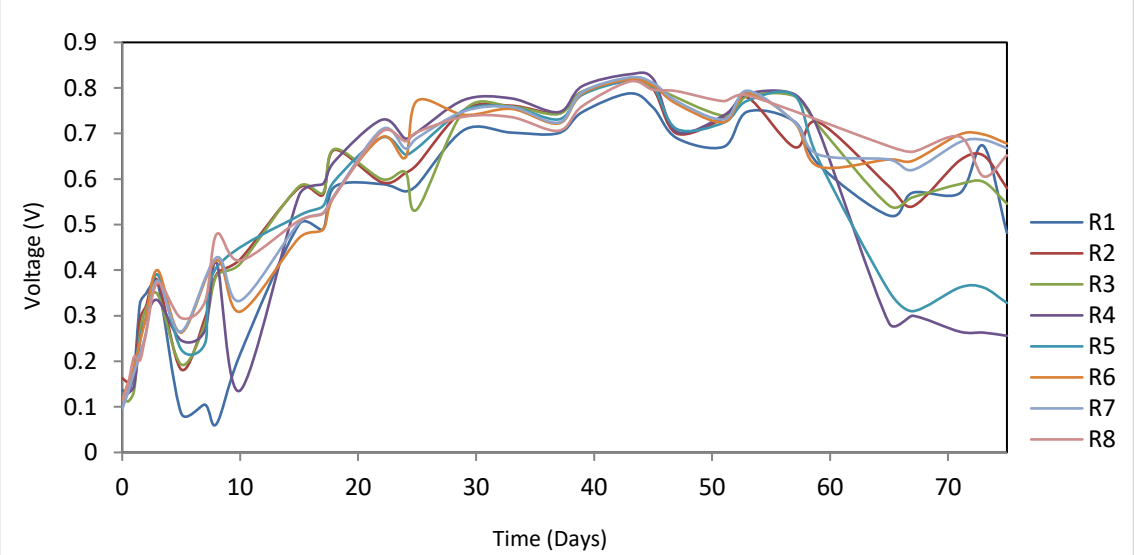

Figure 5-2: *Open circuit voltage during start-up period of 122L reactor with independent electrical connections*

Following start-up, every two neighbouring electrodes were connected in parallel as described in the equivalent circuit in Figure 3-7 (B) in order to additionally examine the hypothesis of performance improvement for the middle electrodes.

The purpose of this study was to examine the start-up of the multi-electrode microbial fuel cell reactor also with regard to ambient temperatures, specifically in the context of Scotland. In Edinburgh, where the reactor was commissioned throughout the study, the temperature generally varies from 9^o to 19^{o}C, rarely falling below -5^o or rising above 22^{o}C (Met Office, 2016). The microbial community used in these experiments was mesophilic, with an optimum temperature of between 20-45^{o}C (Willey, Sherwood and Woolverton, 2011), so both adaptation and successful operation under the aforementioned conditions was not guaranteed. The temperature recorded after the 15th day started off at 12.1^{o}C and increased slightly till day 57, after which a further higher increase occurred with the temperature reaching slightly over 20^{o}C on the last day of *phase 1A*. Figure 5-3,

below, depicts the average OCV output between the eight electrodes of the system against temperature fluctuations throughout this phase. Even though it could be argued by visual comparison that a correlation between temperature and open circuit voltage exists, that would in fact be a false argument. Statistical analysis (Pearson's correlation 0.263, *p* value 0.25), revealed that, perhaps surprisingly, no significant correlation exists between temperature and the increase or overall behaviour of the OCV during start-up. Lower temperatures are generally associated with slower metabolic paths, which would affect different types of microorganisms, which means that achieving a successful adaptation of a mesophilic culture to Scottish ambient temperatures could prove to be a bottleneck. However, low temperatures are also associated with the suppression of methanogenesis, which is particularly interesting in this case due to the origin of the initial inoculum, thus possibly allowing for other competitive processes such as electrogenesis to develop instead (Jadhav and Ghangrekar, 2009). The gas collection points on this reactor were located on the rear side, and for the duration of the study no gas accumulated on the area or was captured, thus rendering the examination of the hypothesis incomplete at this point. This result is in accordance with similar attempts in the past, during which the operation of pilot-scale reactors was not significantly affected by temperature (Heidrich et al., 2014). However, this constitutes a demonstration of a pilot-scale reactor starting-up during adverse, lower temperatures, thus highlighting the success of the adaptation process.

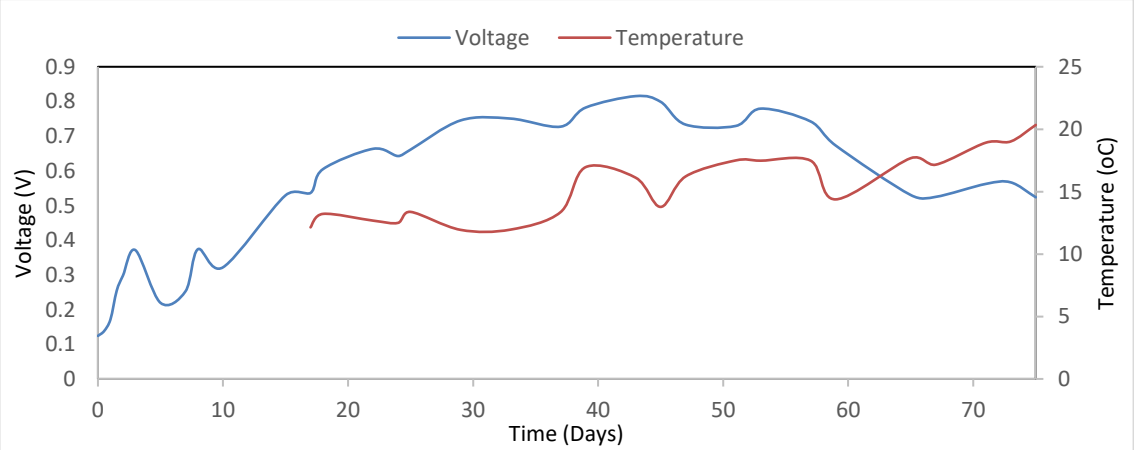

Figure 5-3: *Correlation between average open circuit voltage of 122L reactor and temperature*

5.3.2 *Open circuit profiles of parallel-independent reactor (phase 1B)*

Following the 75-day start-up process, the prototype reactor's performance is examined in the following *phase 1B*. As described in relation to the 24-hour interval switch from

open to closed circuit method described in *Chapter 3*, open circuit voltage was recorded after the connection of the electrodes in parallel mode in order to establish a baseline of performance, which could be used as a control of the process (Logan, 2012). As demonstrated in Figure 5-4, upon re-connection the OCV started from lower levels: 0.433 V for R_1, 0.436 V for R_2, 0.448 V for R_3 and the lowest, of 0.329 V for R_4, and needed approximately nine days to reach relatively maximum points of 0.586 V, 0.648 V, 0.576 V and 0.641 V for R_1, R_2, R_3 and R_4 respectively, which can be considered a new period of electrical adaptation. Throughout the study, the OCV seems to have performed steadily, with a relative deterioration by the 93rd day. By comparing the levels of voltage output between *phases 1A* and *1B* it can be noticed that the OCV output of the latter settled at a lower level which can be attributed either to deterioration due to biofouling (Zhang et al., 2014) or, as was discussed in the previous chapter, to parasitic losses similarly to closed circuit potential due to differences in potential between the connected electrodes (Ren et al., 2014). However, as was also mentioned above, the parallel connection seems to have a stabilising effect on the performance of the electric output.

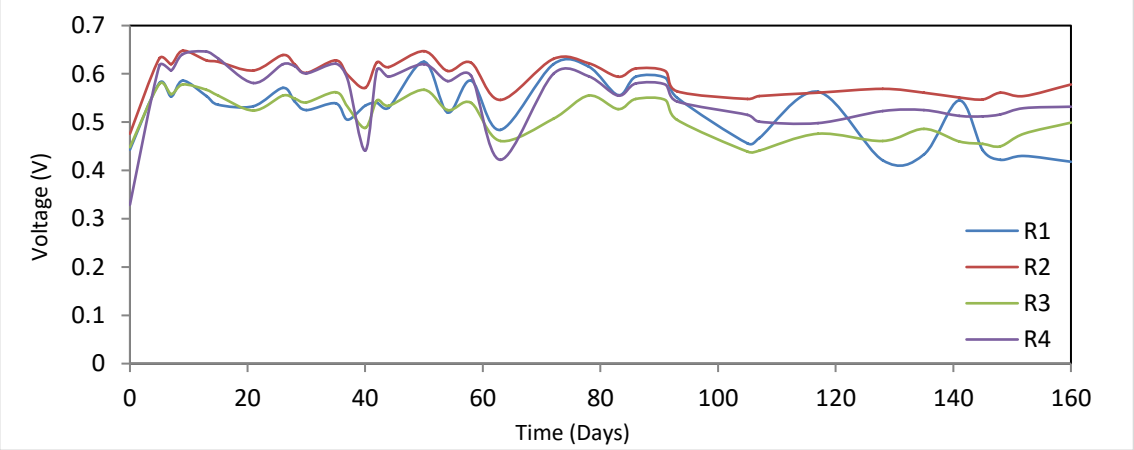

Figure 5-4: *Open circuit voltage of four electrodes of 122 L reactor after the introduction of parallel connections*

5.3.3 *Closed circuit profiles of parallel-independent reactor (phase 1B)*

During *phase 1B*, each pair of electrodes was connected to an independent circuit including an R_{ext}=1 Ω. Figure 5-5, which follows, depicts the current development. For all four electrodes, current generation started from a similar level, at 0.257 A, 0.298 A, 0.268 A and 0.277 A for R_1, R_2, R_3 and R_4 respectively. However, as can be seen, there was considerable fluctuation for R_4 during the first 40 days which seemed to stabilise

further on. A possible explanation for that behaviour could be the highly fluctuating influent tCOD values, which will be examined later on. In general, current output demonstrated a surprisingly steady performance, especially when considered with regard to the length of operation, which for *phase 1B* was over 160 days. Specifically, the average current outputs throughout the study were 0.283±0.022 A, 0.311±0.025 A, 0.273±0.028 A and 0.302±0.062 A for R_1, R_2, R_3, and R_4 respectively. Adding the operational period of 160 days to the start-up period of 75 days, the reactor operated for a total of 235 days, which certainly ranks the reactor as one of the longest field trials attempted, which can be verified by the literature review summary in Table 2-4.

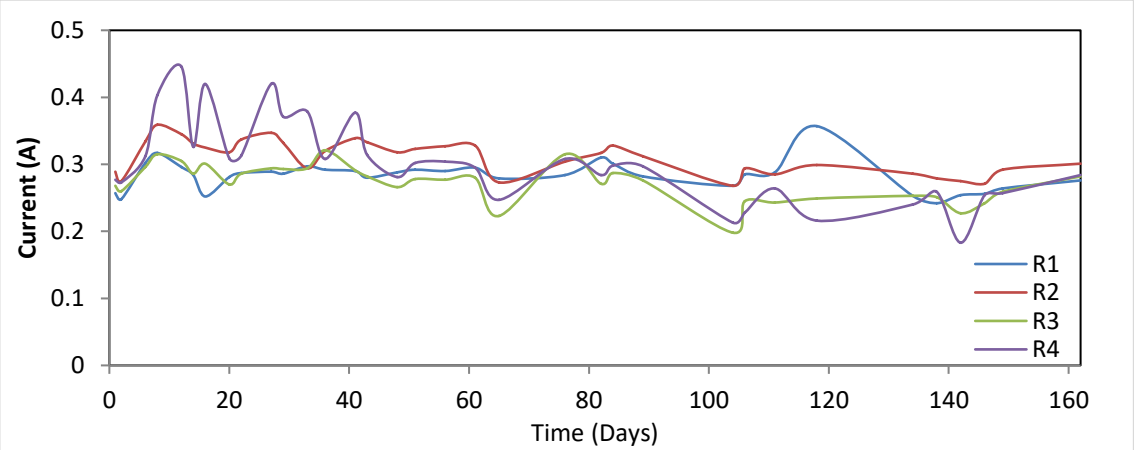

Figure 5-5: *Closed circuit current generation of four independent electrodes of 122 L reactor at* R_{ext}*=1* Ω

At this point a comparison should be made with the results of the previous chapter in terms of the independent and parallel connections. According to previous findings both from this study and similar research (Ren et al. 2014), the current and generally electrical performance in a multi-electrode MFC of independent electrode pairs should reduce from the first in place across to the last, mostly due to the reduction in the available sources of carbon (in this case, the four electrodes are eight electrodes with every two connected in parallel, but in relation to the overall reactor they can be considered as four independent circuits in a multi-electrode system). However, this is not found in the performance of the 122 L reactor. Unlike the findings for the 14 L reactor, in this case the current output develops at similar levels for all four electrodes. Therefore, at this stage it can be deduced that the 122 L multi-electrode reactor is a much more complicated system, and that further research on the large scale side is needed to clarify its performance.

In order to examine the overall performance of the reactor throughout this experimental period in more depth, Table 5-2 summarises the average values of power, and the coulombic efficiency in relation to each electrode, whereas power density and tCOD removal efficiency are examined in overall terms for the reactor. Additionally, at this point the energy balance for the system is introduced through normalised energy recovery and energy consumption, which in this case is only through the pumping system. Similarly, the latest parameters are presented with regard to the reactor as a whole rather than for each electrode independently. Power generation varied from 0.08 to 0.10 W (specific values presented on Table 5-2) for each independent electrode with the sum of the power generated averaged at 0.35±0.07 W. Coulombic efficiency reached high levels compared to the field trials reported in the prior literature (Pant et al., 2010; Wei, Liang and Huang, 2011; Janicek, Fan and Liu, 2014). Starting from R_1 leading to R_4, coulombic efficiency reached averages of 36.08±16.35 %, 39.79±18.67 %, 37.79±16.59 % and 38.97±19.99 % respectively. Similarly to the performance of current, coulombic efficiency, which is an initial indictor of the performance of the reactor both from electrical and effluent quality perspectives, maintained similar levels for all four electrodes.

In the set-up of the current study, as was explained earlier, the main source of energy consumption was the pump, which was calculated at 0.0033 kWh/m^3 according to Equation 3-16. The average normalised energy recovery for the reactor was maintained at 0.64±0.13 kWh/m^3, thus leading to a positive energy balance of 0.6367±0.13 kWh/m^3.

Table 5-2: *Average electric performance of each electrode and of the 122 L reactor as an overall*

	Power (W)	Power Density (W/m^3)	E_{tCOD} (%)	CE (%)	NER (kWh/m^3)	Energy Consumption (kWh/m^3)	Energy Balance (kWh/m^3)
R_1	0.08±0.01			36.08±16.35			
R_2	0.10±0.02			39.79±18.67			
R_3	0.08±0.01			34.79±16.59			
R_4	0.09±0.04			38.97±19.99			
Reactor	0.35±0.07	7.14±1.44	83.45±14.98	37.41±17.62	0.64±0.13	0.0033	0.6367±0.13

NER has only been introduced recently as a concept; therefore, data from studies in the field are mostly derivative (Ge et al., 2013). NER has only recently been studied as part of the experimental process at laboratory scale (Xiao et al., 2014b), and most recently, at

pilot-scale in a stackable reactor (Dong et al., 2015). However, it should be considered as a key performance indicator if MFCs are to be used to generate useful electricity even as a secondary purpose (He, 2013). Ge et al. (2013) indicated that according to the reactor's NER profile, the current study could be compared to the performance achieved by a smaller scale reactor in the range of 20 L, which demonstrates the successful scale-up of the current design.

Since performance in relation to temperature is one of the main objective of this chapter, the temperature was monitored similarly to before during *phase 1B*. Figure 5-6 depicts the normalised energy recovery of the reactor over time in correlation to the temperature recorded within the reactor. The maximum temperature recorded was 25.2^{o}C, while the lowest reached down to 3.3^{o}C, which is very low for an originally mesophilic microbial community, as was mentioned during the examination of the start-up. Statistical analysis (Pearson's correlation 0.731, p value <0.001) revealed a significant positive correlation between the two values. Therefore, it is concluded that the increased reactor temperature led to a subsequent increase in the rate of energy recovery. By comparison with the previous examination of temperature and open circuit voltage where no dependence was found, it can be argued overall that the process of start-up is not dependent on temperature, meaning that the microbial community will inevitably adapt to lower temperatures than optimum, and lead to an increase in electric output. Following that, however, the performance of the reactor follows the expected path, meaning that the lower temperatures slow metabolic reactions. Given the latter effect of temperature on energy recovery, it could be hypothesised that higher temperatures during start-up might have resulted in faster adaptation, and thus a shorter start-up period. The latter findings are also in accordance with the previous research into anaerobic treatments of wastewater, where temperature was proven to be a system limitation (Bowen et al., 2014). From a holistic point of view, the reactor has shown a fundamental ability to perform electrically in the relatively cold Scottish environment, creating a positive energy balance, with the potential to produce even higher power outputs in warmer environments.

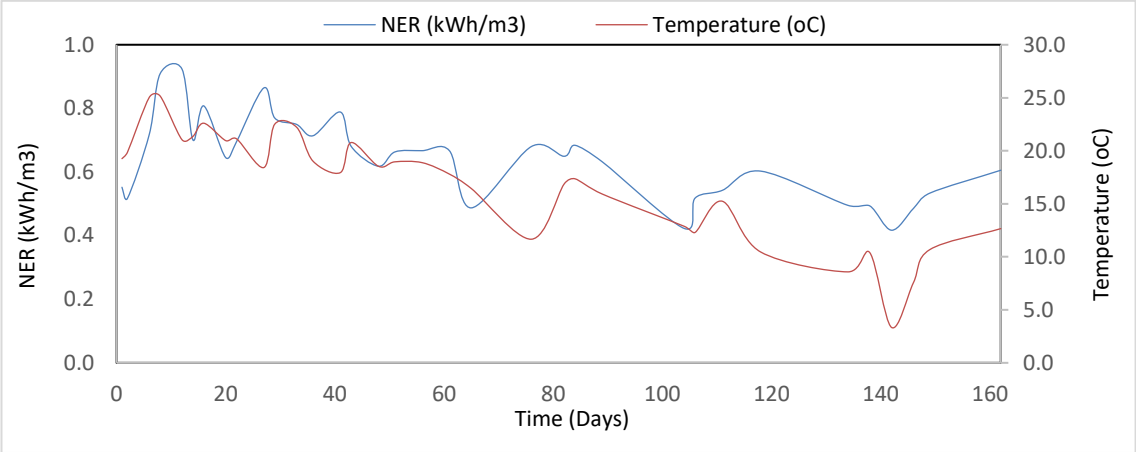

Figure 5-6: *Operational NER against temperature in the 122 L reactor*

5.3.4 *Effluent quality of parallel-independent reactor (phase 1B)*

tCOD is a key performance parameter in wastewater treatment efficiency, so it was recorded throughout the experimental period, and Figure 5-7 depicts the levels of influent and effluent as well as the tCOD removal efficiency in relation to time. As can be seen, the influent values for tCOD considerably fluctuated throughout the trial. The underlying reason for that is possibly that the influent was transported on site (Heriot-Watt University, Edinburgh, UK) from the provider's site (North British Distillery, Edinburgh, UK) in bulk volumes approximately once a week and was kept on site, therefore there was an increasing possibility of influent deterioration. Additionally, since the ultimate objective of this project was to examine the potential of integrating the MFC technology downstream of an anaerobic digester, and since this effluent was not available on time, a mix of spent wash derived effluent was provided with higher original tCOD values and was diluted in order to simulate lower tCOD values as would be expected for AD effluent. This process, in collaboration with the positioning of the influent route (which was placed on the bottom of the reception tank), could have led to increased tCOD readings. Influent tCOD reached a maximum of 5110 mg/l and a minimum of 280 mg/l, with an average value of 2170±957 mg/l. The effluent tCOD values fluctuated over time, with a much lower variance than for the influent, which is possibly the main contributor to that fluctuation. The maximum effluent value reached 1255 mg/l while the minimum was 10 mg/l with an average of 303±2238 mg/l. The average tCOD removal efficiency achieved by the prototype reactor was 83.7±15.5 %, with a maximum of 99.3 % and a minimum at 28.8 %.

Effluent tCOD values and tCOD removal efficiency, as depicted in the figures below, were much more variable during the first half of the examination period. Specifically, until approximately the 100th day, both the second highest and the lowest removal efficiency values were recorded, and similarly for influent values, the highest influent value and tCOD removal were both recorded. According to electrical performance during the start-up period, a steady performance was achieved even before the 75th day. However, according to the tCOD findings, a steady process was only achieved after the 100th day, with the average tCOD value being at 210±137 mg/l. Overall, the important conclusion at this point is that the prototype reactor has managed to achieve and fundamentally prove a high tCOD removal efficiency, which is similar and even surpasses those of relevant field trials, as can be verified by the summary of literature review in Table 2-4, especially considering the adverse conditions, such as Scottish ambient temperatures and fluctuating influent organic loads.

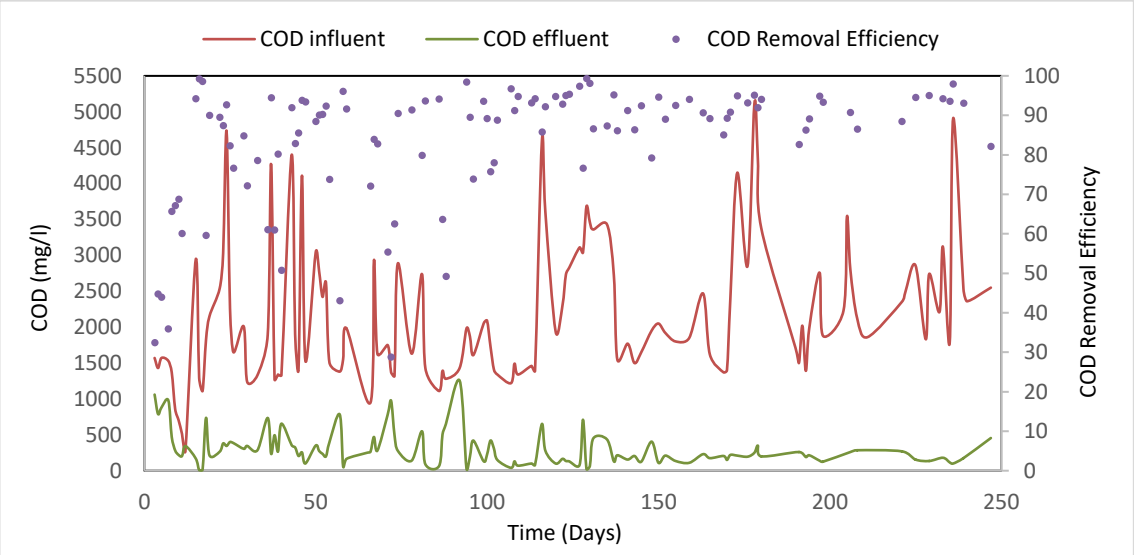

***Figure 5-7**:tCOD performance throughout the overall period of examination*

pH is another key indicator of effluent quality, and is also considered to be one of the fundamental parameters affecting microbial growth and performance. The wastewater collected was consumed as soon as possible and was replenished quite often but some deterioration might have occurred in storage (more often replenishment of fresh wastewater was not possible due to big volumes needed for the pilot reactor). However, pH data were collected when the influent was replenished. Influent pH was fixed at approximately 7 with the addition of sodium bicarbonate as and when was necessary (original pH values are not presented in this research), in order to maintain an

environment suitable for the operation of anaerobic granular biomass. However, as can be seen in Figure 5-8, the pH level demonstrated some peak moments at both higher and lower than the desired level. The average value to influent pH was recorded at 6.9±0.4, with a maximum peak at 8.4 and a minimum at 5.4. The effluent pH value was relatively steady during the experimental period, with an average of 7.4±0.5 while a few maximum values were recorded at an average of 8.8±0.2. The effluent pH value appears to be basal at the points correlating with temperature (pH was monitored in all four coupled electrode pairs, but differences were found to be minimal, therefore the pH value recorded in this graph is the average between the four coupled pairs).

At this point it could be argued that an increase in temperature could possibly lead to a subsequent increase in the reaction rate and create a more favourable environment for microorganisms, resulting in more activity and thus the consumption-depletion of hydrogen ions, creating a basal solution environment. Additionally, the transport of cations other than protons might according to the literature also lead to increased pH values. The overall performance in every case seems unaffected, with pH returning to its neutral level. This observation again strengthens the importance of the complexity of real wastewaters and multi-electrode systems, and is an inconclusive result regarding the cause of the pH increase (Rozendal, Hamelers and Buisman, 2006; Jadhav and Ghangrekar, 2009).

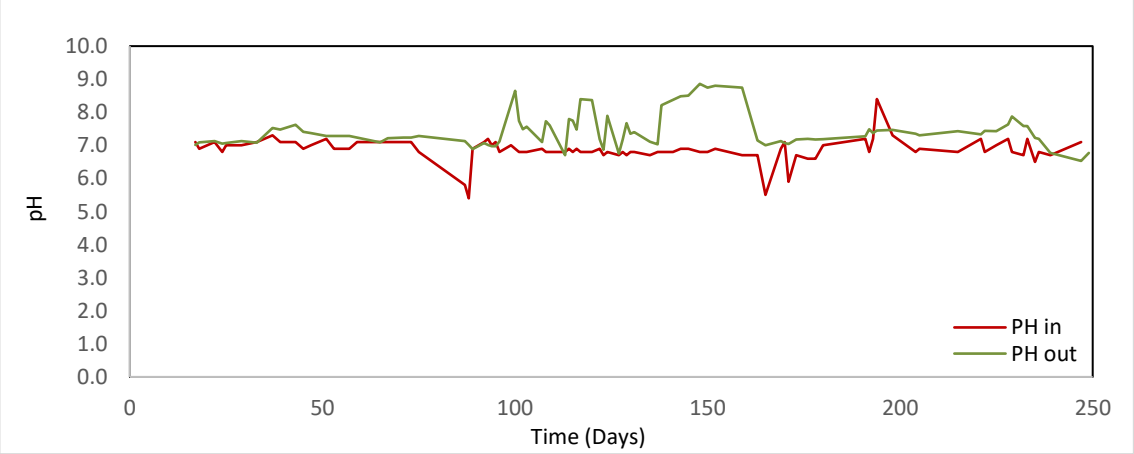

Figure 5-8: *Influent and effluent pH values throughout the overall examination period*

5.3.5 ***Refurbishment for future use (phase 2)***

Following the aforementioned preliminary steps for establishing the successful initial operation of the prototype reactor in ambient temperatures for one specific value of R_{ext},

phase 2 of the preliminary experiments took place. One of the purposes of this study, linking back to the key objectives set out at the start of the thesis, was to create a system capable of operating in an industrial setting as the regular effluent treatment solution. For this reason, it was concluded that refurbishing the reactor and examining the implications of long term operation was a key step. Additionally, in order to examine the reproducibility of the results without constructing a new reactor, it was decided that the current reactor should be separated into two identical, 'half' sub-reactors. This section describes that process of refurbishment in an attempt to standardise the procedure along with findings regarding the effects of long term operation on the reactor.

A precise description of the separation and new sub-reactors regime is given in detail in Chapter 3, however a summary is also given here for convenience. The liquid flow within the original reactor was separated at the end of the fourth channel, allowing for the creation of two, multi-electrode sub-reactors each consisting of two electrodes, thus it could still be classified as multi-electrode. The effluent from the front rear sub-reactor, hereafter referred to as the MFC_{R1+R2}, exited the sub-reactor and was externally connected to the rear end uniting to the back rear MFC, hereafter referred to as the MFC_{R3+R4}. A new influent port was created for the latter, similarly positioned at the front rear. The liquid flows were therefore separated, and even though the reactor was seemingly unaffected on its exterior, it now consisted of two identical sub-reactors.

In the context of the refurbishment process, the adapted microbial community was considered invaluable, and it was therefore decided that it should be harvested, maintained and re-inoculated into the new sub-reactors. The biomass was therefore extracted from the original reactor and was stored in anoxic conditions for the remainder of the maintenance process. All eight anodes were removed, detached and cleaned in 0.05M hydrochloric acid aqueous solution in order to remove all remaining attached biomass, thoroughly rinsed with distilled water, and were left to naturally dry in ambient temperature. Lastly in the removal and restoration process, the inner reactor was fully cleaned and any remaining biomass and wastewater emptied.

Figure 5-9 depicts the state of the cathodic windows, specifically depicting the biofouling observed on the membrane that was coated in contact with the anodic compartment. Figure 5-9 (A) shows a greatly affected cathode, highlighting the extent of the biological

fouling, while Figure 5-9 (B) shows an example of a healthy membrane where minimal to almost no biofouling has occurred. Biofouling has been reported in recent research similarly attempting to address the issue of long term performance and effects on microbial fuel cells. A steep deterioration of cathode potential has been attributed to this phenomenon (Zhuang et al., 2012a; Zhang et al., 2014). However, due to the destructive nature of the inspection process, no evidence could be extracted at an earlier stage. The proportion of the cathodic windows affected was approximately at 75 % with windows affected throughout the course of the influent, with one third of that greatly affected as shown in Figure 5-9 (A). Even though the deterioration of the cathodic membrane quality was obvious for a considerable part of the reactor, it was decided to proceed with the refurbishment process due to the main objective of this project, which was to view the realistic performance of a pilot-scale MFC in the long term, rather than to view this system as a one off application.

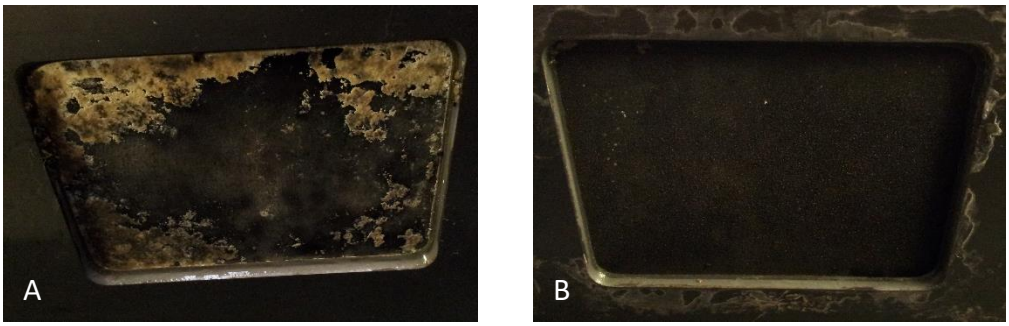

Figure 5-9: *Example of cathode condition due to biofouling at the point of refurbishment; (A) greatly affected membrane and (B) healthy membrane with minimum fouling*

Following the latter part, the anodes were connected back in place within the reactor in an identical order to that previously used. The electrochemically active biomass was re-inoculated into the reactor and the start-up process was initiated. It is important to note at this point that the hydrochloric acid solution used as electrolyte in which the cathode carbon cloth strips were tapping in order to absorb and transport it in the cathode element, was not used from this point onwards, for two reasons: firstly, because mechanical failures of the lower compartment where the solution was kept led to leakages of electrolyte solution, and secondly because as weak as that solution was, it was decided to address chemical leakages prior to further use. The latter also led towards a less complicated system which would be closer to a realistic and practical industrial design.

5.3.6 ***Re-start process of modified 122L reactor (phase 3)***

Phase 3 was initiated as the start-up after maintenance and the retro-fitted changes in the architecture of the prototype reactor. For the purposes of this part, open circuit voltage was recorded, but the general electrical operation of each electrode remained unchanged: a 24-hours interval of open to closed circuit. Figure 5-10, below, depicts the development of the OCV from day 0 of the inoculation to the twelfth day of operation for both MFC_{R1+R2} and MFC_{R3+R4} respectively. At electrode R_1 the OCV was 0.127 V upon inoculation and reached a relatively steady performance state after day 5 at approximately 0.415 V, whereas electrode R_2 started off at 0.194 V reaching 0.497 V. With regard to the duplicate sub-reactor, the OCV for R_3 started off at 0.145 V, finally reaching a 0.429 V maximum, similarly to R_4 where the OCV started at 0.168 V and reached aroud 0.47 V.

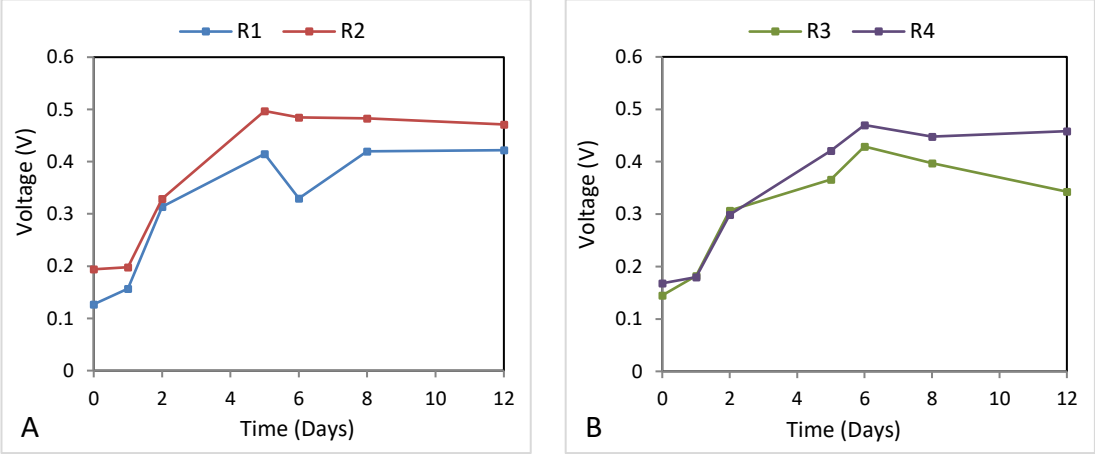

Figure 5-10: *Open circuit voltage during re-start of sub-reactors after modifications and refurbishment for (A) MFC_{R1+R2} and (B) MFC_{R3+R4}*

In comparing the level of OCV achieved compared to the previous operational regime, it can be seen that it was currently lower by approximately 0.2 V.

Two distinct points of interest emerge from the successful re-inoculation and re-start process. On the first level regarding performance, the OCV achieved seems to have been lowered compared to the previous finding, however that was to be expected and is attributed to the removal of the catholyte solution which was previously acting as an enhancement of the oxygen reduction process in the cathodic compartment. Additionally, the initial NR impregnated in the anode materials facilitating electron transfer is considered to have reduced the efficiency due to not being renewed. On a qualitative

basis in terms of duplicate similarity, the two sub-reactors demonstrate similar behaviour in relation to various aspects of performance. As can be seen in Figure 5-10, the OCV in both sub-reactors started at similar levels, followed by an exponential increase after the first day before they reached maximum performance at a little higher than 0.4 V for R_1 and R_3 on the fifth and sixth day respectively, and a little lower than 0.5 V for R_2 and R_4. The latter also demonstrates the similarity of specific electrodes within the multi-electrode sub-reactors. The OCV development demonstrated an overall exponential behaviour which would be expected in the case of a microbial growth-dependent process.

5.3.7 *Modified 122 L MFC with sub-reactors and external resistance (phase 3)*

Upon the successful re-start of the 122 L reactor, now divided into two identical sub-reactors, and the reaching of a steady state in terms of OCV, the purpose of this experiment was to establish the performance of the prototype under various external resistances, and also with regard to flow rate.

As can also be seen in the description of the experimental process, all four electrodes were first connected to an R_{ext}=100 Ω, followed by R_{ext}=50 Ω and finally R_{ext}=25 Ω. The same process was repeated after the hydraulic retention time was reduced to 1 day. Figure 5-11 (A) and (B) depict the current achieved under the various external resistances applied during the two flow regimes over time. Specifically, Figure 5-11 (A) refers to the first sub-reactor, and Figure 5-11 (B) to the duplicate sub-reactor.

Starting on a qualitative basis, the current achieved for the two electrodes of the first sub-reactor, as depicted in Figure 5-11 (A), during the initial experimental period when the HRT was fixed at 4 days, were almost on identical levels during R_{ext}=100 Ω and R_{ext}=50 Ω, with a slight deviation during R_{ext}=25 Ω. Specifically, the current between the two electrodes R_1 and R_2 reached an average of 2.38±0.11 mA, followed by 4.17±0.10 mA and 6.92±0.29 mA respectively. Current performance was slightly different when the HRT was reduced to 1 day. Similarly to the current production during the longer HRT, the current generation during R_{ext}=100 Ω was almost identical between the two electrodes, reaching an average between the two of 2.40±0.10 mA. However, during R_{ext}=50 Ω, R_1's current generation was slightly lower, averaging 4.36±0.10 mA over time, than R_2, which reached an average of 4.89±0.05 mA over the experimental

period. Similarly, during R_{ext}=25 Ω the current produced for R_1 was 7.23±0.18 mA, while for R_2 it was slightly higher at 8.01±0.09 mA. Prior to further investigation of this, it should be noted that the current produced during various external resistances and between both hydraulic retention times was surprisingly steady over time, which can also be verified by the low standard deviation values reported above. Regarding the variation of current production between R_1 and R_2 during HRT=1 day at R_{ext}=50 Ω and R_{ext}=25 Ω, it should be noted that according to the prototype performance of the 14 L reactor described in the previous chapter, this should not have been the case. According to the previous findings and the literature review (Ren at al., 2014), the first electrode would be expected to produce higher levels of current, possibly due to the higher carbon sources available in the influent stream. However, that does not seem to have been the case neither at this point nor during the start-up process, during which according to Figure 5-10, the OCV for both R_2 and R_4 seems to be higher than that achieved by R_1 and R_3 respectively. Further research is required since this seems to be at odds with prior findings.

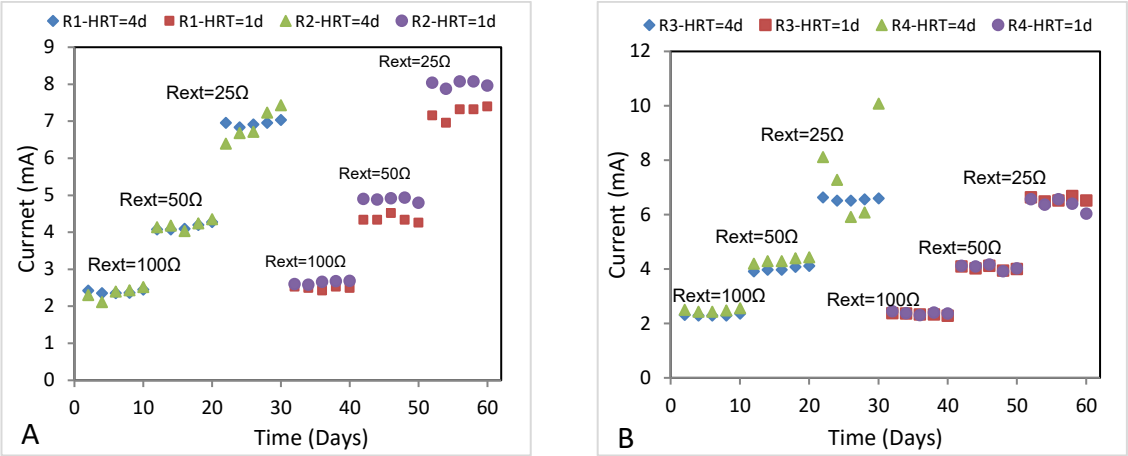

***Figure 5-11**: Current generation under various external resistances (100, 50 and 25Ω) and HRTs (4 days and 1 day) for (A) MFC_{R1+R2} and (B) MFC_{R3+R4}*

In order to verify the multi-electrode system's performance, the duplicate sub-reactor is examined and presented in Figure 5-11 (B). As can be seen above, the current generation during both HRT=4 days and HRT=1 day was almost identical between R_3 and R_4 during each external resistance regime, both between themselves and in correlation to the HRT regime itself. The average current generation between R_3 and R_4 for HRT=4 days was at 2.40±0.10 mA and 4.17±0.18 mA for external resistances of 100 Ω and 50 Ω specifically. When latterly the HRT was reduced to 1 day, the current generation ranged between 2.36±0.05 mA and 4.05±0.08 mA for R_3 and R_4 at 100 and 50 Ω respectively.

An anomaly was only noticed with regard to the current generated from R_4 at HRT=4 days at an external resistance of 25 Ω. The maximum peak was 10.08 mA, while the average generation through the electrode over time was at 7.50±1.70 mA, with the current generated at R_3 at an average of 6.57±0.05 mA. Any similar behaviour at HRT=1 day and at an external resistance of 25 Ω was not noticed, with the current between R_3 and R_4 being almost identical, at an average of 6.48±0.18 mA.

In addition to data on the generated current, power output is also presented in Figure 5-12. Due to the mathematical relationship between current and power expressed in Ohm's law, the same trends were expected in power outputs. Therefore, on a qualitative basis, the remarks made for current development are noticed as being further highlighted in the power graphs. Specifically, in relation to sub-reactor MFC_{R1+R2} during HRT=4 days, the average performance for R_1 was 0.57±0.02 mW, 0.86±0.04 mW and 1.21±0.03 mW at external resistances 100 Ω, 50 Ω and 25 Ω respectively. Similarly, for R_2, power generation was 0.56±0.07 mW, 0.88±0.05 mW and 1.19±0.15 mW for external resistances of 100 Ω, 50 Ω and 25 Ω respectively. Reducing the hydraulic retention time to 1 day resulted in power generation of 0.62±0.02 mW at 100 Ω, 0.95±0.04 mW at 50 Ω and 1.31±0.06 mW at 25 Ω for R_1, whereas for R_2 in the same conditions, power generation of 0.70±0.03 mW at 100 Ω, 1.19±0.03 mW at 50 Ω and finally, 1.60±0.03 mW at 25 Ω was measured. During the longer HRT regime, power output between R_1 and R_2, as shown in Figure 5-12 and the reported values, ranged between roughly the same levels. However, the increase of influent flow rate through the HRT reduction resulted in slightly higher power outputs for R_2 than R_1.

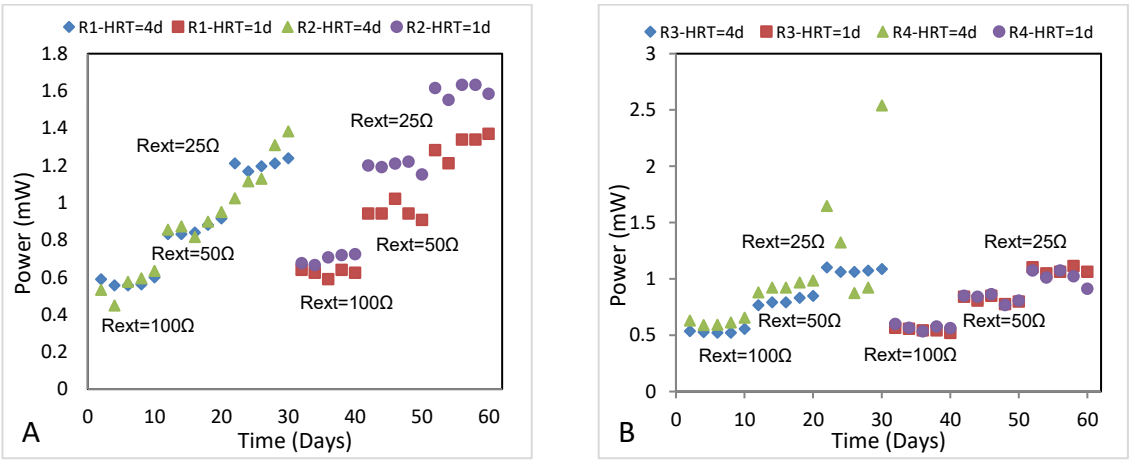

Figure 5-12: *Power production over time for various external resistances (100, 50 and 25Ω) and HRTs (4 days and 1 day) for (A) MFC_{R1+R2} and (B) MFC_{R3+R4}*

Looking at the duplicate sub-reactor performance, the previously noted irregularities in performance for electrode R_4 during HRT=4 days at an external resistance of 25 Ω can also be noticed in the power profile, where the peak was 2.54 mW and the overall average power output was 1.46±0.68 mW. The deviation is the highest recorded. In relation to performance under the remaining resistances, power output was 0.62±0.03 mW and 0.94±0.04 mW for 100 Ω and 50 Ω respectively. Power output for R_3 during HRT=4 days was at 0.53±0.01 mW, 0.81±0.03 mW and 1.08±0.02 mW at external resistances of 100 Ω, 50 Ω and 25 Ω respectively. The reduction of HRT to 1 day led to power output at 0.55±0.02 mW, 0.81±0.03 mW and 1.08±0.03 mW at 100 Ω, 50 Ω and 25 Ω respectively for R_3, while for R_4 the respective values were 0.57±0.02mW, 0.83±0.04mW and 1.02±0.03mW. A comparative study between the replicate sub-reactors within the 122 L reactor confirms the similarity of performance at respective HRTs and at various external resistances. As demonstrated in the prior research in the field of microbial fuel cells, performance both in terms of current and of power output was considerably higher at the lower external resistance.

As a summary of the electrical performance recorded in the present research, power density is presented in Table 5-3, below, while the tCOD removal efficiency is also included in order to subsequently examine coulombic efficiency and create an energy balance. However, at this point, the reference unit used is each sub-reactor as a system rather than each separate electrode, as described in previous similar approaches. Since specific values are presented for each case, the examination at this point is qualitative. The power density during an HRT of 4 days showed a minimal deviation between the two sub-reactors at each external resistance when maximum power density was achieved by sub-reactor MFC_{R3+R4} at 0.1044±0.0284 W/m^3 at the minimum external resistance of 25 Ω. The tCOD removal efficiency will be examined in more detail in the following section, but according to Table 5-3 the maximum efficiency during HRT=4 days was achieved at an external resistance of 25 Ω for both sub-reactors, reaching 81.8±4.4 % for MFC_{R1+R2} and 78.1±11.8 % for MFC_{R3+R4}. Overall removal efficiency during the longer HRT steadily increased with the reduction of external resistance for both sub-reactors. Similarly, coulombic efficiency reached a maximum of 0.91±0.49 % for the second sub-reactor, while for the first the equivalent value was 0.81±0.25 %, both occurring at an external resistance of 25 Ω. Given the nature of coulombic efficiency, maximum output was expected at the lowest level of external resistance.

A reduction in hydraulic retention time did not affect performance in terms of when the maximum power density was observed in relation to the different external resistances. For both sub-reactors, maximum density was observed at R_{ext}=25 Ω and was 0.1196±0.0036 W/m^3 for MFC_{R1+R2} and 0.0862±0.0033 W/m^3 for MFC_{R3+R4}. Similarly, coulombic efficiency and tCOD removal efficiency were highest during the application of the lowest external resistance at 74.5±10.9 % for E_{tCOD}, 0.28±0.15 % for CE for MFC_{R1+R2}, and 75.2±9.0 % for E_{tCOD} and 0.24±0.14 % for CE for MFC_{R3+R4}. The qualitative performance of the two sub-reactors during the lower HRT shows comparable results, validating the findings.

***Table 5-3**: Summary of electrical performance and energy balance for MFC_{R1+R2} and MFC_{R3+R4} at various external resistances and HRT regimes*

HRT		R_{ext} (Ω)	Power Density (W/m^3)[1]	E_{tCOD} (%)	CE (%)	NER (kWh/m^3)[2]	Energy Consumption (kWh/m^3)	Energy Balance (kWh/m^3)
4d	1st sub-reactor	100	0.0465±0.0034	66.5±5.3	0.47±0.11	0.0042±0.0003	0.0033	0.0009
		50	0.0715±0.0035	79.3±4.5	0.55±0.15	0.0064±0.0003	0.0033	0.0031
		25	0.0985±0.0068	81.8±4.4	0.81±0.25	0.0089±0.0006	0.0033	0.0056
	2nd sub-reactor	100	0.0473±0.0016	70.1±3.8	0.44±0.10	0.0043±0.0001	0.0033	0.0010
		50	0.0716±0.0030	73.4±6.7	0.60±0.19	0.0065±0.0003	0.0033	0.0032
		25	0.1044±0.0284	78.1±11.8	0.91±0.49	0.0094±0.0026	0.0033	0.0061
1d	1st sub-reactor	100	0.0543±0.0012	67.8±10.6	0.10±0.05	0.0012±0.00003	0.0033	-0.0021
		50	0.0881±0.0025	71.0±11.3	0.17±0.09	0.0020±0.00006	0.0033	-0.0013
		25	0.1196±0.0036	74.5±10.9	0.28±0.15	0.0027±0.00008	0.0033	-0.0006
	2nd sub-reactor	100	0.0457±0.0015	69.0±10.5	0.09±0.04	0.0010±0.00003	0.0033	-0.0023
		50	0.0674±0.0028	72.3±8.4	0.14±0.07	0.0015±0.00006	0.0033	-0.0018
		25	0.0862±0.0033	75.2±9.0	0.24±0.14	0.0019±0.00008	0.0033	-0.0014

(1) : Power density is normalised over reactor volume (see definition in section 3.3)
(2) : NER is energy recovery per volume of treated wastewater (see definition in section 3.3)

Having established that best performance occurs at the minimum external resistance, this section moves on to a comparison between the two HRT regimes, where it can be observed that power density on a sub-reactor basis was slightly higher during HRT=1 day for MFC_{R1+R2}. Specifically, it increased by approximately 16.8 %, 23.2 % and 21.4 % at 100 Ω, 50 Ω and 25 Ω respectively. In contrast to that, power density decreased for MFC_{R3+R4} by 3.4 %, 5.9 % and 17.4 % respectively. Similarly, tCOD removal and coulombic efficiency in most cases decreased with a reduction in HRT. As was mentioned earlier, maximum tCOD reduction efficiency and coulombic efficiency occurred at R_{ext}=25 Ω, but the values corresponding to that external resistance regarding tCOD decreased from 81.8 % to 74.5 % for the first sub-reactor and from 78.1 % to

75.2 % for the second, and similarly regarding coulombic efficiency decreased from 0.81 % to 0.28 % for the first sub-reactor and from 0.91 % to 0.24 % for the second.

On a first level of examination, the outcome of the comparative study is in favour of the longer retention time since it resulted in higher values in the majority of cases, especially for the highest performance achieved at R_{ext}=25 Ω in relation to the three parameters examined. However, a full consideration not only involves the absolute value but also the impact of the reduction of HRT from 4 days to 1 day on a qualitative basis. The reduction in reference allowed for a four times higher volume of influent to be treated within the reactor. By examining the volume of influent treated and the optimum performance independently of each other, the achievement of the passing through the reactor of a higher volume for argument's sake regardless of the tCOD removal efficiency and electrical performance is neither sustainable nor the purpose of this experiment. However, the four times higher volume achieved here was treated at the cost of only slightly lower treatment efficiency and power density output. Therefore, for the purposes of a robust industrial system for a possible first level of wastewater treatment, a reduction of HRT to 1 day should be considered possible, and to have been successful on this occasion.

Normalised energy recovery was also examined during the various external resistances and influent flow regimes. Looking back to the definition of NER, it can be seen that it depends on both power and influent flow rate. Given the earlier findings relating to power, it is only reasonable that NER increased along similar lines with the reduction of external resistance. Indeed, maximum NER was achieved at R_{ext}=25 Ω specifically at 0.0089±0.0006 kWh/m^3 for MFC_{R1+R2} and at 0.0094±0.0026 kWh/m^3 for MFC_{R1+R2}. However, since the power output slightly increased in the case of the first sub-reactor and similarly decreased for the second while the influent flow rate increased four times, it is only to be expected that the NER dramatically decreased with the reduction of HRT. Indeed, NER decreased to 0.0027±0.0008 kWh/m^3 for the first sub-reactor and at 0.0019±0.0008 kWh/m^3 for the second.

Energy consumption, as is the overall case in this study, is solely due to the pumping system and was calculated as before at 0.0033 kWh/m^3. Essentially, it is only dependent on the hydraulic pressure head, and since that remained unchanged over time, energy

consumption therefore remained at the same level even after an increase in the influent flow rate. A balance was subsequently calculated for each case with regard to the three different external resistances for the two separate cases of hydraulic retention times, of 1 day and 4 days, and the results are presented in Table 5-3. Maximum recovery was achieved at an external resistance of 25 Ω for both sub-reactors at HRT=4 days, at 0.0056 kWh/m^3 and 0.0061 kWh/m^3 respectively. However, as can clearly be noticed, the reduction in HRT lead to a negative energy balance for both sub-reactors, though with a most efficient balance created at an external resistance of 25 Ω at -0.0006 kWh/m^3 for MFC_{R1+R2} and -0.0014 kWh/m^3 for MFC_{R3+R4}. Therefore, the balance for the latter indicates that more energy is put into the system that could possibly be recovered based on the system's power production.

Since the rationale of NER is the measurement of the energy recovered in relation to the volume of the effluent treated in a reactor, the subsequent decrease here shows that because power output did not considerably increase with an increase in the influent flow rate, thus lower energy is recovered per volume of treated effluent at the lower HRT. Therefore, on a decision matrix of optimum performance, decisions would have to be prioritised according to the above findings, by asking: is it more important to have higher energy harvested by an MFC, or is it more preferable to maintain a desirable treatment efficiency while being able to increase the volume of treatment given that industrial scale wastewater treatment is the scope of this MFC? Which, then, is the point of trade off?

5.3.8 *Modified 122 L MFC with sub-reactors and effluent quality (phase 3)*

During the previous section, tCOD removal efficiency was examined in relation to electrical performance and, specifically coulombic efficiency. In this section, tCOD development is focused upon. The unit used is the sub-reactor as a system, thus Figure 5-13, below, includes the tCOD values of the influent, a comparison between tCOD effluent values for MFC_{R1+R2} and MFC_{R3+R4}, and tCOD removal efficiency values throughout the overall duration of the experiment.

Throughout the current study period under examination, as verified by Figure 5-13, the level of influent tCOD fluctuated, reaching a minimum value of 1145 mg/l and a maximum of 3050 mg/l during the higher HRT phase, and 1300 mg/l to 3790 mg/l during the reduced HRT respectively, while average values were 2071±566 mg/l and

2407±786 mg/l respectively. The influent used during *phase 3* was anaerobic digestion liquid digestate which, as mentioned earlier, was provided by the local distillery. However, the trials were conducted at the Heriot-Watt University site, thus the influent was transported and maintained on site leading to a prolonged residence time within the influent container, which could have possibly led to the settlement of solids, a deterioration in effluent quality, and the formation of granules on the lower levels of the effluent was also noticed. The aforementioned issues, in conjunction with the influent pumping point and the sampling point, might have resulted in unrepresentative values of tCOD influent in relation to the original quality. However, the values depict the tCOD influent value at the point of sampling, and reflect the realistic value of the influent entering the reactor.

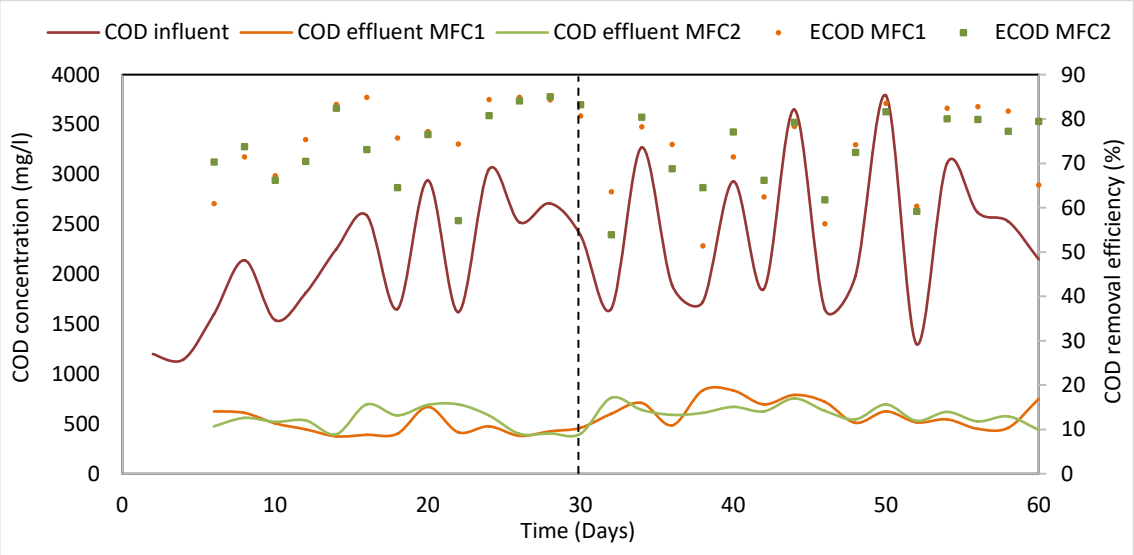

***Figure 5-13**: tCOD profile for sub-reactors MFC_{R1+R2} and MFC_{R3+R4} (the dashed line indicates the point of HRT change from 4 days to 1 day)*

Table 5-4 reports the tCOD removal efficiency in relation to various operational parameters which are now examined in more detail. During HRT=4 days in MFC_{R1+R2}, upon previously establishing a steady state of performance, E_{tCOD} gradually increased from 66.5±5.3 % to 79.3±4.5 % and finally to 81.8±4.4 % with reductions in external resistance from 100 Ω to 50 Ω and eventually to 25 Ω. Similarly, in the duplicate reactor MFC_{R3+R4} during the same conditions, the tCOD removal efficiency increased from 70.1±3.8 %, to 73.4±6.7 %, reaching 78.1±11.8 %. The subsequent decrease of HRT to 1 day and the reinstatement of the 100 Ω external resistance resulted in a reduced removal efficiency at 67.8±10.6 % for the first replicate and 69.0±10.5 % for the second. During

the following stage, the external resistance was reduced to 50 Ω and the removal efficiency recorded was 71.0±11.3 % for MFC_{R1+R2} and 72.3±8.4 % for MFC_{R3+R4}. During the latter part of the experimental, the tCOD removal efficiency relatively increased further to 74.5±10.9 % and to 75.2±9 % for MFC_{R1+R2} and MFC_{R3+R4} respectively.

Similarly, in the previous examination of electrical performance and NER in this study it was demonstrated that the lower external resistance amongst the levels used in this experiment demonstrated the most efficient tCOD removal. Overall, throughout the duration of the experiment the duplicated sub-reactors demonstrated a fundamental ability to treat anaerobic digestion liquid digestate.

In further examining effluent quality, pH and electrical conductivity were recorded for the influent and effluent of both sub-reactors on a 10-day basis, at the end of each external resistance cycle, and the recorded levels are presented in Table 5-4. The influent pH values ranged from 7.2 up to 7.6, with similar levels for effluent from MFC_{R1+R2} and MFC_{R3+R4} during the longer hydraulic retention time. During the lower HRT period, the influent pH level slightly shifted towards more basal values resulting in higher effluent pH values ranging from 7.6 to 8.0. Electrical conductivity is an important factor influencing effluent quality, with higher levels increasing the power output of MFCs (Cheng and Logan, 2011). During this study, the EC fluctuated both for influent and effluent, with influent values ranging from the lower level of 1930 µS/cm to the maximum of 3260 µS/cm. For MFC_{R1+R2}, the conductivity of the effluent ranged from 1640 µS/cm to 3260 µS/cm and for FC_{R3+R4} from 1260 µS/cm to 3420 µS/cm. As a generic overview, values for both influent and effluent fluctuated around similar levels for the same sample, which is consistent with prior results reported by similar trials during which the EC of domestic wastewaters remained relatively unchanged during the MFC treatment (Ren, Ahn and Logan, 2014). The divergent performance for the sample at day 20 during which EC considerably increased after the MFC treatment could be attributed to complex organic compounds being degraded, resulting in smaller charged molecules which may have increased the solution's conductivity (Dong et al., 2015). Throughout the experiment, conductivity was kept at levels possibly lower than typically found in strong effluent, but enough to ensure the effective performance of the sub-reactors (Feng et al., 2014).

Table 5-4: *PH and electrical conductivity values on a 10-day basis throughout the period of 60 days for MFC_{R1+R2} and MFC_{R3+R4}*

		pH			EC (μS/cm)		
HRT		Influent	MFC_{R1+R2}	MFC_{R3+R4}	Influent	MFC_{R1+R2}	MFC_{R3+R4}
	D0	7.8			2020		
	D10	7.2	7.4	7.6	2060	1640	1260
4d	D20	7.3	7.2	7.3	1930	2400	2180
	D30	7.4	7.4	7.6	2660	2620	2820
	D40	7.5	7.6	7.7	3200	3260	3420
1d	D50	7.5	7.9	8.0	2720	1900	2540
	D60	7.6	7.9	8.0	2780	2700	2780

The total suspended solids, phosphates, nitrates and sulphates were also recorded for a similar regime, and the levels for influent and effluent for both MFC_{R1+R2} and MFC_{R3+R4}, along with subsequent removal efficiencies are presented in Table 5-5 and Table 5-6 respectively. For MFC_{R1+R2}, in relation to tSS, the influent values of the samples ranged from 914 mg/l up to slightly above 1043 mg/l during the longer HRT, while for shorter HRT the values ranged at slightly higher levels, from 1023 mg/l up to 1255 mg/l. Removal efficiencies were calculated ranging from 82.9 % up to 89.2 % for HRT=4 days and from 78.3 % up to 88.5 % for the shorter HRT. Performance in relation to the aforementioned parameter does not seem to be correlated either to the levels of external resistance or the hydraulic retention times. On the contrary, tSS removal seems to have reached a high level at the beginning of the experiment, which was then maintained throughout the process. Overall tSS removal efficiency was high throughout the trial and consistent with results previously reported regarding diverse effluents such as those in the brewing and dairy industries (Mardanpour et al., 2012; Dong et al., 2015).

According to both Table 5-5 and Table 5-6, sulphate reduction appears to have been achieved at a considerable level for both sub-reactors, with one exception when the sulphate level increased by 40.6 %. The sulphate influent values fluctuated considerably throughout the experiment from 2.11 mg/l to 7.45 mg/l. The recorded reduction could be attributed to anaerobic mechanisms during which the sulphate is reduced to hydrogen sulphide, and similar results were reported in prior research (Zhang et al., 2013b). Even though complete removal was achieved in certain cases, the levels of sulphate were very

low in the influent compared to values found in similar effluents (Mohana, Acharya and Madamwar, 2009; Zhang et al., 2013b), however this warrants further study, since sulphate reduction is a process antagonistic to electrogenesis and it could be hypothesised that its suppression might lead to increased electric output.

Table 5-5: *MFC $_{R1+R2}$ chemical analysis on a 10-day basis throughout the period of 60 days*

		Nitrate NO_3^- (mg/l)			**Phosphate PO_4^{3-} (mg/l)**			**Sulphate SO_4^{3-} (mg/l)**			**tSS (mg/l)**		
HRT		Influent	Effluent	% Red.	Influent	Effluent	% Red.	Influent	Effluent	% Red.	Influent	Effluent	% Red.
	D0	0.32			113			1.06			914		
	D10	0.98	0.35	**64.3**	168	116	**30.7**	7.45	1.58	**78.1**	1027	176	**82.9**
4d	D20	0.41	0.45	**-9.1**	125	129	**-3.5**	7.43	2.82	**62.1**	1043	112	**89.2**
	D30	0.45	0.3	**32.7**	131	131	**0**	3.64	0.5	**85.9**	948	112	**88.2**
	D40	BDL*	BDL	N/A**	151	148	**1.63**	2.11	BDL	**100**	1255	202	**83.9**
1d	D50	BDL	BDL	N/A	159	127	**19.8**	5.56	2.22	**60.1**	1041	225	**78.3**
	D60	BDL	BDL	N/A	270	248	**8.3**	4.81	4.19	**12.9**	1023	118	**88.5**

* *BDL: Below detection limit*
** *N/A: Not applicable due to below detection levels*

Table 5-6: *MFC $_{R3+R4}$ chemical analysis on a 10-day basis throughout the period of 60 days*

		Nitrate NO_3^- (mg/l)			**Phosphate PO_4^{3-} (mg/l)**			**Sulphate SO_4^{3-} (mg/l)**			**tSS (mg/l)**		
HRT		Influent	Effluent	% Red.	Influent	Effluent	% Red.	Influent	Effluent	% Red.	Influent	Effluent	% Red.
	D0	0.32			113			1.06			914		
	D10	0.98	0.24	**75.9**	168	116	**29**	7.45	1.35	**81.9**	1027	176	**82.9**
4d	D20	0.41	0.32	**22.6**	125	130	**-4.3**	7.43	1.66	**77.6**	1043	81	**92.2**
	D30	0.45	0.19	**57.2**	131	130	**0.7**	3.64	5.1	**-40.6**	948	122	**87.1**
	D40	BDL	BDL	N/A	1551	151	**0**	2.11	BDL	**100**	1255	140	**88.8**
1d	D50	BDL	BDL	N/A	159	145	**8.7**	5.56	2.89	**48.1**	1041	192	**81.6**
	D60	BDL	BDL	N/A	270	159	**41.1**	4.81	2.52	**47.6**	1023	114	**88.9**

BDL: Below detection limit
** *N/A: Not applicable due to below detection levels*

Nitrates and phosphates are key effluent quality parameters since both are nutrients essential to microbial growth. However, it is precisely because of this contribution that their excess can lead to eutrophication, so they have to be removed through treatment (Correll, 1998; UNEP, 2016). Throughout this trial, both the influent and effluent values of phosphate and nitrate fluctuated without any particular trend developing. Specifically, for nitrates, performance varied from an increased effluent concentration of 9.1 % to a maximum decrease of 64.3 % for MFC_{R1+R2} and a removal of 22.6 % to 75.9 % for MFC_{R3+R4} during the longer HRT. During HRT=1 day, nitrate levels were found to be below the detection level; assessment was therefore impossible. Phosphate increased by

a maximum of 3.5 % for MFC_{R1+R2} while the maximum removal reached 30.7 %. Similarly, in MFC_{R3+R4}, in one instance phosphate increased during the MFC treatment by 4.3 % while the reduction in concentration reached a maximum of 41.1 %. The outcome of this analysis is therefore inconclusive. The behaviour of nitrates and phosphates due to treatment with an MFC should be examined in more depth and possibly with a sampling regime in order to identify more specific trends. A suggestion could be made to look at total nitrogen and total phosphorus instead, especially since the ratios between the aforementioned and carbon considerably affect microbial growth and the treatment of effluents, as previously recorded in relevant prior research (Ammary, 2004).

5.4 Chapter conclusions

In this chapter, a pilot scale 122 L reactor was deployed in Heriot-Watt University operating on diluted spent wash, the main whisky distillation process liquid residue. A successful reduced start-up period was achieved and the pilot was demonstrated to be capable of sustainably treating the wastewater stream as a stand-alone technology, while maintaining a positive energy balance. Temperature was a main focus of the chapter, and the correlation between that and start-up and performance during constant discharge was examined. As a result, the reactor was proven to achieve treatment in the ambient Scottish environment.

The chapter went on to establish a refurbishment protocol which was further successfully implemented for the re-deployment of the reactor on anaerobic liquid digestate. The initial results demonstrated a successful re-start, and the further optimisation of performance was examined in relation to external resistance. The conclusion of this chapter demonstrated the potential of the reactor to be similarly used as a complementary technology to anaerobic digestion, setting the ground for the next chapter which follows a pilot plant integrated in the existing processes in a local distillery.

Chapter 6 - Integration of the microbial fuel cell in a whisky effluent treatment process

6.1 Introduction

Following the preliminary examination of the MFC prototype reactor operating complementary to anaerobic digestion technology, a field study was set up with the purpose of integrating the microbial fuel cell technology into an existing wastewater treatment facility. Two 122 L microbial fuel cells (MFCs) were deployed on site in Scotland, using anaerobic digestion liquid digestate as process influent in order to examine long term performance in terms of wastewater treatment and electricity generation in a realistic, industrial environment. The initial studies in the previous chapter focused on diluted spent wash and a short term (60-day) experiment on ADLD to investigate the potential for MFCs to be integrated into existing processes in order to work complementary to existing wastewater treatment technologies. Following the two initial long term operational stages, the reactors were operated in a continuously closed circuit mode in order to examine the time until the possible failure of the system while harvesting maximum power, and if so, to identify the reasons driving failure.

6.2 Methods and system set-up

6.2.1 *Field site*

The pilot reactors were installed and operated at the effluent treatment facility running in the North British Distillery situated in the city of Edinburgh, Scotland, UK (55°56'19.2"N, 3°14'11.8"W). The effluent treatment plant is operated on site, treating approximately 120 m^3 of spent wash on a daily basis, maintaining the company's commitment to environmentally respectful and conscious whisky production and compliance with trade effluent discharge regulations.

6.2.2 *Integration of prototype in the existing treatment process*

The pilot reactors were placed in a sealed, covered area, which was protected from weather conditions but was subject to ambient temperatures. The process influent was collected after a mix of spent wash based effluents underwent anaerobic treatment, so it could therefore be characterised as anaerobic digestion liquid digestate, after the screening point during which the excess of biomass exiting the AD stream was removed. The influent was collected from the higher screening point with piping in a 200 L

container, as described in Chapter 3.2.6, thus gravity eliminated the need for additional mechanical pumping. The two reactors were operated hydraulically in parallel, resulting in duplicate results and volumes of wastewater treated. Gas extraction points were introduced on the lid, on the middle of the anodic compartment (see Figure 6-1), showing the standard white polypropylene tubing), starting from the second channel and at every two channels onward. The gas extraction points on the rear of the reactor were permanently sealed off. This modification was introduced due to indications in earlier experiments of gas accumulating on the specific area rather than where the extraction points on the rear had previously been put.

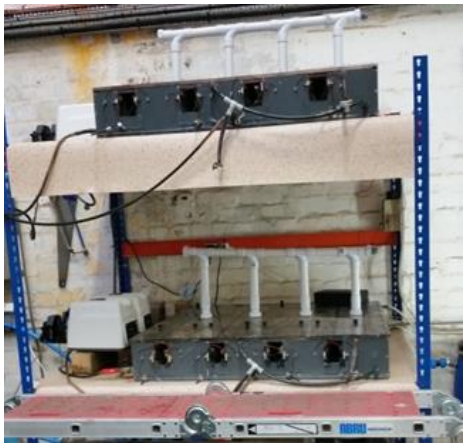

Figure 6-1: *Photograph of the pilot installation in situ at the North British Distillery wastewater treatment plant*

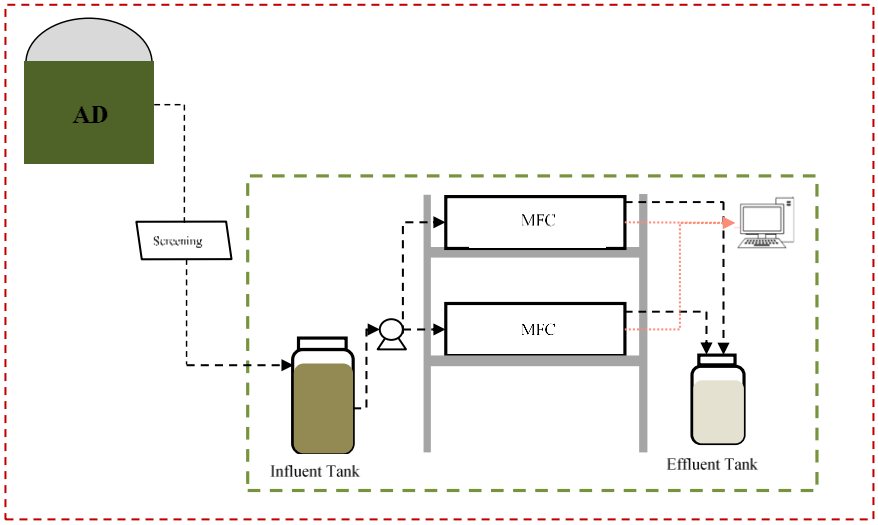

Figure 6-2: *Schematic diagram of reactors integrated in the existing wastewater treatment plant at North British Distillery*

6.2.3 *Reactor configuration*

Concerning the set-up of the reactor, the internal effluent circulation, and the electrode connections, each one of the duplicate reactors was operated in the same way as adopted during the latter part of the previous experimental period. Each MFC reactor was internally divided into two sub-reactors with separate influent feeds in serpentine internal circulation, each with two independent electrode pairs, thus characterised as a multi-electrode MFC. Each electrode pair consisted of two anodes and two cathodes connected in parallel between themselves as described in Figure 3-8 (B).

The reactors and sub-reactors will be referred to as follows. The two 122 L reactors are referred to as $MFC_{R1\text{-}R4}$, consisting of two sub-reactors, MFC_{R1+R2} and MFC_{R3+R4}, and $MFC_{R5\text{-}R8}$, consisting of two sub-reactors MFC_{R5+R6} and MFC_{R7+R8}. Therefore, all four sub-reactors can be regarded as identical.

6.2.4 *Operational conditions*

During *phase 1* and *phase 2*, the reactors were electrically operated on a two-day transition cycle from open to closed circuit. During *phase 1* (with a duration of 4 months), the organic load rate was fixed at 0.6 kg tCOD/(m^3d) (according to the average values during overall operation), resulting in a hydraulic retention time of 4 days. During *phase 2* (with a duration of 3 months), the organic load rate increased to 2.4 kg tCOD/(m^3d), resulting in a hydraulic retention time of 1 day. Throughout these two phases, R_{ext} for each coupled electrode pair was fixed and regularly reviewed at 500 Ω.

Following these two phases, during *phase 3*, a further reduction in hydraulic retention time through an increased organic load rate was unsuccessfully attempted. This was not successful due to mechanical failures, and therefore, HRT was maintained at 1 day. However, the difference represented by *phase 3* lay in the operation of the reactor in terms of monitoring of electrical performance. As described in Chapter 3.3, all four electrode pairs, thus eight in total in the duplicated reactors, were operated on a continuously closed circuit mode under various external resistances, while connected to a data acquisition system recording with at hourly time intervals. For the latter part of *phase 3* the coupled electrode pairs were operated at R_{ext}=22 Ω as according to the polarisation curves, this was the resistance at which maximum power was observed at the majority of electrodes. As was described in the literature review conducted continuously since the beginning of

the project, the field of microbial fuel cells is rapidly developing in several directions, reflecting its nature as a multidisciplinary field. Research on a basic laboratory scale is undoubtedly necessary, but industrial pilot scale trials and long term studies will also shed more light in the field. The purpose of the final experimental *phase 3* in the current study was to further study the performance of the reactor, now successfully integrated into the existing treatment process, while at the same time examining a different anode material. Its performance until relative failure, or more precisely, its performance development throughout time in an integrated wastewater treatment system is examined both through power curves and continuous discharge.

6.3 Results and discussion

6.3.1 *Integration into the existing process and initial operation (phases 1 and 2)*

Upon inoculation, the start-up period of the reactors was initiated during which the MFCs were operated in open circuit until they reached a steady maximum potential. Following the establishment of microbial operation and as described earlier, each electrode pair was operated in a 24-hour open to 24-hour closed circuit mode. The open circuit voltage output throughout *phase 1* and *phase 2* of the experimental process was used as a control of the process, and is presented as follows in Figure 6-3, below, for $MFC_{R1\text{-}R4}$, for both sub-reactors MFC_{R1+R2} and MFC_{R3+R4} and in Figure 6-5 for $MFC_{R5\text{-}R8}$, similarly for both sub-reactors MFC_{R5+R6} and MFC_{R7+R8}.

With regard to the first 122 L reactor, it can be seen that the OCV started at 0.054 V for R_1 and at 0.032 V for R_2, while for the second sub-reactor it began at 0.092 V for R_3 and 0.074 V for R_4 upon inoculation. The OCV sharply increased within the first four days when a maximum point was reached at 0.374 V, 0.430 V, 0.406 V and 0.403 V for R_1, R_2, R_3 and R_4 respectively. This period is thus acknowledged as a successful start-up and the introduction to *phase 1*, during which HRT was set at 4 days and closed circuit mode was implemented. The OCV went through a period of slight decrease until approximately the 22nd day, after which it stabilised at averages of 0.299±0.009 V and 0.349±0.018 V for R_1 and R_2 of the MFC_{R1+R2} sub-reactor, and 0.300±0.012 V and 0.318±0.013 V for R_3 and R_4 of MFC_{R3+R4}.

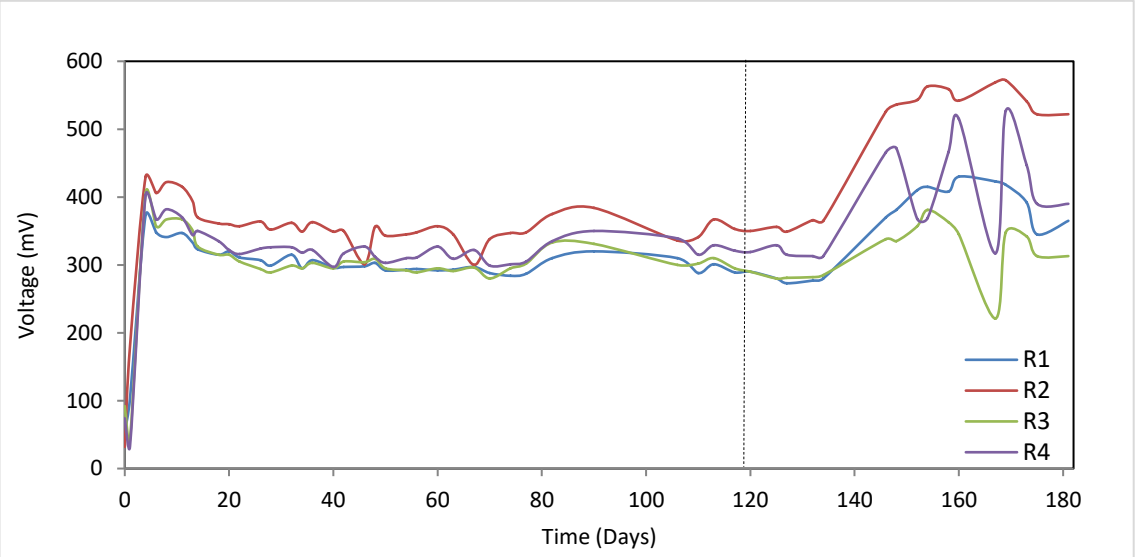

Figure 6-3: *Open circuit voltages of 122 L MFC_{R1-R4} reactor over time (the dashed line indicates the change from HRT of 4days to 1 day)*

Following successful operation at HRT=4 days, hydraulic retention time was further decreased by increasing the feeding rate, in order to increase the capacity of volume treated. On the 119th day, influent flow rate was gradually increased until the desirable HRT was achieved. Open circuit voltages for the two sub-reactors were recorded and are presented above (on the right-hand side of the dashed line in Figure 6-3). It can be seen that OCV remained unchanged for the following 15 days at roughly similar average values as before. After the 15th day an increase clearly occurred in every electrode in both sub-reactors. Specifically, OCV for R_1 increased to 0.381 V, for R_2 to 0.536 V, for R_3 to 0.335 V, and to 0.472 V for R_4. Following this period, performance was not steady for either of the sub-reactors, as it can be seen that OCV moderately fluctuated in R_1 and R_2 of MFC_{R1+R2} and fluctuated even more sharply in R_3 and R_4 of the second sub-reactor.

In relation to performance under closed circuit, which is when the 'useful' power output occurs, Figure 6-4 shows the current output for *phase 1* and *phase 2*. Every electrode was operated independently and was continuously connected to an external resistance of 500 Ω. After the start-up process was finished, all four electrodes of the two sub-reactors exhibited a considerably steady performance. Specifically, for MFC_{R1+R2}, current was maintained at an average of 0.564±0.028 mA for R_1 and 0.640±0.028 mA for R_2, while for MFC_{R3+R4} current output was maintained at similar values of 0.580±0.042 mA and 0.624±0.033 mA for R_3 and R_4 respectively.

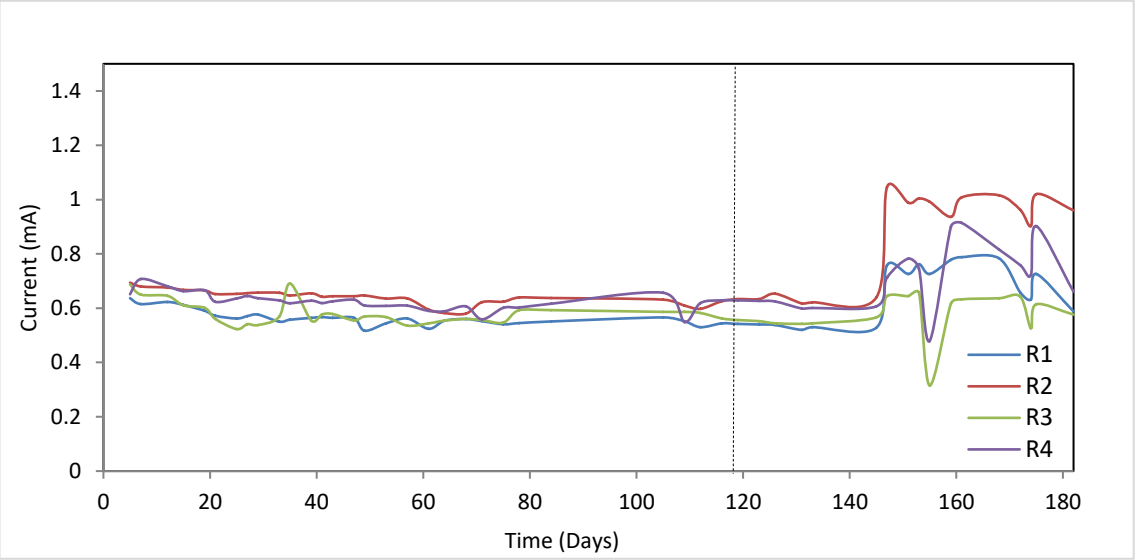

Figure 6-4: *Closed circuit voltages of 122 L MFC_{R1-R4} at 500Ω external resistance reactor over time (the dashed line indicates the change from HRT of 4 days to 1 day)*

Moving on to the next phase in the reduction of HRT from 4 days to 1 day, it was observed that current generation exhibited a similar behaviour as it had for the previously examined open circuit voltage. Current generation maintained the average levels seen previously, however following the 145th day, it sharply increased to a peak of 0.758 mA for R_1 and 1.046 mA for R_2 and for R_3 and R_4 the peaks were 0.645 mA and 0.713 mA respectively. Following these peaks, current generation fluctuated considerably until the end of the experimental period.

On an overall basis, consistency was observed between the two neighbouring sub-reactors during *phase 1*, with R_2 and R_4 producing a slightly higher current output than R_1 and R_3. In *phase 2*, the observed initial sharp increase can be correlated to the behaviour of a biological community after adaptation to a new feeding regime. In comparison to the standard growth curve of a microorganism, the current output demonstrates the initial steady lag phase of adaptation, followed by an exponential phase of increase in microbial growth, manifested here in the exponential increase of electricity generation, followed by a stationary phase of steady output. Given that an MFC is primarily a biological process, it is only reasonable that the electrogenic community would follow the standard growth curve triggered by the increase in the organic load rate. However, following the initial stationary phase, overall performance through the latter period demonstrates a relatively unsteady system, possibly indicating that the increase in feeding rate is higher than that which the microbial community can tolerate in order for that to provide a steady, reliable

system. Additionally, sharp decrease of current generation on several occasions during this last part could possibly be due to blockages noticed in the feed leading to obstructions and short periods of decreased flow thus, decrease in the availability of organic matter.

The two sub-reactors analysed above formed part of the first 122 L reactor, and the similarities in the performance will be further discussed later, however, the performance of the duplicate set, MFC_{R5+R6} and MFC_{R7+R8}, part of the 122 L MFC_{R5-R8}, will be examined presently. Open circuit voltage is the first parameter examined in relation to electrical performance. Following inoculation, when the OCV started at 0.255 V for R_5, 0.174 V for R_6, 0.158 V for R_7 and 0.203 V for R_8, all four electrodes demonstrated sharp decreases to 0.053 V, 0.020 V, 0.010 V and 0.035 V respectively, followed by sharp increases to 0.526 V, 0.556 V, 0.553 V and 0.497 V respectively within the first six days. The sharp initial decrease could possibly be attributed to a microbial 'shock' due to the change in feeding conditions. The ongoing performance following for the remainder of the HRT period of 4 days varied for the various electrodes, as Figure 6-5 details. For MFC_{R5+R6} and specifically for R_5, the OCV reached a maximum of 0.621 V then stabilised for the remainder of the 4 days HRT period at a similar level of 0.620±0.014 V, while R_6 exhibited more fluctuation, stabilising after the 13th day at approximately 0.512±0.026 V. For MFC_{R7+R8} and specifically for R_7, the OCV, as shown below, fluctuated particularly between the 14th and the 70th day, and later slightly increased, achieving an average of 0.424±0.068 V. Finally, the OCV for R_8 following the start-up period stabilised at the lowest recorded average of 0.342±0.052 V.

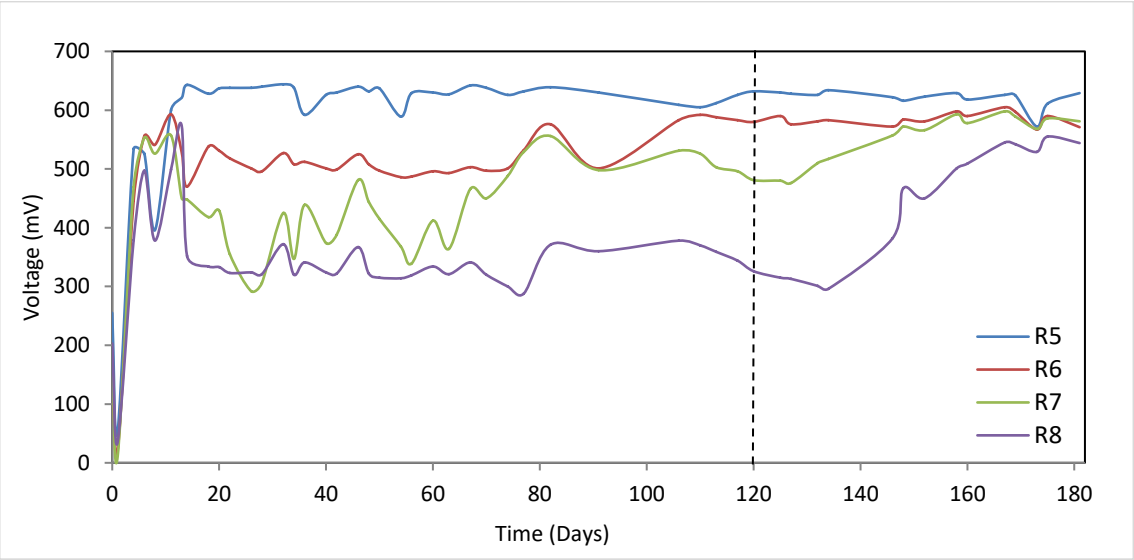

***Figure 6-5**: Open circuit voltage of 122 L MFC_{R5-R8} reactor over time*

On the 120th day, when the HRT was gradually reduced to 1 day, as verified by Figure 6-5 above, the OCV for both electrodes of MFC_{R5+R6} remained unaffected at 0.620±0.014 V for R_5 and 0.585±0.010 V for R_6. The performance for both electrodes of MFC_{R7+R8} demonstrated a quite different behaviour. Following the 127th day, the OCV for R_7 increased at a lower rate than R_8, for which the OCV sharply increased after the 134th day at a maximum of 0.555 V.

For both MFC_{R5+R6} and FC_{R7+R8}, the current density in the context of the closed circuit performance starting on the fifth day is presented in Figure 6-6, for which every electrode was connected independently to an external resistance of 500 Ω. In common with the OCV, the current generation for the aforementioned sub-reactors fluctuated throughout the experimental period in both *phase 1* and *phase 2*. Specifically, for the first sub-reactor during *phase* 1 involving 4 days HRT, the current generation for R_5 started at 0.594 mA and reached a maximum of 1.010 mA, and later on achieving an average of 0.954±0.059 mA. The current generation for R_6 achieved a relatively steadier level of 0.844±0.042 mA. In relation to the second sub-reactor, MFC_{R7+R8}, current generation for R_7 fluctuated before achieving a relatively steadier performance after the 78th day with an average reaching 0.746±0.110 mA, unlike R_8 which demonstrated a steadier and lower current generation of 0.611±0.027 mA.

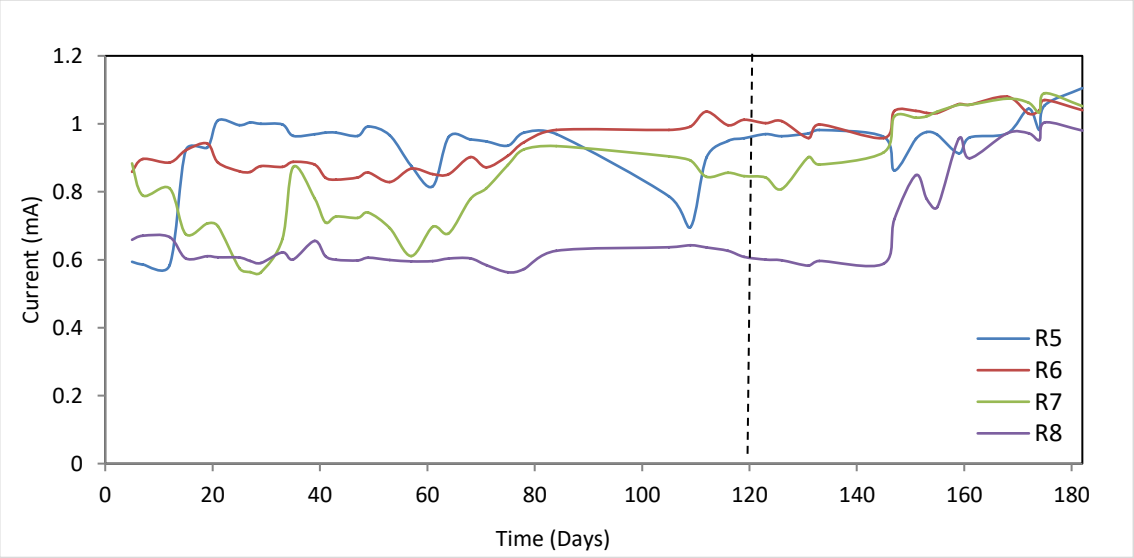

***Figure 6-6**: Closed circuit voltage of 122 L MFC_{R5-R8} reactor at 500Ω over time*

As Figure 6-6 verifies, the reduction in the HRT from 4 days to 1 day during *phase 2* had contradictory effects on the two sub-reactors. For MFC_{R5+R6}, the current generation of

both R_5 and R_6 remained relatively unchanged throughout the increase in influent flow rate with average generations of 0.957±0.081 mA and 1.024±0.033 mA for R_5 and R_6 respectively. Comparison of the two average values for R_5 and R_6 between *phase 1* and *phase 2* only reveals a slight increase for the latter electrode. Different behaviour is noticeable with regard to MFC_{R7+R8}. For R_7, current generation slightly increased after the 145th day, increasing from an average of 0.865±0.035 mA to 1.046±0.023 mA for the remainder of *phase 2*. The current generation of R_8 increased at a higher rate after the same day until the 159th day from an average of 0.609±0.021 mA to 0.962±0.033 mA, which was maintained for the remaining period.

As described above, the current generation in the MFC_{R5+R6} sub-reactor seems to have been relatively unaffected by the change in organic load caused by the HRT reduction. If examined in detail, only R_5 seems to generate an increased current and even then only slightly, especially compared to the R_7. A hypothesis requiring further investigation could be made at this point: it is possible that the performance recorded is the maximum current that could be generated by the specific microbial community with regards to the electrogenic microorganisms. In addition, as will later be examined in more detail, tCOD removal efficiency remained at relatively steady levels, so a reasonable deduction would be that the excess of organic matter present in the stream due to increased OLR was consumed by microbial activities other than electrogenesis. Given that the original microorganisms are anaerobic, that process would be expected to be methanogenesis. However, gas generation was checked for through liquid displacement, with none found, suggesting that the gas either escaped through pathways other than the gas collection points or dissolved in the liquid stream, or that the above hypothesis itself is wrong. Therefore, further research could address the phenomenon of relatively unchanged current generation by the MFC_{R5+R6} electrodes.

In correlating the current performance of both MFC_{R5+R6} and MFC_{R7+R8} to the performance of the 14 L MFC reactor previously described, an overall consistency is noticeable between the output of the first electrodes in relation to the influent points; R_5 and R_7. Using the average values mentioned earlier, during *phase 1*, both R_5 and R_7 demonstrated higher current production relative to R_6, and R_8 respectively; 0.954±0.059 mA and 0.746±0.110 mA compared to 0.844±0.042 mA and 0.611±0.027 mA respectively. This performance, as described in relevant research and as has been

shown here, is indicative of a greater organic load being available when entering the reactor, which subsequently decreases in moving towards the back of the reactor (Ren et al., 2014). However, the higher rate of increase in current generation for R_8 in relation to R_7 during *phase 2* might indicate a higher organic load being introduced in the reactor than the electrogenic community of R_7 could consume in the time provided, thus allowing for higher organic content to reach R_8, subsequently increasing the rate and value of the current produced. Similar contradictory behaviour was monitored by Winfield et al. (2011) where, in a series of hydraulically connected MFCs, the reactors in the middle recorded higher voltage outputs when fed with higher concentrations of acetate than in a first case using lower concentrations. The quantitative data which would be needed for the hypothesis to be verified is not available; therefore, the argument requires further examination during which the collection of values and/or effluent analysis in each chamber would be necessary.

Finally, in relation to this part of the experiment, a short comparison between all four sub-reactors should be made. By combining and summarising the results and conclusion made above, it can be deduced that the sub-reactors within the $MFC_{R1\text{-}R4}$ 122 L reactor demonstrated similar trends, whereas the sub-reactors within the $MFC_{R5\text{-}R8}$ had different trends, both in regards to the amount of current generated and the response to the reduction of HRT. Therefore, amongst all four sub-reactors, reproducibility cannot be verified. In order to address this issue and for future applications analysis of the microbial community is necessary. Such an analysis will provide an insight on potential differences in the microbial communities of each anode and each reactor and a correlation between the microbial content and electrical performance will be possible.

After the start-up period which lasted for only 5 days for both sub-reactors of the 122 L reactor $MFC_{R1\text{-}R4}$ and for approximately 14 days for $MFC_{R5\text{-}R8}$, the effluent quality performance was measured and is presented below. Even though the start-up times were slightly different for the four sub-reactors, sampling for effluent quality started on the 5^{th} day for all of them and pH and electrical conductivity data were recorded according to the methods discussed in Chapter 3.4. In Table 6-1, the two parameters are presented and compared in relation to the relative hydraulic retention time for the two 122 L reactors since the samples for both were collected at the very rear end of the reactors where the streams of the two sub-reactors were merged and exited together. As could be verified

during the longer HRT of 4 days, the pH variation was minimal from the influent stream at 7.6±0.2 to the effluent for both MFC_{R1-R4} and MFC_{R5-R8}, exiting at averages of 7.7±0.2 and 7.8±0.3 respectively. Similarly, during the optimisation of HRT at 1 day, the change in pH was minimal with the value being reduced by 0.2 for MFC_{R5-R8} while the rest remained steady.

Electrical conductivity demonstrated a slightly different pattern of development. For the first operational period the values recorded are shown below, and as can be seen, the average conductivity from the influent stream to the effluent stream increased, by 341 µS/cm for MFC_{R1-R4} and by 298 µS/cm for MFC_{R5-R8}. In contrast, the increase recorded during the shorter HRT was almost halved, recording a change by 65 µS/cm and by 102 µS/cm in MFC_{R1-R4} and in MFC_{R5-R8} respectively. This result is consistent with those recorded by previous experiments, and can be linked to the degradation of more complex compounds due to the biological treatment that increases the ionic strength. Achieving and maintaining higher levels of conductivity in the MFC reactors is of great importance since increased conductivity has been linked to increased power outputs (Feng et al., 2008; Cheng and Logan, 2011). If the increase in conductivity is due to this phenomenon, then the 'lower increase' monitored during the increase in the organic load rate could then be linked to the less effective degradation of more complex compounds, thus indicating a less effective treatment performance during the later period. However, further research and in-depth chemical analysis of the effluent would be necessary in order to verify that argument.

Table 6-1: *Changes in the average values for conductivity and pH for both reactors*

	PH			**EC (µS/cm)**		
HRT	Influent	MFC_{R1-R4}	MFC_{R5-R8}	Influent	MFC_{R1-R4}	MFC_{R5-R8}
4d	7.6±0.2	7.7±0.2	7.8±0.3	2841±422	3182±448	3139±449
1d	7.6±0.3	7.7±0.3	7.6±0.3	2690±277	2755±492	2792±351

The levels of influent and effluent tCOD as well as the removal efficiency of both sub-reactors within MFC_{R1-R4} during *phase* 1 of HRT=4 days are presented in Figure 6-7. It should be noted at this point that the sampling ports for the separate sub-reactors for both 122 L larger reactors failed after the first 50 days of operation. The recovery of

samples led to an unintended extraction of biomass which on the one hand led to the microbial community being compromised, and on the other hand led to false high effluent tCOD values. For that reason, results are not presented for *phase 1* after that day. It can be seen in particular that the influent tCOD varied greatly throughout the period, with the minimum value reaching as low as 430 mg/l and the maximum as high as 4610 mg/l, while the average level was calculated at 1525±1109 mg/l. Unlike the influent, the effluent exiting both sub-reactors demonstrated a considerable stability except in a period of approximately 15 days for MFC_{R3+R4} when the output seems to have been higher, correlating to the respective increase of the influent value. Additionally, in order to steady the effluent output, the two sub-reactors demonstrated almost identical performance both before and after the 15-day period of variance of the second sub-reactor, as Figure 6-7 verifies, with overall averages of 285±62 mg/l and 384±219 mg/l for MFC_{R1+R2} and MFC_{R3+R4} respectively. Values for the removal efficiency of tCOD greatly varied, and given the steady performance in relation to the effluent output, that could be a result of the great variance in the influent tCOD. E_{tCOD} reached as low as 35.45 % and 29.77 %, and as high as 93.88 % and 94.54 %, while the average values were 73.78±16.16 % and 68.12±17.71 % for MFC_{R1+R2} and MFC_{R3+R4} respectively.

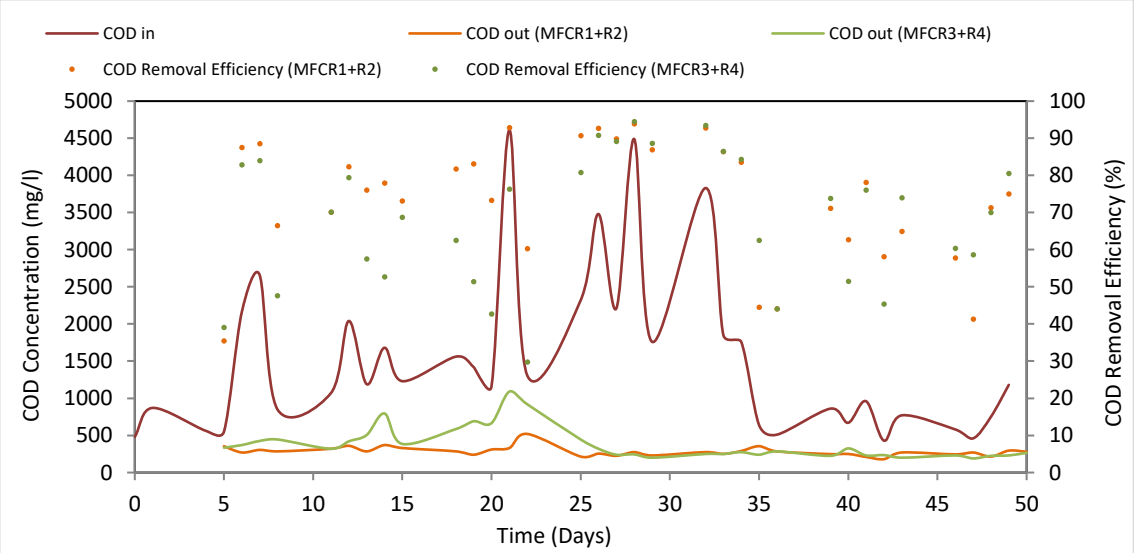

Figure 6-7*: t*COD performance for HRT=4 days for MFC_{R1+R2} and MFC_{R3+R4}

The second 122 L reactor demonstrated a different performance in relation to the effluent levels of tCOD, which varied between the two sub-reactors thus leading to varying removal efficiencies, which in some cases (specifically for $MFC_{R7+}R_8$) even reached a negative value. Average tCOD values for the effluent streams were 360±330 mg/l and

593±184 mg/l for MFC_{R5+R6} and MFC_{R7+R8} respectively, achieving a removal efficiency of 72.57±16.13% and 50.35±28.46 %. By comparing the values of the average removal efficiency of the four sub-reactors, it is evident that the first three of the four achieved very similar results, but the last one demonstrated approximately 25 % lower removal efficiency.

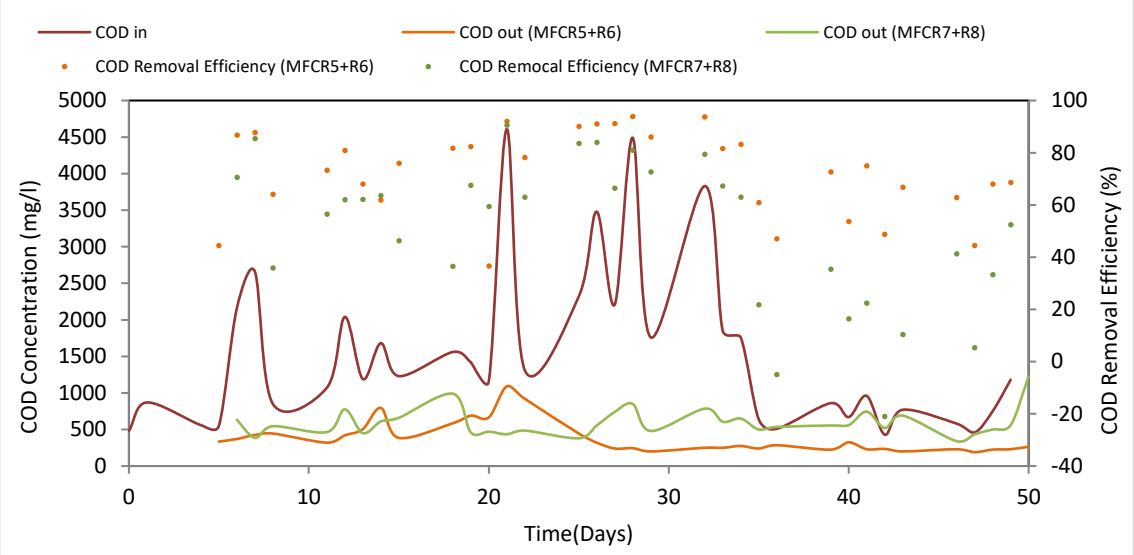

Figure 6-8: *tCOD performance for HRT=4 days for MFC_{R5+R6} and MFC_{R7+R8}*

After the failure of the sampling ports, sampling of effluent quality resumed for *phase 2* on the 120th day. However, the only ports that could provide a sample without leaked biomass were at the very last compartment. This was a point at which effluents exiting the two sub-reactors were already combined into one final stream exiting the 122 L reactor. Therefore, the results for *phase 2*, refer to the combined stream of MFC_{R1+R2} and MFC_{R3-R4}, shown in the figure below as MFC_{R1-R4} and MFC_{R5-R8} respectively. It is assumed for the purposes of further analysis that the tCOD value is identical for the two sub-reactors. tCOD influent greatly fluctuated over time during HRT=1 day as it is shown in Figure 6-9 for MFC_{R1-R4} and in Figure 6-10 for MFC_{R5-R8}. Effluent tCOD values and on tCOD removal efficiency are also shown in these figures. Average influent tCOD values was 1971±813 mg/l, and for effluent values it is evident that relatively steady outputs were achieved during the reduced HRT period. Specifically, average tCOD effluent values were 501±112 mg/l for MFC_{R1-R4}, and 498±105 mg/l for MFC_{R5-R8}. However, tCOD removal efficiency, which was obviously affected by the fluctuation of influent, similarly fluctuated. 70.59±12.48 % tCOD removal efficiency was achieved by MFC_{R1-R4}, and 70.97±11.49 % was achieved for MFC_{R5-R8}.

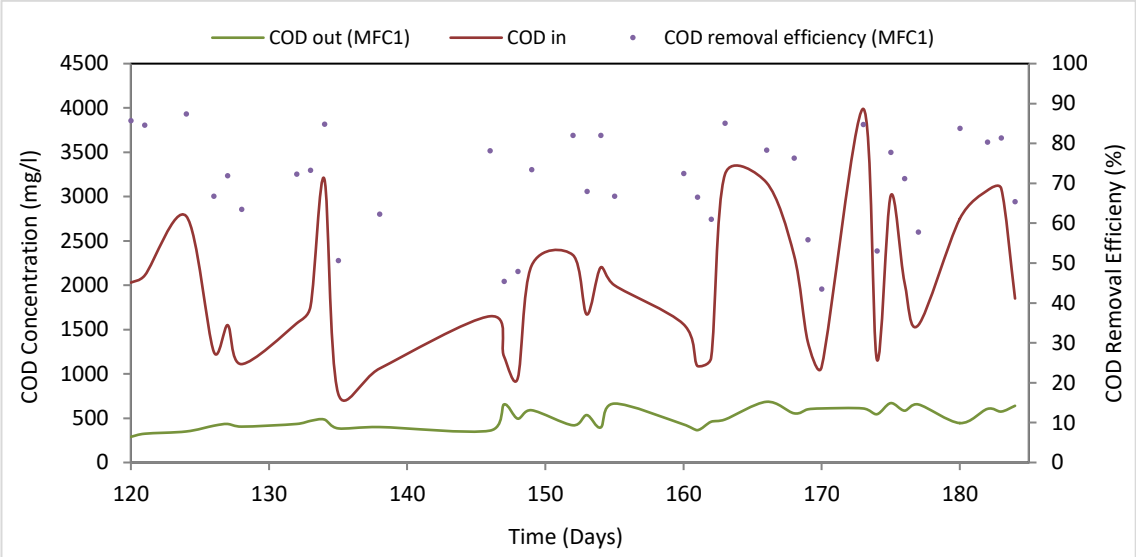

Figure 6-9: *tCOD performance at HRT=1 day* $MFC_{R1\text{-}R4}$

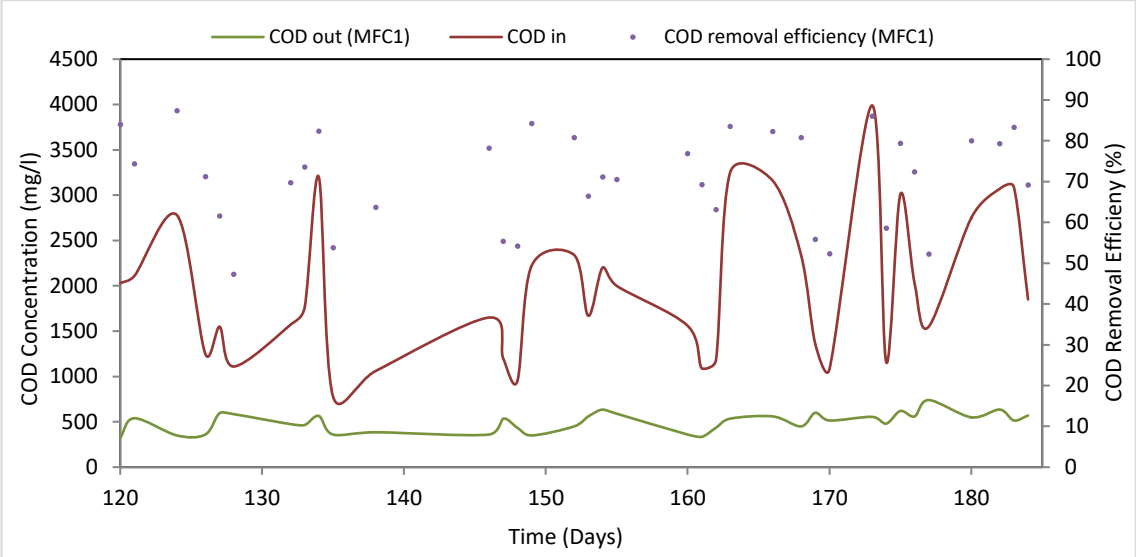

Figure 6-10: *tCOD performance for HRT=1 day for* $MFC_{R5\text{-}R8}$

The tCOD values achieved were almost identical for the two reactors in this case, and what is of additional interest is that for $MFC_{R1\text{-}R4}$, a slightly increased tCOD effluent value was achieved after the 145th day. This could relate back to the sharp increase in current generation shown in Figure 6-4. However, if the increase of current generation could be connected to a reduction of tCOD removal efficiency, an indication of which is an increase in final effluent value, then it could be argued that tCOD reduction was not achieved directly due to electrogenic activity, but was possibly due to the synergetic or antagonistic activities of the microorganisms present in the reactor. For this argument to be verified or dismissed, more insight into the microbial community would be necessary in order to identify the species involved and their activities. However, due to the

destructive nature of the sampling process, such an investigation was not possible in the experiment, so further research would be necessary to address the relationship between an increased electrical current and the possible adverse effects on tCOD removal efficiency.

Additionally, by comparing the average values achieved during *phase 1* and *phase 2* it can be seen that for both sub-reactors of $MFC_{R1\text{-}R4}$, the increase of organic load rate resulted in higher tCOD values exiting at the final point, which therefore had an adverse effect on effluent treatment. No conclusive comparison can be made for the second reactor since the values for *phase 2* are higher than those of MFC_{R5+R6} but lower than MFC_{R7+R8}, thus making it impossible to directly link the decrease of HRT to performance in terms of effluent quality.

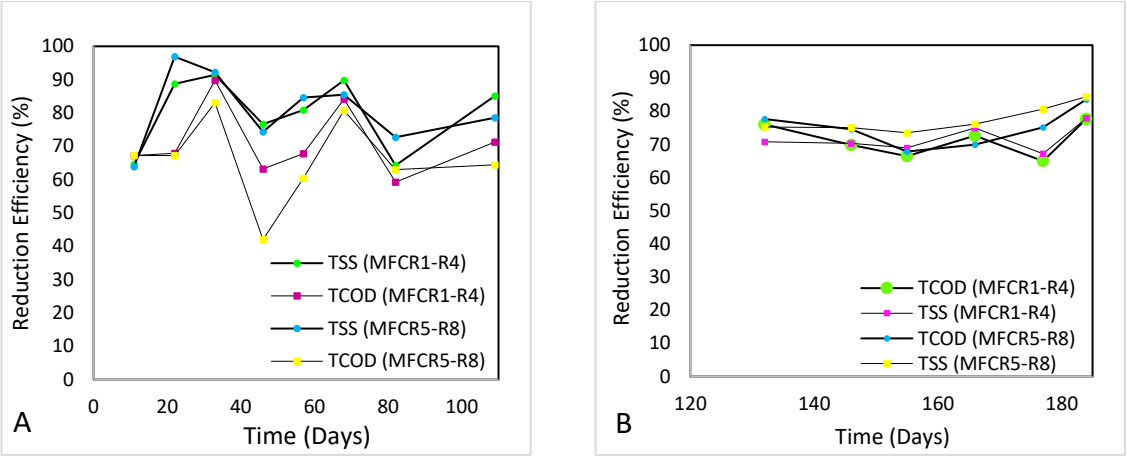

Figure 6-11: *Total suspended solids during (A) phase 1 and (B) phase 2*

As a last step in this experimental period, the tSS value was measured using the same principle described earlier. Average values were reported on a weekly basis, and are summarised in Figure 6-11, in (A) for *phase 1* during HRT=4 days and in (B) for *phase 2* for HRT=1 day. The removal efficiency of solids equally varied, with values ranging in a similar way to those for tCOD. However, it would be more appropriate to say that given the total tCOD value is affected by the suspended solids content in a total measurement (no filtration or centrifuge), a variance in the figure for total solids removal would similarly affect the removal of tCOD, which can also be seen above. Overall, during *phase 1* between the two sub-reactors of $MFC_{R1\text{-}R4}$, 80.07±17.34 % of total suspended solids were removed, while for $MFC_{R5\text{-}R8}$ the average removal rate was 80.33±14.00 %, an almost identical performance for the two reactors. Finally, during

phase 2 the respective totals of suspended solids removed were 74.32±13.77 % and 76.95±11.97 % which was marking a reduction in efficiency. This is in accordance with the previously made argument that effluent quality is adversely affected by the reductions in the treatment cycle and can more clearly be seen here in the context of total suspended solids.

6.3.2 *In situ refurbishment process of modified 122L MFC with sub-reactors*

Upon the completion of *phase 1* and *2*, the first experimental cycle aimed at integrating an MFC into an existing whisky co-products treatment plant was carried out. In order to further examine the MFC's operation under a different electrical regime (continuous discharge method) and until the relative failure of the system, the two MFC reactors were refurbished in situ according to the previously established procedure. The anodes were removed and the adapted microbial community was harvested. The anodes were then rinsed with distilled water, according to the maintenance process followed in section 5.3.5 for the retro-fit of the prototype reactor. Following the first cleaning process, the anodes were then placed in a weak hydrochloric acid solution (0.05M HCl) for two hours in order to remove the remaining organic matter prior to their re-use, before being thoroughly rinsed for the second time with distilled water. The cathodes were cleaned with distilled water. Biofilm, similar to that observed during the first refurbishment of the Heriot-Watt reactor was observed on the surface which had been in contact with the anodic compartment, and was fully removed with fine cloth while exercising caution in order to avoid damaging the coated cathode surface; a process also described in an earlier study by Zhang et al. (2014). Finally, the two reactors were filled with fresh water, in order to assess potential leakages, and fix any which were found. No leakages were observed and therefore, re-inoculation was carried out.

The harvested adapted biomass was re-inoculated into the reactors, enriched with fresh anaerobic granular biomass collected from the anaerobic digester operating in the distillery at a 1:1 ratio. Serial transfusions of adapted microbial communities have been found by researchers to be an effective way of utilising adapted microorganisms to strengthen the performance of electrogenic communities, while minimising the time needed for start-up (Logan, 2008; Cusick et al., 2011).

Additionally, during the later *phase-3*, the anodic electrodes of the MFC_{R1+R2} sub-reactor, R_1 and R_2, were replaced with the design described in Figure 3-4 (A) in order to further examine the suitability of the materials for the 122 L prototype. Lastly, solely for the start-up process and for a single application, the cathodes were sprayed with HCl solution (0.1M) on the air breathing side in order to mimic the original design including the electrolyte absorbed from the carbon cloth member in the cathode structure, to enhance the cathode reaction (Fedorovich, 2012). The hydraulic retention time was maintained at 1 day, as had previously been achieved, unless stated otherwise.

6.3.3 *How long until failure? Electrical performance according to power curves (phase 3)*

During *phase 3* the reactors were operated continuously under external resistance (unlike the previous electrical regime), and connected to a data acquisition system. Various resistances were examined, and one sub-reactor, MFC_{R1+R2} was also operated with a different anode. The results during this phase are examined in two different ways in relation to electrical output. To begin with, in order to explore the effects of the different materials and construction used in the anodes of the first sub-reactor, a comparison is established of the respective anodic potential of MFC_{R3+R4}. Additionally, the power output of each electrode is compared through power curves, therefore tracing it in relation to current over two different time periods. Finally, power density is used in this section to describe the development of performance over time, as was previously done. Therefore, in the later part of this phase, a comparison of these two methods is attempted. For effluent quality, all the major parameters are monitored, including pH, tCOD and Tss.

Upon the establishment of a successful re-start up period, the anodic potentials against the current of each electrode of the two sub-reactors of MFC_{R1-R4} were recorded and are presented in Figure 6-12, (A) for R_1 of MFC_{R1+R2} against R_3 of MFC_{R3+R4}, and (B) for R_2 of MFC_{R1+R2} against R_4 of MFC_{R3+R4}. This was necessary in order to be able to establish the differences in electrical performance between the two constructions and materials used. In the figure below, it might appear that electrode performance was almost identical between R_1 and R_2 and R_3 and R_4. However, a significant difference can be noticed if compared against current generation. The potential of R_1 and R_2, which were made entirely of woven carbon tow, sharply decreased with the increase in current generation with the maximum value of -428 mV achieved at the minimum current of 0.071 mA, and

the minimum potential of -281 mV at 5.442 mA for R_1, while for R_2 respective values were -418 mV at 0.115 mA and -257 mV at 8.300 mA. Unlike carbon tow, the complex construction based on carbon cloth, conductive adhesive and activated carbon granules (which were only initially impregnated with catalyst) maintained very similar levels of potential against current generation with the first ranging from a maximum of -437 mV at 0.085 mA to a minimum of -413 mV at 13.842 mA for R_3, and a maximum -442 mV at 0.182 mA against a minimum of -358 mV at 22.558 mA.

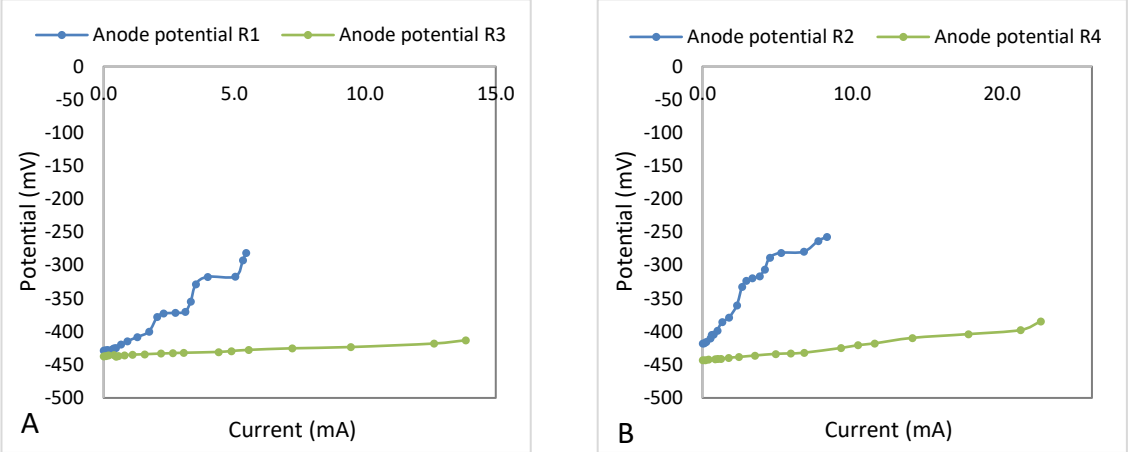

Figure 6-12: *Comparison of anode potential over current of (A) R_1 vs R_3 and (B) R_2 vs R_4*

It is clear with regard to the potential generated by the complex design anodes that even though it starts at the same levels, it can be maintained while achieving considerably higher current levels. This can be contributed to the lower internal resistance and higher surface area, which in this case was difficult to estimate. However, historically, taking into consideration the materials in principle, the complexity of the second design has contributed towards a higher potential (Rabaey et al., 2005; Logan et al., 2007). Additionally, the relatively linear nature noticed for the complex anode design indicates that activation and concentration losses in the electrode are negligible (Larminie and Dicks, 2003).

Power curves were also plotted in order to monitor the development of performance over the following six months. Specifically, they were plotted beginning with the establishment of the start-up process and after six months for each electrode, and are presented in Figure 6-13. The maximum power varied between the electrodes, so an average value would not be a representative value. Instead, a comparison between electrodes of identical construction is attempted. The maximum power output for R_1

reached 0.660 mW and had only slightly decreased to 0.549 mW after six months, unlike R_2, the power output of which increased during the same period from 1.004 mW to 1.243 mW. On the one hand this indicates the long term suitability of the cloth electrode, while on the other hand the increase in the case of R_2 could be linked to a better adaptation and attachment of the microbial structure, resulting in more efficient electron movement (Rabaey et al., 2005; Logan, 2008). However, apart from indications in relevant research, an analysis of the microbial community would be necessary in order to identify the potential differences and eventually gain more precise insight into the reason behind the increase in power output.

The performance of the identical complex electrodes demonstrated similar trends for the remaining six. The maximum power output for R_3 cannot be directly compared to that of R_4 because the first achieved 2.394 mW while the latter reached 6.917 mW. This is in accordance with the findings of Chapter 5, according to which the output of the first electrode in the row is lower than the second, possibly due to an excess of nutrients passing into the second anodic chamber due to an excessively high feeding rate. The power outputs of R_5 and R_6 were at similar levels at the start of *phase 3*, achieving 7.013 mW and 6.361 mW respectively, while R_7 and R_8 had a power output of 10.736 mW and 9.547 mW respectively. As is verified in Figure 6-13, over the course of the following six months the maximum power output for all six complex anodic electrodes decreased to an average of 25 % of the original output, leading to outputs of 0.864 mW, 1.275 mW, 0.619 mW, 2.988 mw, 2.487 mW and 2.381 mW for R_3, R_4, R_5, R_6, R_7 and R_8 respectively. Overall, it is evident that the relatively uninterrupted operation led to a considerable deterioration in performance. However, a last point should be raised here, which is that even with the evident deterioration in power output, the complex anodic electrodes made from carbon cloth, conductive adhesive and graphite granules have still clearly outperformed those made from carbon tow. Even though estimation of the surface area of the latter is very difficult, this could be attributed to the fact that the complex design has a higher surface area, leading to higher power outputs.

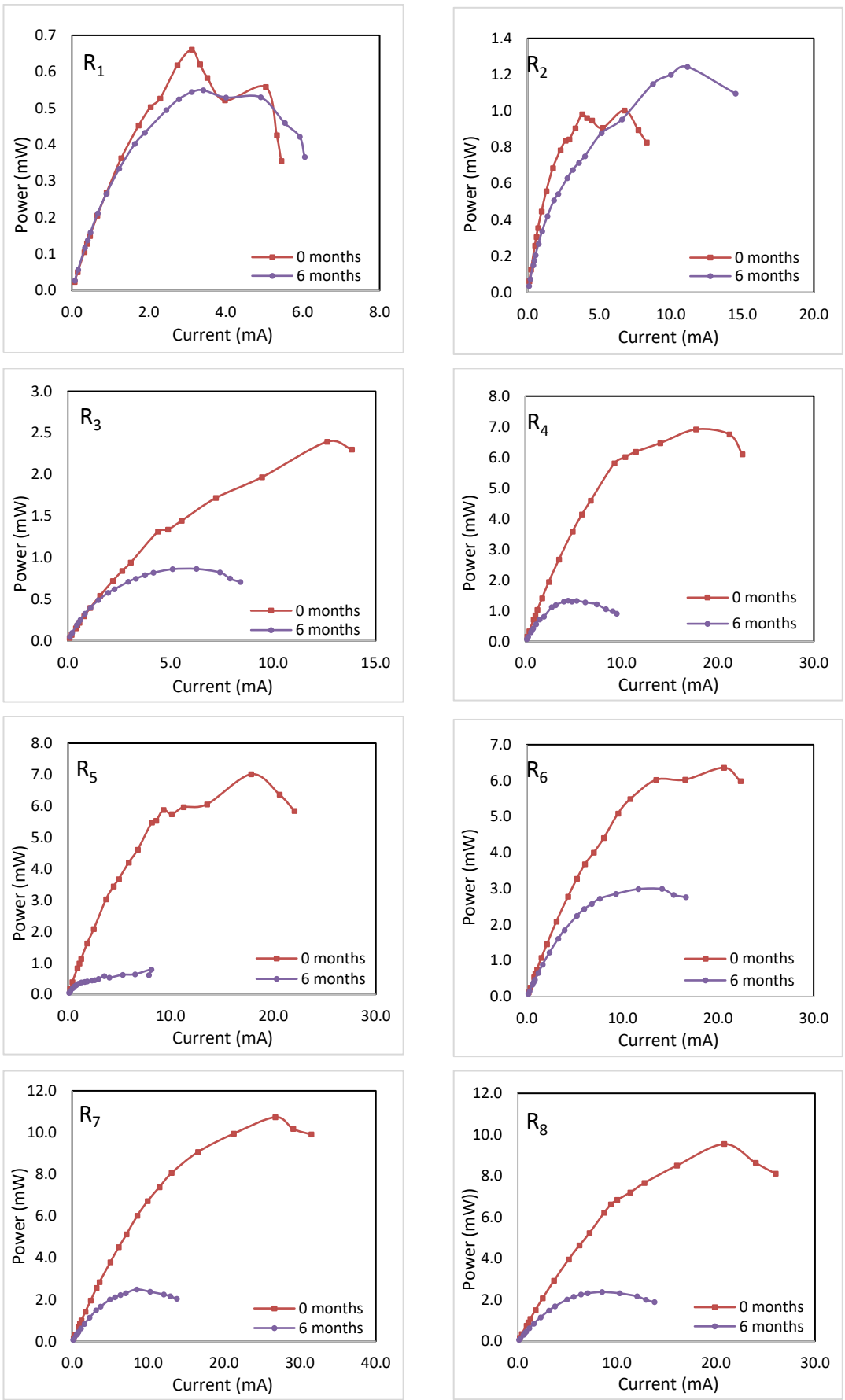

Figure 6-13:*0 and 6 months' deterioration in performance according to power curves for each electrode*

6.3.4 *How long until failure? Performance according to current generation under different external resistances (phase 3)*

Within the period of six months until the relative failure decision point, two different external resistances were implemented as long term working resistances: 10 Ω for the first 50 days, and then for the remaining time every electrode was operated according to the external resistance for which the majority of the electrodes achieved their maximum power points which was 22 Ω.

Figure 6-14 (A) depicts the power outputs for MFC_{R1+R2} and MFC_{R3+R4} as sub-reactors and not as single electrodes, while Figure 6-14 (B) depicts the power for MFC_{R5+R6} and MFC_{R7+R8} respectively. Power was chosen for analysis and presentation instead of other electrical indicators, such as current, as it would allow for a direct comparison between this representation of MFC performance and the power output as presented above through the power curves. As can be verified, the performance during *phase 3* greatly varied between the sub-reactors. During the first 50 days, the power output for MFC_{R1+R2} demonstrated a steady performance at an average 1.662±0.615 mW with minimal peaks, unlike MFC_{R3+R4}, for which the power output greatly fluctuated from a maximum of 17.632 mW to a minimum of 1.182 mW, with an average of 4.338±2.572 mW. MFC_{R5+R6} demonstrated a steady performance similar to MFC_{R1+R2}, with an average power output of 1.557±0.477 mW. It can also be seen that unlike what is suggested from the power curves previously described, the levels of power output achieved by the tow design are in fact almost identical (with regards to average value) to the complex design. The power output of MFC_{R7+R8} demonstrated a wide fluctuation similar to the second sub-reactor, moving from a minimum of 0.367 mW to a maximum of 10.394 mW, while the average output was calculated at 4.304±2.451 mW.

In summing up the results over the first 50 days of *phase 3*, it can be noticed that they are divided into two groups: two of the sub-reactors demonstrated significant fluctuations in their performance, whereas the remaining two showed a steady power output with very little variance. The possible reasons why this happened can be mostly attributed to blockages and to the technical failures experienced particularly throughout the last stage of the reactors' life in relation to the overall integration. Biofouling, both on the inner and outer sides of the cathode, was either noticed or expected as per the previous findings, which certainly negatively affected oxygen uptake by the cathodes. Maintenance during

the first operational period of 50 days was not attempted, but it would be expected that a simple cleaning of the outer cathode area should lead to an increase in power output, as previous research has also indicated (Zhang et al., 2013b, Zhang et al. 2014). Concerning the system set-up and integration into the existing process, blockages in the influent piping which led to biofouling of the pipe work were regularly noticed. The built-up solids in the piping would lead to an increased tCOD value, which would then also lead to an irregular power output. However, if that was the main reason for the fluctuating power output, then it should have been recorded for every sub-reactor given that the influent feed was common to all four. Two out of the four sub-reactors demonstrated considerably steady outputs; therefore, further research to address this issue is necessary.

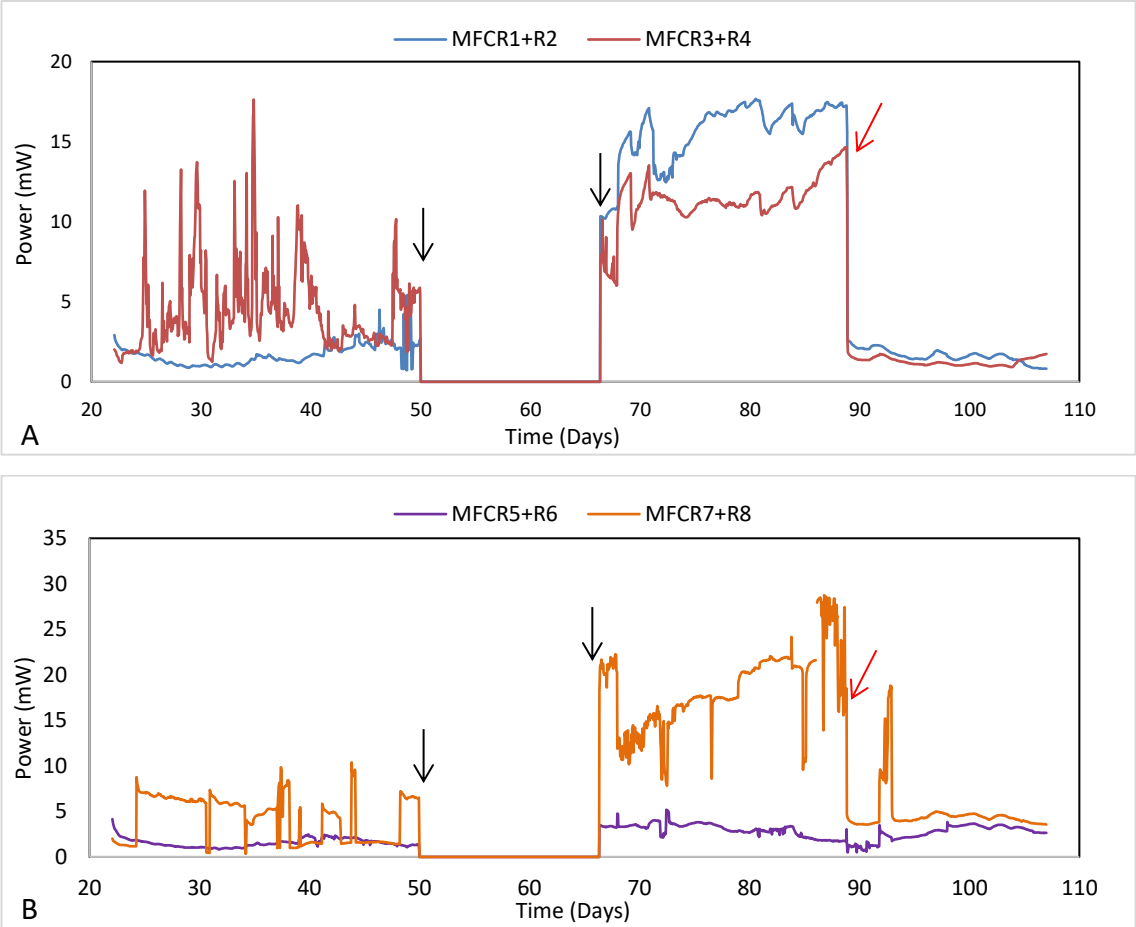

Figure 6-14:*Power output of the two 122 L reactors presented at a sub-reactor level; (A) sub-reactors* MFC_{R1+R2} *and* MFC_{R3+R4} *and (B) sub-reactors* MFC_{R5+R6} *and* MFC_{R7+R8}

For practical applications of MFC technology and its integration into industrial scenarios, it is important to be able to examine performance in adverse conditions. For this reason, in order to examine the effects of potential blockages in the feed, a situation in which the feed was completely ceased and the MFCs were virtually 'unplugged' was attempted. It

is often the case that industrial effluent treatment establishments do not operate continuously but rather according to demand, or their processes are paused for a specific period for maintenance. For a period of approximately 15 days, the feed was therefore stopped, and the sub-reactors were switched to open circuit mode and the microbial community was left in suspension. The two black arrows in Figure 6-14 indicate the shut-down and re-start of the four sub-reactors respectively, during which they were left in 'sleep mode'.

Open circuit voltage during 'sleep mode' was reached within the first day and demonstrated surprising stability, which can be also verified, but there was some variance, with average values at 274±11 mV, 467±18 mV, 377±23 mV and 695±6 mV for R_1, R_2, R_3 and R_4 respectively in the first reactor, while for the second 122 L reactor the average values were 605±26 mV, 608±16 mV, 634±7 mV and 613±7 mV for R_5, R_6, R_7 and R_8. Following this period of 'sleep mode', when all sub-reactors successfully recovered and maintained their maximum potential, every electrode was connected back to an external resistance of 22 **Ω**, which corresponded to the maximum power point resistance for the majority of the working electrodes.

Figure 6-14 shows that upon reconnecting the electrodes under the external resistance, the power generation sharply recovered within the first few hours. Additionally, an increasing trend, which was steadier than previously seen was noticeable, with average power output of 15.610±1.924 mW and 11.334±1.568 mW for MFC_{R1+R2} and MFC_{R3+R4} respectively, while for MFC_{R5+R6} and MFC_{R7+R8} average values were at 3.020±0.681 mW and 18.514±4.331 mW, up until the 88th day. This performance contrasted with previous results, especially for the MFC_{R1+R2} and MFC_{R5+R6} sub-reactors which had previously demonstrated steady yet considerably lower power output.

In order to determine that the increase in power was due to increased microbial function and not due to corrosive current, it was decided to clean the working electrodes and implement maintenance on the external electrical connections, without interrupting the anodic electrodes and microbial community (see the red arrow point in Figure 6-14). The power output recorded after the cleaning process demonstrated a steady performance but at much lower levels than before, thus verifying that the performance has been overestimated due to a galvanic current attributed to failing, corroded electrical

connections. It was established that the true external resistance was considerably higher, resulting in wrongly estimated power outputs; this can be considered a point of failing performance. For the remaining period of approximately 18 days, the power outputs were steady apart from a peak noticed at MFC_{R7+R8}, which was possibly due to electrical connection failure as had happened previously, with average values of 1.630±0.391 mW, 1.262±0.236 mW, 2.624±0.819 mW and 4.709 mW achieved for MFC_{R1+R2}, MFC_{R3+R4}, MFC_{R5+R6} and MFC_{R7+R8} respectively. Therefore, if it is accepted that the performance prior to the cleaning of the electrical connections was due to the galvanic current, that this was therefore not the 'true' power, the latest power values should be considered representative of performance under R_{ext}=22 Ω.

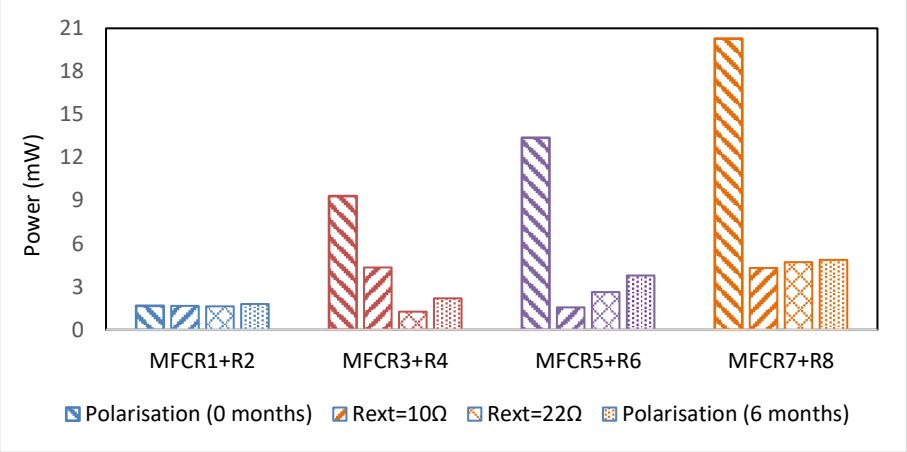

Figure 6-15: *Comparative power performance of the four MFC sub-reactors according to polarisation data at 0 months and 6 months and performance under R_{ext}=10 Ω and R_{ext}=22 Ω*

In order to summarise the power performance under the different working conditions over time and to emphasise the necessity of both polarisation curves and continuous performance under an external resistance, Figure 6-15 is presented above. The power according to the polarisation data at 0 and 6 months is represented as well as the average long term performance under external resistance values of 10 Ω and 22 Ω. The original arguments can be verified, as for MFC_{R1+R2}, power was maintained over time except at relatively lowest levels. On the other hand, the performance of the complex electrodes clearly sharply deteriorated with time, keeping in mind that a single spray of HCl solution was applied to the cathodes upon start-up. Therefore, even though the carbon tow can be said to demonstrate long term sustainability and credibility, it is still outperformed by the complex anodes. Finally, as was suggested before, polarisation curves tend to

overestimate the power output potential of an MFC, highlighting the necessity of a long term examination to gain a more 'realistic' insight into an MFC's working performance.

That said, the value which truly brings together treatment and electrical efficiency and which might have shown a different pattern of development throughout time is coulombic efficiency. Therefore, the Table 6-2, below, summarises E_{tCOD} and coulombic efficiency at different R_{ext} for the two reactors with different anodes. Even though the maximum power point was observed to be at an external resistance of 22 **Ω** for the majority of the electrodes, it is noticed that coulombic efficiency was greater at the external resistance of 10 **Ω**, with the maximum value achieved by electrode R_4 at the average of 7.61±2.63 %, followed by R_1 and R_2. These results in regards to their quality can be verified by Figure 6-15, where it can also be seen that R_1 had the poorest performance. This performance can be attributed to the different material used in these two electrodes which was carbon tow, and as it was also verified by the specific polarisation curves, it was outperformed by the complex anode construction. However, tCOD removal efficiency demonstrated a different behaviour for the sub-reactor with the carbon tow. The tCOD removal efficiency for MFC_{R1+R2} was the second highest reported during R_{ext}=10 **Ω** at an average of 67.14±9.64 % and the third highest for R_{ext}=22 **Ω** at an average of 84.88±5.98 %. This could be attributed to the fact that the carbon tow anode possibly acted as a filter, removing compounds contributing to the tCOD value. In both cases, in relation to tCOD removal efficiency, greater results were monitored during the external resistance of 22 **Ω**.

An energy balance was also performed for all four MFC sub-reactors for this last period of examination. The consumption of the pumps was calculated according to Equation 3-16 at 0.0033 kWh/m^3 for the pump feeding MFC_{R1+R2} and MFC_{R3+R4}, while for the pump feeding MFC_{R5+R6} and MF_{R7+R8}, energy consumption was calculated at 0.0003 kWh/m^3. The normalised energy recovery was also calculated according to the methods previously presented and the energy balance for the sub-reactors is presented below, in Table 6-2. After the sub-reactors were cleaned it was concluded that the increased power outputs were due to galvanic current because of considerable deterioration of the electrical connections. Therefore, an energy balance was produced for the second half of the operation under R_{ext}=22 **Ω**, the period for which it was concluded that the electricity production of the electrodes was solely due to the microbial community's function and not due to additional galvanic current. Energy recovery

demonstrated a slightly different behaviour. The specific values can be seen in the table below and it is obvious that for MFC_{R1+R2} and MFC_{R3+R4} more energy was recovered during operation under a 10 Ω external resistance, whereas for MFC_{R5+R6} and MFC_{R7+R8} NER was higher during R_{ext}=22 Ω. Keeping that in mind, examining the performance of the sub-reactors from Figure 6-15 in relation to power production, it can be noticed that MFC_{R1+R2} and MFC_{R5+R6} have maintained a steady performance both under external resistance of 10 Ω and 22 Ω, unlike MFC_{R3+R4} and MFC_{R7+R8} for which power fluctuated. This fluctuation, and the fact that for the latter two sub-reactors' power generation achieved a low, yet steady value after the cleaning, can be explained by that galvanic current occurred in occasions resulting in a higher, yet not real positive energy balance. Therefore, results regarding NER are rather difficult to correlate. In every case these results are approximately lower by a factor of ten in relation to recovery recorded in literature (Dong et al., 2015).

Table 6-2: *Summary of coulombic efficiency, tCOD removal efficiency, NER and energy balance*

	E_{tCOD} (%)		**CE (%)**		**NER (kWh/m^3)**		**Energy Balance**	
	10	22	10	22	10	22	10	22
MFC_{R1+R2}	67.14±9.64	84.88±5.98	0.93±0.27 1.14±0.3	0.48±0.15 0.77±0.22	0.001539	0.001508	-0.001761	-0.000179
MFC_{R3+R4}	66.95±9.49	85.70±6.01	2.30±1.54 7.61±2.63	0.61±0.19 0.44±0.14	0.004017	0.001167	0.000717	-0.000213
MFC_{R5+R6}	56.11±28.4	83.89±7.13	3.63±5.95 3.71±6.29	0.19±0.05 0.34±0.13	0.001442	0.002430	0.000114	0.000213
MFC_{R7+R8}	68.74±8.83	87.43±4.5	2.28±0.48 1.16±0.26	0.42±0.16 0.78±0.25	0.003986	0.004361	0.000369	0.000406

Finally, examining the overall system energy balance, it can be seen that negative values are recorded during both external resistances for MFC_{R1+R2}, which hosted the carbon tow anodes. This result supports the conclusion of this study, that the complex design electrode has provided a better electrical performance than the carbon tow. For the rest of the sub-reactors, mixed results are obtained. The energy balance was negative for MFC_{R3+R4} during operation under the 22 Ω external resistance, while the highest energy harvest was achieved by the same sub-reactor for the lower external resistance. Overall, it can be argued that the levels of energy harvested at this point are low contributing to

the notion that the MFC construction is failing. In comparison to prior results of this study, this can be considered the case. However, if compared to established wastewater treatment technologies such as the activated sludge process, which can consume 0.1-0.2 kWh/m^3 (McCarty, Bae and Kim, 2011), the MFC prototype sub-reactors proved that, even during what can be argued as the end of their life, they still consumed considerably less energy for treatment and in some cases made a small contribution.

6.3.5 *Effluent quality until relative failure (phase 3)*

With regard to effluent quality pH, total COD and total suspended solids and their subsequent removal efficiencies are examined for the latest part of the experiment, *phase 3*. Table 6-3 summarises the effluent quality in relation to the average maintained throughout the system on a sub-reactor level for the remaining six-months period. Specifically, tCOD is further examined in order to examine possible failure in more detail, as was done with power output. It is noticeable that the pH remained almost unaffected by the MFC treatment, maintaining a level of just above 7.7 for the $MFC_{R1\text{-}R4}$ reactor and just above 7.8 for $MFC_{R5\text{-}R8}$. In terms of suspended solids reduction, relatively high removal efficiencies were maintained, with minimal indications of failing performance. The highest removal was achieved at 73.44±14.44 % by MFC_{R1+R2}, the anode of which was the carbon tow. This can be attributed to the bulkier construction and the more complex pathways created by the tow, which possibly acted as a filter keeping solids in suspension from exiting into the effluent stream. Unlike the tow construction, even though the granule-based anodic electrode provided higher power outputs, it allowed for more solids to pass through, resulting in lower, yet still satisfactory removal efficiencies ranging from 57 % to 70 %.

Table 6-3: *Summary of effluent quality for the four sub-reactors (average values) until relative failure*

	tCOD (mg/l)	**E_{tCOD} (%)**	**tSS (mg/l)**	**E_{tSS} (%)**	**PH**
Influent	1342±654		640±380		7.7±0.3
MFC_{R1+R2}	261±80	76.31±12.21	161±97	73.44±14.44	7.7±0.3
MFC_{R3+R4}	300±83	73.26±12.89	181±117	70.09±16.51	7.7±0.3
MFC_{R5+R6}	237±94	80.35±9.26	263±150	57.55±25.33	7.8±0.4
MFC_{R7+R8}	269±88	77.15±9.97	233±102	60.01±19.63	7.8±0.4

Specifically looking at tCOD development during *phase 3*, as can also be verified by Figure 6-16 (and as monitored throughout the integration of the pilot construction in the wastewater treatment process), the influent tCOD values fluctuated considerably from 540 mg/l to 3237 mg/l while the average value was 1342±654 mg/l. Removal efficiencies developed at the same levels, with the average removal of the carbon tow based anode achieving the third highest rate, as can be seen in the table above. However, it is evident that the tCOD effluent values achieved throughout *phase 3*, during which the failure of the reactors was examined, were relatively steady and remained as such throughout the six months. Therefore, in effluent quality terms, the reactors remained in good working condition even though the electricity generation considerably declined after six months to a minimal level, as described previously. At this point it could therefore be argued that removal efficiency was correlated to activities other than electricity generation.

Prior research in the field has found that possible antagonistic microbial activities were responsible for COD removal, rather than electricity. According to Zhang et al. (2013b), a carbon balance revealed that the sulphate reduction process consumed considerably more carbon than electricity production did. For this reason, sulphates were examined throughout the latter part of *phase 3* and, in a departure from the findings reported by prior research, it was revealed that the values for the ADLD used as influent in this study were notably low. This could be attributed to the fact that the whisky distillation co-product has undergone anaerobic digestion as one of the initial steps of its treatment. Related research has shown that sulphates are converted to hydrogen sulphide by sulphate-reducing bacteria during anaerobic processes, inhibiting the process, and giving the characteristic smell to AD, but reducing the sulphates in the effluent stream. Therefore, for the purposes of this application, sulphate reduction probably does not act antagonistically to electricity generation due to its limited availability. Therefore, in order to address the mismatch of electricity production and its declining trend to a successful effluent treatment, further chemical analysis is necessary along with an analysis of the microbial community and its development until the point of relative electrical failure.

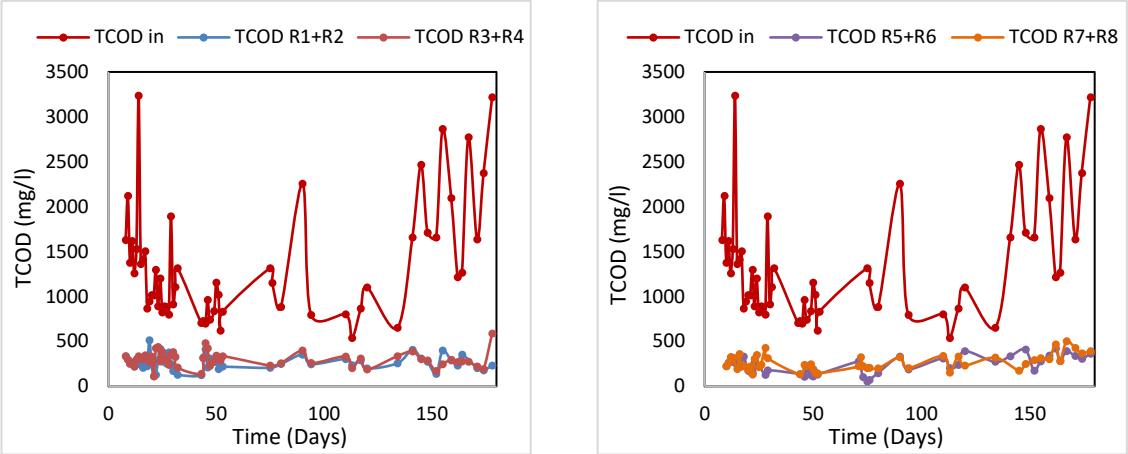

Figure 6-16: *Influent and effluent tCOD concentrations during phase 3 for (A) sub-reactors MFC_{R1+R2} and MFC_{R3+R4} and (B) MFC_{R5+R6} and MFC_{R7+R8}*

6.4 Perspective on the integration of the prototype reactor into existing treatment processes

On the first level, the lessons learned from the long process of integrating the pilot set-up within an existing treatment process are mostly of industrial or technical interest. Throughout the long experimental process, a variety of re-occurring issues were experienced. Due to the position of the pilot set-up within the process, ADLD was collected with a gravity-driven feed rather than through pumping. Therefore, biofouling was a significant concern throughout the process. The chosen feeding tube experienced very frequent clogging due to its relatively small diameter and insufficient pressure. In order to address that issue, constant maintenance was necessary, and aside from that, a sudden release of built-up solids was experienced. In relation to the collection system, due to insufficient mixing, colloidal solids were formed and frequently passed through the system. Finally, again due to insufficient mixing, the anaerobic microorganisms present in the influent eventually formed granular structures which were found to pass through the system. This uneven feeding regime, resulting in a greatly varying influent tCOD value, could not be attributed to an unsuccessful anaerobic process, but was instead due to engineering failures. These issues could be addressed in a future application either through an increased retention time, which here was proven to lead to subsequently higher tCOD removal efficiencies, an increased surface area per volume of reactor, and certainly with a better overall engineering of the system. This would allow for a faster transfer of effluent through the piping system, a lower residence time within collection systems, and even adequate mixing. In perspective, these should not be considered as issues due to the fact that if a further scale-up was planned and implemented, then process engineering

would ensure secure, adequate and necessary flows of effluent throughout the treatment process.

As could possibly be expected and as suggested in previous pilot studies (Logan, 2012; Janicek, Fan and Liu, 2014), albeit with regard to considerably shorter periods, the chosen materials became an issue towards the end of the reactors' life. Even though stainless steel was chosen for the external connections, they eventually degraded leading to corrosion issues and galvanic current. Subsequently, the electrical potential of the reactors was falsely overestimated. Maintenance can address that issue in the short-term, however, in the long term (which is the main goal), realistic applications should be reconsidered in terms of the selection of materials on an industrial scale. Given that materials are one of the main constraints to MFC commercialisation, it is necessary that this issue is addressed, possibly by following the example of already-commercialised industrial applications such as chemical treatment-based methods.

Additionally, for the purposes of this study, specific effluent parameters were monitored, including the basic ones of effluent quality determination, pH, tCOD, tSS and in some cases conductivity and a variety of micronutrients. However, in order to better determine these, to examine reasons for the failure of the MFC process in more depth, and to detect possible inhibiting processes, a full effluent characterisation is necessary as has also been previously suggested by Greenman et al. (2009) and Janicek, Fan and Liu (2014).

Even though these technical and engineering factors have adversely affected the overall output of the present study, it still managed to demonstrate a relatively successful integration of MFC technology into an existing treatment process for whisky distillation by-products. In the current model, the spent wash undergoes anaerobic digestion and subsequently regularly goes into an aerobic polishing step in order to meet the standards necessary for final discharge to the sewers. What has been suggested through the present investigation of this process is that the MFC prototype can work complementary to anaerobic digestion, unlike much prior research that has suggested that MFCs are competitors to AD technology (Pham et al., 2006). With some years still to go until full scale commercialisation, MFCs could prove a successful alternative to aerobic processes, that unlike MFC technology, consume large amounts of energy for their operation.

In many respects, this study has not confirmed the great power outputs reported in similar prior studies of laboratory scale experiments, in controlled environments, usually using artificial substrates. It is also certainly still some distance away from full scale commercialisation at its current outputs. However, if used along with other attempts of a similar kind, of MFCs in industrial environments, in realistic conditions, at ambient temperatures, with little maintenance and on real wastewater substrates, it is anticipated that the experience gained will lead to a fully successful application

6.5 Chapter conclusions

This chapter discusses the last of the field experiments carried out in this study. During this last part of the examination, a pilot set-up was integrated into an existing treatment facility. The set-up, consisting of two 122 L multi-electrode reactors, was successfully operated in the industrial environment for over a year, treating anaerobic digestion liquid digestate. This proved the MFC's potential to be used in the future after AD treatment, possibly instead of established but energy intensive technologies. The pilot demonstrated a long term, robust treatment potential since failure regarding electrical performance was found to be only due to technical issues, which are believed to be relatively easy to address in future applications. In terms of the wastewater treatment process, no failure was detected.

The chapter went on to examine two different experimental anode designs and concluded with the preferred design between the two. Experimental data collected during this later part are used in the following chapter in order to investigate the potential for using a simple electrochemical model to describe the performance of the pilot-scale prototype developed in this study. The present chapter, as part of the overall study, has shed some light on the field applications and integration in a real industrial environment of MFCs in the wastewater treatment sector.

Chapter 7 - Development of electrochemical model

7.1 Introduction

In this chapter, a basic electrochemical model is developed based on the activation, ohmic and concentration losses, occurring in a standard fuel cell of any kind, as has been described with reference to the polarisation curve in Chapter 2.8. The model was developed by subtracting the various losses from the thermodynamically-predicted voltage of a typical fuel cell. The model parameters were then estimated in *OriginPro* and the ohmic resistance (R_{ohm}) was used as the comparative parameter. Subsequently, R_{ohm} was calculated experimentally for all six electrode pairs (two complex design electrode pairs per sub-reactor), and compared with the value generated from the programme. The purpose of this chapter is to examine whether this simplified model derived from the standardised fuel cell characteristics can be used to describe the performance of a pilot scale MFC operating on real, industrial wastewater.

7.2 Materials and methods

The ohmic resistance of each electrode was determined with the current interrupt method. In this method, when the current is interrupted, ohmic losses are instantly eliminated (Clauwaert et al., 2009), resulting in a steep increase of potential E_R as can be seen in sections 2 and 3 of Figure 7-1, in potential that is proportional to the R_{ohm} and current I produced before interruption.

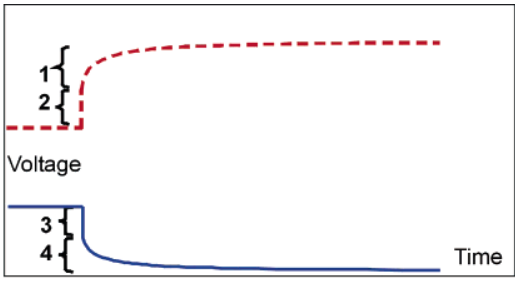

Figure 7-1: *Anodic and cathodic potential profile over time when applying the current interrupt method to determine ohmic resistance of the electrode*
(Source: Logan et al., 2006, p.5186)

According to Ohm's law ohmic resistance can be calculated as:

$$R_{ohm} = {}^{E_R}/_{I} \quad \textit{(7-1)}$$

The additional increase of potential, albeit at a slower rate, represents the electrode overpotential which occurs during current production (Logan et al., 2006). Since, as can

be seen, the ohmic losses disappear instantly, it is very important for the equipment used to be able to receive electrical samples down to fractions of a second. For this reason, the data acquisition system used during the latest part of the operation of the 122 L reactors collected voltage samples at a rate of 100 msec. Therefore, the experiment aiming to validate the model was carried out in the latter part of the previous operation, just before the end of life of the 122 L reactors, a fact which should be taken into consideration when examining and evaluating the results. Eight different external resistances on the ohmic spectrum were used (680, 470, 330, 220, 150, 120, 82 and 65Ω), and the experimental R_{ohm} refers to the average of the values calculated by them. As was mentioned earlier, the *OriginPro* data analysis software was used for the theoretical calculation of R_{ohm} based on the values obtained in the polarisation curves.

7.3 Results and discussion

7.3.1 *Electrochemical model development*

For all electrochemical systems, the real voltage output under a specific external load can be described by subtracting the various losses from the thermodynamically predicted voltage (Larminie and Dicks, 2003), as follows:

$$\boldsymbol{V = E_{thermo} - \eta_{act} - \eta_{ohmic} - \eta_{conc}} \quad \textit{(7-2)}$$

Where essentially, the real voltage (V) is the predicted potential difference between the two electrodes (E_{thermo}) minus the voltage losses due to kinetics (η_{act}), ohmic polarisation (η_{ohmic}) and losses due to mass transport (η_{conc}) respectively. For the following equations, 'a cell' will be regarded as one anode and cathode pair; thus, the following can be applied separately to each electrode in the multi-electrode reactor. Specifically, for each electrode the Tafel equation describes the activation overpotential as:

$$\boldsymbol{E = E_q + \frac{RT}{(1-a)nF} ln \frac{I_d}{i_o}} \quad \textit{(7-3)}$$

Where E refers to the electrode potential; E_q is the equilibrium potential of the electrode; R is the universal gas constant; T is the temperature; a is the charge transfer coefficient; n is the number of electrons involved in the electrode reaction; F is the Faraday constant; I_d is the current density and i_o is the exchange current density. In order to simplify the aforementioned equation constant B is introduced:

$$E = E_q + B\,ln\frac{i}{i_o} = E_q + B(ln\,i - ln\,i_o) = E_q - B\,ln\,i_o + B\,ln\,i$$
(7-4)

The first part of the equation can therefore be considered as a constant value A_{an} for the anodic electrode, and A_{cat} for the cathodic one along with B_{an} and B_{cat} respectively, resulting in:

$$E_{an} = A_{an} + B_{an}\,ln\,i$$
(7-5)

$$E_{cat} = A_{cat} + B_{cat}\,ln\,i$$
(7-6)

Returning to Equation 7-2, ohmic resistance for each electrode can be described as:

$$\eta_{ohmic} = IR_{ohm}$$
(7-7)

But in order to be consistent with the equation for voltage loss, the equation has to be expressed in terms of current density. To do so, the equation can be expressed as:

$$\eta_{ohmic} = iSR_{ohm}$$
(7-8)

Where i is the current density in mA/m^2, S is the cross sectional surface area of the electrode and in m^2 and R_{ohm} is ohmic resistance.

Moving the last component of equation 7-2, concentration losses are expressed as:

$$\eta_{conc} = c\,ln\left(\frac{i_L}{i_L - i}\right)$$
(7-9)

Which occur both for the anode and the cathode, where c is a constant depending on the operational conditions of every fuel cell and i_L is the limiting current density. An alternative approach that has no theoretical basis but was empirically established, has been used in the early stages of fuel cell description (Larminie and Dicks, 2003):

$$\eta_{conc} = mexp(ni)$$
(7-10)

This last equation has been shown to provide a good fit with the experimental results produced previously, and will therefore be used for the purposes of this study. However,

if the above equation is to be used, it should be noted that the logarithmic model does not work well at low currents, especially at zero, where OCV occurs.

Equation 7-2 can therefore be expressed in relation to the operating cell voltage by extracting the aforementioned irreversibilities from the cell's open circuit voltage:

$$\boldsymbol{V = E_{thermo} - (A_{an} + B_{an}\, ln\, i) - (A_{cat} + B_{cat}\, ln\, i) - iSR_{ohm} - mexp(ni)}$$
(7-11)

$$\boldsymbol{V = E_{thermo} - (A_{an} + A_{cat}) - (B_{an} + B_{cat})\, ln\, i - iSR_{ohm} - mexp(ni)}$$
(7-12)

The first part of the equation relates to the open circuit voltage, therefore the equation can be further simplified to:

$$\boldsymbol{V = V_{oc} - B\, ln(i) - iSR_{ohm} - mexp(ni)}$$
(7-13)

7.3.2 *Non-linear fit and analysis of polarisation curves*

The polarisation curves extracted for *phase 3,* as described previously (see Chapter 6.3.3), after six months of operation were used to perform a non-linear curve fit in *OriginPro*. The values of the parameters were calculated automatically by the software. The anodic electrodes of one of the four sub-reactors, MFC_{R1+R2}, were solely constructed from carbon fibre. Therefore, an estimation of the cross sectional surface area is very difficult to extract, so validation of the model was only attempted for the standardised electrode constructions of MFC_{R3+R4}, MFC_{R5+R6} and MFC_{R7-R8} (Figure 3-5), for which the area was calculated at 0.2994 m^2. Table 7-1, below, summarises the results obtained from the software.

Table 7-1*: Ohmic resistance (Ω) for each electrode as generated by OriginPro*

	R_3	**R_4**	**R_5**	**R_6**	**R_7**	**R_8**
R_{ohm} (Ω)	22.3010	42.7015	31.2035	32.9396	36.9681	31.8279

For the values generated and shown above, Figure 7-2 demonstrates the fitting of the polarisation curves for each standardised electrode, with the dotted line representing the curve and the red line representing the fitting according to the software.

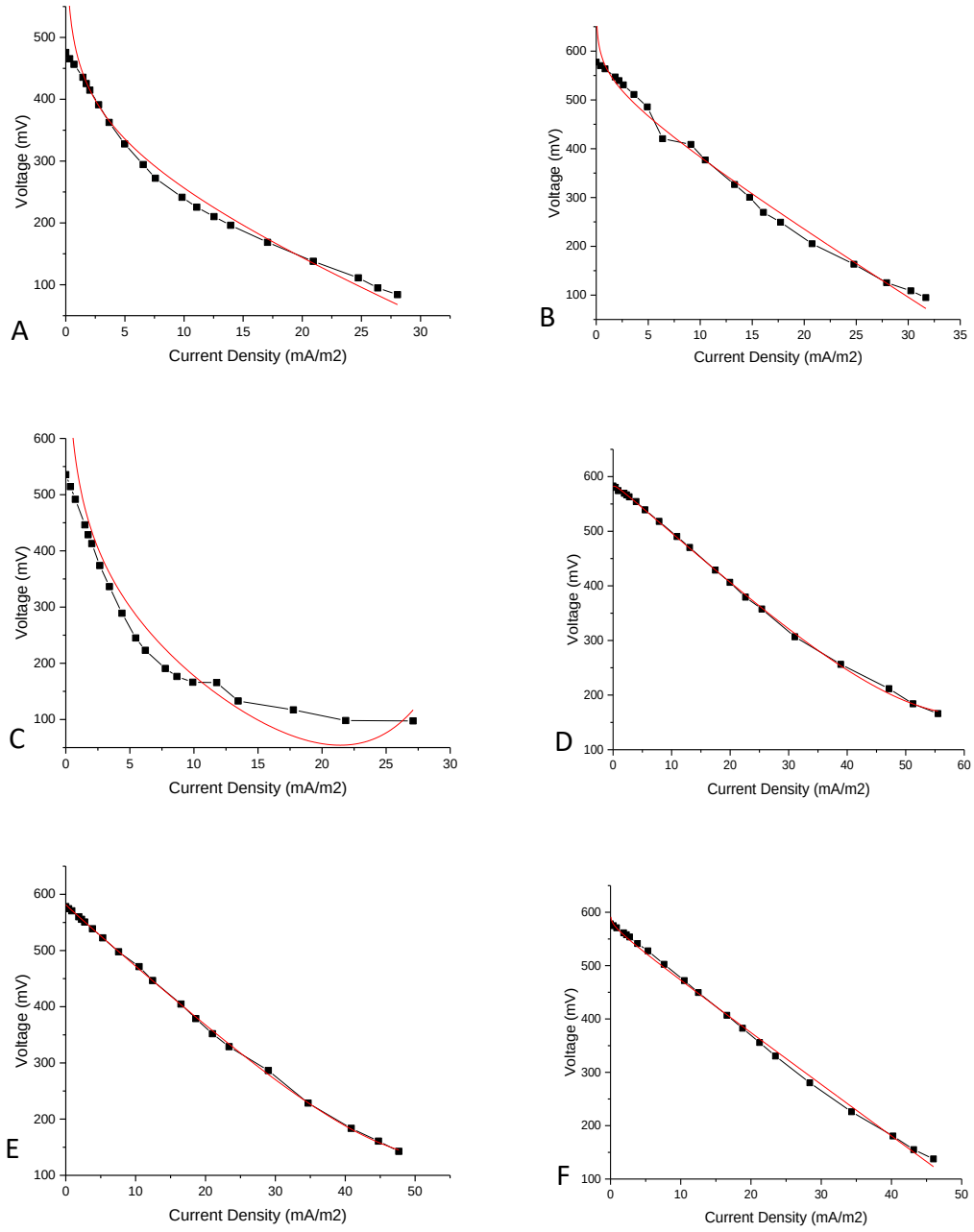

***Figure 7-2**: Non-linear fit of polarisation curve for electrodes (A): R_3, (B): R_4, (C): R_5, (D): R_6, (E): R_7 and (F): R_8 as generated by OriginPro*

In order to validate the model and the parameters, ohmic resistance was measured for each electrode pair for the second part of *phase 3* (six months after re-inoculation) through the current interrupt method. The following table summarises the results of the experimental estimation for average ohmic resistance, as calculated from the various external resistances applied.

***Table 7-2**: Average ohmic resistance (Ω) and respective standard deviation*

	R_3	R_4	R_5	R_6	R_7	R_8
R_{ohm} (Ω)	9.1445	15.1499	2.8915	3.7014	5.0643	4.2140
Stdev	0.3216	0.9817	0.8183	0.2498	0.4341	0.3566

A comparison of Tables 7.1 and 7.2 reveals a discrepancy between the results obtained through the electrochemical model and from the current interrupt method for experimental calculations. The ratio between the experimentally-derived ohmic resistance and the model-derived figure is presented in Table 7-3. It can be seen that between the two electrodes R_5 and R_6 for MFC_{R5+R6}, and R_7 and R_8 for MFC_{R7+R8}, the ratio is at similar levels, but in the case of R_3 and R_4, the ratio slightly varies. This result potentially reveals a trend of deviation between the two values in the data. The result is also in disagreement with prior research. Wen et al. (2009), as discussed earlier, used a more detailed model regarding the estimation of concentration and activation losses, which however was similarly based on the voltage of the electrode through an abstraction of the various losses from the thermodynamically predicted electrode voltage. In their research, ohmic resistance was estimated both experimentally and through the model, and was found to be consistent, rendering the model useful for describing the performance of an open air cathode MFC operating on brewery wastewater.

***Table 7-3:** Ratio between experimentally and model derived ohmic resistance*

	R_3	R_4	R_5	R_6	R_7	R_8
R_{exper}/R_{model}	0.4100	0.3548	0.0927	0.1124	0.1370	0.1324

Further research is necessary in order to address the deviation reported here, since no additional information points towards a reason for this trend. It could be however argued that in the prior research in the field of MFC modelling, the models developed, unlike Wen et al. (2009), describe the losses occurring in greater detail (Marcus, Torres and Rittmann, 2007; Oliveira et al., 2013; Ortiz-Martínez et al., 2015). Additionally, all the aforementioned research was conducted using laboratory scale MFCs, and the majority of it was on artificial or simple substrates, unlike the present study where the model was attempted on a 122 L prototype operating on whisky distillation derived wastewater. Both of these conditions may have affected the complexity of the reactions and the general

interactions occurring in the device, thus rendering the electrochemical model oversimplified and incapable of describing such a complex system. It is therefore suggested that the simplicity of the model against the complexity and size of the application resulted in the deviation identified between the experimental and theoretical results, indicating that the model was possibly not fit for this purpose.

However, through a further analysis of the part of the polarisation curve used in this chapter, i.e. the curve of voltage over current density, it can be observed that for electrodes R_4, R_6, R_7 and R_8 the loss observed is ohmic, while there is clearly no evidence of activation and concentration losses. As discussed in Chapter 2-7 and specifically depicted in Figure 2-5, ohmic losses occur in medium level current generation and are linear, thus it is recognised that for these electrodes, it is the only kind of loss present. This kind of loss is a voltage drop due to the resistance components of the cell, involving both of the anodic and the cathodic electrodes and their interconnections as well as the resistance to the flow of ions in the electrolyte and through the exchange membrane (Scott and Hao Yu, 2015; Larminie and Dicks, 2003).

There are several ways to further reduce ohmic losses and subsequently contribute to the optimisation of cell performance. Both from the anodic and the cathodic perspective, the reduction of electrode spacing can lead to lower ohmic losses as this way, protons have a shorter distance to travel to the cathode, while the orientation of the electrodes has been investigated as an additional way to achieve ohmic resistance reduction. Additionally, since ohmic resistance is also related to the interconnections between the electrodes, the choice of appropriate connecting materials can further contribute to a reduction in internal resistance (Rismani-Yazdi et al., 2008). Also, with regard to the components of the cell, optimising the physical properties of the membrane used in order to reduce its inherent resistance or possibly even working with membrane-less MFCs, could decrease ohmic losses (Rismani-Yazdi et al., 2008; Larminie and Dicks, 2003). Finally, increasing the conductivity of both the electrodes and the electrolytes (in the anode and cathode) could contribute to decreased ohmic losses since the flow of ions would be less hindered (Rismani-Yazdi et al., 2008; Larminie and Dicks, 2003; Logan et al., 2006).

The picture is slightly different for electrodes R_3 and R_5. Even though ohmic losses appear to be similar with the other electrodes, Figure 7-2 shows that this occurs only after

approximately 10 mA/m^2 for both electrodes. Activation losses can be observed up to that current. These are caused by the slowed reactions taking place on both electrodes, therefore possible steps for remediation need to be taken for both electrodes. During lower currents, when activation losses occur, electron transfer is slower (Scott and Hao Yu, 2015), so the addition of a mediator in the anode and a catalyst in the cathode could lead to reduction of activation losses. This is because catalysts have been found to exponentially effect the kinetics of oxygen reduction by decreasing the activation energy barriers (Rismani-Yazdi et al., 2008b; Wen et al., 2009). In the 122 L prototype, a mediator had already been impregnated in the anodic electrode. Additionally, in the 122 L prototype the HCl solution used as catholyte during the early stages of this study was likely to have contributed by enhancing the cathodic reaction. It was used only during the early stages, but according to these findings, it is suggested that using it again could lead to reduction of activation losses.

Additionally, an increase of operational temperature of the cell would lead to an increase of the available thermal energy in the system, thus the reactants would be able to obtain sufficient energy to reach an activated state. Increasing the concentration of reactants could lead to a decrease in activation losses (Wen et al., 2009). In the case of the current study, increasing the concentration of the AD liquid digestate in the anodic compartment would affect the performance of the cell in a more complicated way, and would therefore require a more in-depth examination. With regard to the cathode, since the MFC has an open air construction, increasing the air supply could lead to enhanced cathodic reactions but additional energy consumption would also be introduced, therefore sustainability and energy balance considerations would be required. Finally, increasing the possible reaction sites, which can be achieved by increasing both electrodes' surface areas, could optimise activation losses (Wen et al., 2009; Scott and Hao Yu, 2015; Larminie and Dicks, 2003).

7.4 Chapter conclusions

This chapter represents a further step in analysing the performance of the pilot scale multi-electrode system developed in this study. A simple electrochemical model applicable to every fuel cell system has been adapted in order to investigate whether or not it can be used to describe the performance of the current system. The relevant prior research during the last few years in the field of MFC modelling (Ortiz-Martínez et al.,

2015) has demonstrated that the real measurable voltage of an electrode pair can indeed be calculated by subtracting the various losses from the thermodynamically predicted voltage. This study has found a deviation between the theoretical and experimental values of ohmic resistance, while the latter was used as the validation parameter. Therefore, the conclusion has been reached that the electrochemical model developed in this stage is unable to accurately describe the performance of the electrodes. The most probable reason for that lies in the complexity of the developed device against the simplicity of the model, and further research has therefore been suggested in order to develop a more detailed, accurate theoretical model that could be used as a cheaper and faster alternative to experiments in large scale MFCs. The examination of the polarisation curves has provided an insight into the predominant losses occurring in the electrodes of the multi-electrode device, and suggestions were made at this final stage of the current research on how to further optimise the performance of the MFC.

Chapter 8 – Thesis conclusions

The overall aim of this study has been to examine the potential of utilising a microbial fuel cell within the whisky distillation process by integrating a pilot-scale MFC into existing treatment processes to examine its operation complementary and/or alternatively to established processes.

The initial approach in the study focused on optimising the performance of a pilot 14 L plug-flow multi-electrode MFC in relation to electrical connections. The reactor was constructed in scale to the future 122 L prototype, consisting of two anodes and two cathodes. Two different electrical connections were implemented: an independent operation during which the MFC was operated as a multi-electrode construction, and a parallel connection in which the two anodes were connected between themselves, as were the cathodes, to construct one united single electrode. The reason for this experiment was to determine the optimum electrical connection. It was concluded that, either using polarisation curves or the constant current discharge method, the united electrode (in parallel connection) led to a higher power output than when the electrodes were operated as two independent circuits: specifically, the power output during parallel connection was approximately 37.8 % higher than the recorded power output in independent operation. Additionally, the MFC was operated on anaerobic digestion liquid digestate, and demonstrated both a start-up period of 14 to 20 days, which can be considered as an accelerated start-up given that this stage can last up to 103 days (Wang et al., 2009b), and a successful maximum tCOD reduction of 81.9±6.2 %, demonstrating the fundamental ability of an MFC to work in a complementary manner to anaerobic digestion. Finally, during these first pilot trials, according to the constant discharge method it was found that the first electrode (in terms of its relative position to the feed) produced higher power outputs with power being reduced while moving towards the flow of wastewater, which can be linked to the greater availability of organic matter at the beginning of the feed, in accordance with prior results presented for a laboratory scale MFC by Ren et al. (2014). This can be considered as a great step towards more in-depth understanding of large scale multi-electrode MFCs.

The study then continued with the deployment of the 122 L plug-flow multi-electrode MFC reactor. The MFC, consisting of 8 independent anode-electrode pairs, was operated on diluted spent wash, initially achieving a start-up period of 45 days. A rather

unexpected outcome was observed at this point. As part of the main objective, which was the realistic deployment of a pilot-scale MFC, one of the key parameters observed was temperature, and its effect on the start-up and further operation of the reactor were therefore monitored. During the start-up stage, the ambient temperatures ranged from approximately 12^{o}C up to a little higher than 16^{o}C, and no correlation was found with an increase of OCV, a result in line with the recent research suggesting that temperature is not necessarily a limiting factor for bioelectrochemical systems (Heidrich et al., 2014). After establishing a successful start-up, the MFC was operated according to the optimised parallel electrical connection suggested in this study's previous findings. Current and power generation were observed to be constant and at high levels throughout the overall duration of the preliminary studies, similar to the tCOD removal efficiencies achieved. In order to express energy recovery for the prototype MFC, which is one of the key aspects of the technology, the normalised energy recovery was calculated and the prototype reactor was found to produce a positive energy balance. Therefore, it is concluded that the prototype reactor is capable of sustainably treating whisky distillation by-products, thus not only achieving energy savings but also contributing towards an additional energy output. At this point, a positive correlation was observed between the level of energy recovered and temperature, meaning that an increase in operational temperature can lead to an increase in energy recovery. Overall, it appears that temperature does not affect the principle of electricity generation in an MFC allowing for start-up, regardless of the environmental conditions, possibly it instead slows down its development, but upon achievement of a steady state, the MFC is concluded to have a behaviour similar to biological technologies affected by operational temperature (Gerardi, 2003; Jadhav and Ghangrekar, 2009).

As part of the industrial deployment of the technology, a refurbishment protocol was established which includes the harvesting of biomass, the addressing of bio fouling on the cathode surface, electrodes maintenance, and the retro-fit of the 122 L reactor into two sub-reactors to examine reproducibility. The protocol was deployed successfully, moving to the next stage of operation when the serial transfusions of microbial inoculum (previously adapted in the MFC similarly fed with anaerobic digestion liquid digestate for more than 60 days) led to an enhanced start-up process which was now minimized to last only 5 days. Further optimization of the operational parameters was attempted and the hydraulic retention time was proven to be capable in principle of further reduction,

form 4 days down to 24 hours. Interestingly, this study finds that similar levels of power were reported during the reduced HRT as during the longer HRT, so the inability of the reactor to utilize the additional organic input into the system for electricity generation led to negative energy balances, suggesting that additional energy input is required for the treatment of the waste. However, due to the high costs associated with aeration, the technology studied here is still capable of energy savings. Finally, the outcomes regarding the nutrients in the system such as sulphates, phosphates and nitrates were inconclusive.

Up to this point, the plug-flow MFC achieved promising performance when operating both on effluent before the AD and after the AD process. The research went on to examine the integration of MFC technology within an existing treatment process in a local whisky distillery. The pilot layout consisting of two duplicate 122 L reactors, each of which was further equally divided into two sub-reactors, was deployed to operate in a complementary way to anaerobic digestion. The utilization of the adapted biomass, as previously linked to the lower start-up period, was similarly achieved. Interestingly at this point, two major observations were drawn: firstly, that MFC_{R1+R2} and MFC_{R3+R4} within the first 122 L reactor demonstrated almost identical results regarding electrical performance, with similar results found between them regarding tCOD removal efficiency, as did MFC_{R5+R6} and MFC_{R7+R8} within the second 122 L reactor. However, the second major observation was that when compared on a reactor level, the performance was not similar as expected. Additionally, only MFC_{R5+R6} and MFC_{R7+R8} seemed to follow the pattern dictated by the findings in the 14 L reactor at the beginning of this study, according to which the first electrode (in terms of its relative position to the influent feed) produced a higher power output than the following electrodes due to having access to a greater amount of organic feed. When the hydraulic retention time was further reduced down to 24 hours, two additional major outcomes were drawn; on the one hand, the adaptation to the new organic load exhibited an increase similar to a microbial growth curve, possibly linked to the increase of electrogens. On the other hand, beyond this initial increase, the system's stability was compromised for the remainder of the experimental period in terms of electrical performance and tCOD reduction.

During the latter phase of this study, further optimization regarding the anodic materials was examined. Additionally, having established the fundamental ability of the prototype

to be used in a complementary manner to AD, the final issue addressed here was how long the performance of the pilot installation would remain sustainable before being prohibitively impaired by time and physical deterioration. A comparative study between an anodic electrode made entirely of carbon fiber against the standard graphite granule-based construction highlighted the greater potential of the second type with regard to voltage output, concluding that the complex construction graphite granule-based electrode is more suitable for the current development. The long term performance and relative failure of the reactors was examined using two different approaches during this last phase; power curves traced power output over current generated, and the constant discharge method over time was also employed. Interestingly, the fiber anodes exhibited minimal deterioration after six months, and in another case even achieved an increased maximum power after six months, prompting a question regarding more favorable microbial adhesion. However, even in the case of an increase in the maximum power output after six months, the newly achieved level was still at least 50 % lower than the maximum power output achievable through the complex graphite granule construction. The comparative study based on the power curves of the complex electrodes revealed a considerable deterioration of the power output for every electrode, in the most extreme case from 7.01 mW down to 0.79 mW, an approximate 88.7 % reduction within six months.

According to the constant discharge monitoring, the power over time profile revealed a considerably fluctuating performance, which has been linked to the galvanic current generated due to the significant deterioration of the materials involved, which can be addressed in the future with a more appropriate materials selection and maintenance intervention, as was used in this study. Further, concerning electrical performance, apart from the relative failure over the last six months of operation, the prototype reactors interestingly exhibited an ability to maintain their electrogenic potential even in adverse conditions of starvation. An approximately 15-day long starvation of the MFCs was found not to have affected the electrical power output of the reactors, highlighting their potential for use in remote access areas, and as ancillary electricity producing equipment in adverse environments.

Finally, concerning wastewater treatment both in relation to total suspended solids and total COD, the prototype reactors were shown to be able to maintain their efficiency over

time with no notable system failures. The final tCOD effluent concentrations might not have thrived as much as they did in other studies, but the current study has certainly demonstrated the ability of a pilot scale MFC to be integrated into an industrial wastewater treatment process, and its potential to be used as an integral part of a total treatment solution.

The above comments conclude the experimental work carried out for this study, which in its latter phase went on a step further than integration into the development and application of a simple electrochemical model. It was concluded that there is a deviation between the theoretical and experimental values chosen as the validation parameter, and therefore the electrochemical model which has been developed to this stage is not currently able to accurately describe the performance of the electrodes.

From an overall perspective, this study has shed light onto the application and integration of microbial fuel cells in real industrial environments. In the majority of the research performed to date, MFCs have been considered as a stand-alone technology for wastewater treatment. In contrast to that perspective, the present study has provided proof on a larger scale that MFC technology operating in a complementary manner to anaerobic digestion should be considered as an energy efficient, if not energy producing, alternative to energy-intense treatment options such as aerobic treatments. As hopeful as that finding might be for the field of MFCs, the technology has still a long way to go before it can be deployed on a level comparable to these technologies; therefore, future research has a very important role to play in making that happen.

Chapter 9 – Future research and recommendations

This study set out to examine the performance of a pilot scale multi-electrode MFC in the context of the treatment of whisky distillation process by-products. Various aspects of its electrical performance and effluent treatment capabilities were examined and several outcomes were drawn throughout this journey. However, the current study has also raised some new questions, which are set out at this point as a continuation of the current work in order to conclusively outline the issues discovered here regarding the performance of MFCs.

Chapter 4: During the preliminary experiments involving the 14 L reactor it was found that the parallel connection of two electrodes is capable of producing higher power outputs. However, the effect of this electrical connection on tCOD removal efficiency was inconclusive. The parameter was only examined at the rear of the reactor, but in order to study the effect of connections on the MFC in more depth, a sampling point at the end of each electrode would be necessary.

Chapter 5: Due to the conclusions drawn from the previous chapter, every two neighbouring anodes and cathodes in the 122 L reactor were connected in parallel, resulting into the reactor having four coupled electrodes. One main question rose at this point from that decision. Would connecting all eight originally independent sets of anodes and cathodes result in an overall higher power output, or not? A comparative study between a multi-electrode MFC in which all electrodes are connected in parallel, and a multi-electrode MFC in which only some electrodes are connected in parallel could possibly provide an optimised system that could be further scaled-up. Regarding the outcomes of this chapter, it was found that unlike previous suggestions made by this research and by a relevant recent study of Ren et al. (2014), in the 122 L multi-electrode reactor, power outputs from every electrode, both in independent and parallel connections, were found to be at similar levels. Electrodes were not found to follow the rationale according to which a poorer availability of organics moving from the front rear to the back is expected to lead to lower power outputs. Therefore, examination of the carbon content levels in every compartment with an electrode and characterisation of the microbial composition again inn every anodic compartment could possibly provide a better understanding of why the gradual decrease in power outputs was observed in the 14 L reactor, but not for the 122 L reactor.

The effect of temperature on the overall performance of the reactor could be described as contradictory, in that temperature was not found to affect the start-up process but instead to positively affect energy recovery during regular operation. Therefore, a closer examination of temperature would be expected to provide further insight on optimisation. Prior research has produced similarly contradictory results regarding the correlation between these two parameters (Jadhav and Ghangrekar, 2009; Catal et al., 2011; Heidrich et al., 2014). It is therefore suggested that an additional heating element should be examined. The MFC system up to this point was found to produce a positive energy balance, thus it is also suggested for the additional heating element's energy consumption to be included in balance calculations in order to also examine whether higher power outputs possibly offset the energy required by the heating element.

A further reduction in hydraulic retention time through an increased influent flow rate seemed to create a negative energy balance, essentially meaning that more energy is put into the system for treatment than the amount of energy recovered through electricity generation. Given that tCOD removal efficiency was found to be unaffected by this decrease in HRT, further research is necessary in order to identify the microbial metabolic pathways that contribute to activities other than electrogenesis.

Chapter 6: During this stage actual integration of the pilot was carried out in an industrial environment. Issues associated with blockages, connectivity and other practical hindrances should be resolved in future application. However, this is believed to be an issue relatively easy to overcome due to industrial knowledge available.

Regarding the first stage of integration, it has been noted that the reduction of HRT from four days to 24 hours resulted on the one hand in an electrical behaviour similar to a standard microbial growth curve, and on the other hand, to a relatively unsteady reactor. It is therefore proposed that future similar experiments should include a process of identification of the microbial species responsible for electrogenic activity and their enumeration in order to directly correlate electrical trends to microbial growth. In relation to fluctuating performance, the need for more time for adaptation is a possible corrective action. However, closer investigation regarding the correlation between influent organic loading rate, detailed chemical characterisation of the influent wastewater stream and electrical outputs could provide a clearer image of the fluctuation pattern.

Regarding the latter phase of experimentation, suggestions for future research relating to materials and the structural approach to be adopted arise. The graphite brush has been found to be effective mostly due to its increased surface area that allows better microbial adhesion and more points of reaction (Logan et al., 2007; Lanas and Logan, 2013). It is therefore, suggested that it is examined in a comparative study with the existing complex graphite granule-based electrode, which could reveal a further point of optimisation. The cathode used in this study was an optimised construction developed to combine the advantages of the open air cathode while maintaining the input of an electrolyte to enhance oxygen reduction. However, alternative materials can be examined also for the cathode while keeping cost low. Regarding the design of the overall unit and keeping in mind the open air cathode element, optimisation through design alterations is suggested. This reactor in the present study was developed as a plug-flow multi-electrode MFC with a serpentine internal liquid flow. However, incorporating the cathode and an optimised anode into different designs, such as tubular or spiral design, could produce an even better performing design which may possibly be more suitable for scaling-up.

This chapter intended to achieve the potential of integration of MFC technology into an existing treatment process. During this phase the MFC was operated in a complementary manner to an anaerobic digester, and the feasibility of this was demonstrated, but additional treatment was found to be necessary in order to provide holistic treatment options. Therefore, it is suggested that additional treatment options are examined downstream of an MFC to achieve discharge adhering to the environment limits set on a UK and EU level, if not solely to reduce costs from discharge to sewer.

Chapter 7: In this chapter the simple electrochemical model used was not conclusively validated through experimental work. The reason behind that was hypothesised to have been its oversimplified nature. The development of a more detailed set of equations is necessary to accurately describe the performance of a multi-electrode reactor. Research should include the identification and accurate estimation of the parameters in greater detail. Additionally, the inclusion of microbial kinetics in the model and thus, the development of a holistic model taking that aspect also into consideration, would lead to a better defined model able to more accurately demonstrate an MFC's functions.

Further recommendations: From an overall perspective, due to economic constraints, a full chemical characterisation of waste streams was not possible over the long term in this study. However, this is highly recommended in any future studies performed on the prototype. A complete chemical characterisation would provide a holistic overview of the components present and would possibly identify those elements which might be inhibitory to electrogenesis and/or treatment. Within this frame, throughout this study some parameters of effluent quality were closely and continuously monitored, but some secondary parameters, such as phosphates, nitrates and sulphates, were only examined sporadically. It is therefore suggested that future applications of this prototype monitor the cycle of nitrogen, phosphorus and sulphur from the point of waste generation to the final discharge point. Even though such parameters are not strictly regulated, their examination could provide a more detailed picture of the processes occurring in an MFC, and might identify the metabolic pathways which are antagonistic to electrogenesis. For instance, much more carbon was found to be consumed for sulphate reduction than is utilised in electricity generation in a study by Zhang et al. (2013b). Therefore, it would be worthwhile examining whether the suppression of this pathway would lead to higher power outputs.

Possibly one of the greatest inefficiencies in the current flat plate reactor was identified as the collection, characterisation and utilisation of the possible gas produced in the anodic compartment. According to recent relevant research by Ge et al. (2013), and given that an originally anaerobic granular biomass was used as inoculum in this study, any gas generated would mostly be expected to be methane. Therefore, two main experimental suggestions are made here: firstly, the consideration of an alternative MFC design, such as a tubular reactor, and its relative position could help with the gas potentially produced in future experiments. The second suggestion relates to temperature and its effect on methanogenesis and electrogenesis in the MFC reactor. As was described in the literature review, lower temperatures are associated with the suppression of methanogenesis. It would therefore be interesting to examine how the addition of a heating element would affect electrogenesis, but also the production of methane. Optimum energy recovery from the current and any future designs might lie in a combination of the two processes rather than the absolute suppression of the latter in order to promote the former.

Regarding operational parameters, some further improvements to the system might lead to higher levels of energy recovery while maintaining treatment efficiency. Introducing the recirculation of the treated effluent and/or hydraulically connecting two reactors has been found to affect energy recovery and tCOD removal efficiency (Winfield et al., 2011; Jacobson, Kelly and He, 2015). Additionally, the examination of continuous, batch and semi-batch operational modes would be beneficial in determining the optimum operational conditions, especially for the current design of the multi-electrode reactor.

List of references

Aelterman, P., Rabaey, K., Clauwaert, P. and Verstraete, W., 2006. Microbial fuel cells for wastewater treatment. *Water Science & Technology*, 54(8), pp.9–15.

Aelterman, P., Versichele, M., Marzorati, M., Boon, N. and Verstraete, W., 2008. Loading rate and external resistance control the electricity generation of microbial fuel cells with different three-dimensional anodes. *Bioresource Technology*, 99, pp.8895–8902.

Ahn, Y. and Logan, B.E., 2010. Effectiveness of domestic wastewater treatment using microbial fuel cells at ambient and mesophilic temperatures. *Bioresource Technology*, 101, pp.469–475.

Aldrovandi, A., Marsili, E., Paganin, P., Tabacchioni, S. and Giordano, A., 2009. Sustainable power production in a memrane-less and mediator-less syntetic wastewater microbial fuel cell. *Bioresource Technology*, 100, pp.3252–3260.

Allen, R.M. and Bennetto, H.P., 1993. Microbial fuel-cells. *Applied Biochemistry and Biotechnology*, 39(1), pp.27–40.

Ammary, B.Y., 2004. Nutrients requirements in biological industrial wastewater treatment. *African Journal of Biotechnology*, 3(4), pp.236–238.

APHA, 1998. *Standard Methods for the Examination of Water and Wastewater*. *Standard Methods*. Washington DC.: APHA.

Appels, L., Baeyens, J., Degrève, J. and Dewil, R., 2008. Principles and potential of the anaerobic digestion of waste-activated sludge. *Progress in Energy and Combustion Science*, 34, pp.755–781.

Bond, D.R. and Lovley, D.R., 2003. Electricity Production by Geobacter sulfurreducens Attached to Electrodes Electricity Production by Geobacter sulfurreducens Attached to Electrodes. *Applied and Environmental Microbiology*, 69(3), pp.1548–1555.

Bowen, E.J., Dolfing, J., Davenport, R.J., Read, F.L. and Curtis, T.P., 2014. Low-temperature limitation of bioreactor sludge in anaerobic treatment of domestic wastewater. *Water Science and Technology*, 69(5), pp.1004–1013.

Burkitt, R., Whiffen, T.R. and Yu, E.H., 2016. Iron phthalocyanine and MnOx composite catalysts for microbial fuel cell applications. *Applied Catalysis B: Environmental*, 181, pp.279–288.

Caffoor, I., 2008. *Energy Efficient Water and Wastewater Treatment*. *Environmental Knowledge Transfer Networks*.

Canfield, J.H., Goldner, B.H. and Lutwack, R., 1963. *NASA Technical report*. Magna Corporation, Anaheim, CA.

Catal, T., Kavanagh, P., O'Flaherty, V. and Leech, D., 2011. Generation of electricity in microbial fuel cells at sub-ambient temperatures. *Journal of Power Sources*, 196, pp.2676–2681.

Catal, T., Xu, S., Li, K., Bermek, H. and Liu, H., 2008. Electricity generation from polyalcohols in single-chamber microbial fuel cells. *Biosensors and Bioelectronics*, 24(4), pp.849–854.

Cerrillo, M., Oliveras, J., Viñas, M. and Bonmatí, A., 2016. Comparative assessment of raw and digested pig slurry treatment in bioelectrochemical systems. *Bioelectrochemistry*, 110, pp.69–78.

Chae, K.J., Choi, M.J., Lee, J.W., Kim, K.Y. and Kim, I.S., 2009. Effect of different substrates on the performance, bacterial diversity, and bacterial viability in microbial fuel cells. *Bioresource Technology*, 100, pp.3518–3525.

Chaudhuri, S.K. and Lovley, D.R., 2003. Electricity generation by direct oxidation of glucose in mediatorless microbial fuel cells. *Nature Biotechnology*, 21, pp.1229–1232.

Chen, Y.M., Wang, C.T., Yang, Y.C. and Chen, W.J., 2013. Application of aluminum-alloy mesh composite carbon cloth for the design of anode/cathode electrodes in Escherichia coli microbial fuel cell. *International Journal of Hydrogen Energy*, 38, pp.11131–11137.

Cheng, K.Y., Ho, G. and Cord-Ruwisch, R., 2012. Energy-efficient treatment of organic wastewater streams using a rotatable bioelectrochemical contactor (RBEC). *Bioresource Technology*, 126, pp.431–436.

Cheng, S., Liu, H. and Logan, B.E., 2006a. Increased performance of single-chamber microbial fuel cells using an improved cathode structure. *Electrochemistry Communications*, 8, pp.489–494.

Cheng, S., Liu, H. and Logan, B.E., 2006b. Power densities using different cathode catalysts (Pt and CoTMPP) and polymer binders (Nafion and PTFE) in single chamber microbial fuel cells. *Environmental Science and Technology*, 40, pp.364–369.

Cheng, S. and Logan, B.E., 2011. Increasing power generation for scaling up single-chamber air cathode microbial fuel cells. *Bioresource Technology*, 102, pp.4468–4473.

Clauwaert, P., Mulenga, S., Aelterman, P. and Verstraete, W., 2009. Litre-scale microbial fuel cells operated in a complete loop. *Applied Microbiology and Biotechnology*, 83, pp.241–247.

Cohen, B., 1930. The bacterial culture as an electrical half-cell. *Journal of Bacteriology*, 21(1), pp.18–19.

Corcoran, E., Nellemann, C., Baker, E., Bos, R., Osborn, D., Savelli, H., 2010. *Sick Water ? the Central Role of Wastewater Management in Sustainable Development*. *United Nations Environment Programme*.

Correll, D.L., 1998. The Role of Phosphorus in the Eutrophication of Receiving Waters: A Review. *Journal of Environment Quality*, 27, pp.261–266.

Cusick, R.D., Bryan, B., Parker, D.S., Merrill, M.D., Mehanna, M., Kiely, P.D., Liu, G. and Logan, B.E., 2011. Performance of a pilot-scale continuous flow microbial electrolysis cell fed winery wastewater. *Applied Microbiology and Biotechnology*, 89, pp.2053–2063.

Daud, S.M., Kim, B.H., Ghasemi, M. and Daud, W.R.W., 2015. Separators used in microbial electrochemical technologies: Current status and future prospects. *Bioresource Technology*, 195, pp.170–179.

DEFRA, 2012. *Waste water treatment in the United Kingdom*. London.

Dekker, A., Heijne, A. Ter, Saakes, M., Hamelers, H.V.M. and Buisman, C.J.N., 2009. Analysis and Improvement of a Scaled-Up and Stacked Microbial Fuel Cell. *Environmental Science & Technology*, 43(23), pp.9038–9042.

Dewan, A., Beyenal, H. and Lewandowski, Z., 2008. Scaling up Microbial Fuel Cells. *Environmental Science & Technology*, 42(20), pp.7643–7648.

Dong, Y., Qu, Y., He, W., Du, Y., Liu, J., Han, X. and Feng, Y., 2015. A 90-liter stackable baffled microbial fuel cell for brewery wastewater treatment based on energy self-sufficient mode. *Bioresource Technology*, 195, pp.66–72.

Du, Z., Li, H. and Gu, T., 2007. A state of the art review on microbial fuel cells: A promising technology for wastewater treatment and bioenergy. *Biotechnology Advances*, 25, pp.464–482.

Du, Z., Li, Q., Tong, M., Li, S. and Li, H., 2008. Electricity Generation Using Membrane-less Microbial Fuel Cell during Wastewater Treatment. *Chinese Journal of Chemical Engineering*, 16(5), pp.772–777.

Dumas, C., Basséguy, R. and Bergel, A., 2008. Microbial electrocatalysis with Geobacter sulfurreducens biofilm on stainless steel cathodes. *Electrochimica Acta*, 53, pp.2494–2500.

Dumas, C., Mollica, A., Féron, D., Basséguy, R., Etcheverry, L. and Bergel, A., 2007. Marine microbial fuel cell: Use of stainless steel electrodes as anode and cathode materials. *Electrochimica Acta*, 53, pp.468–473.

Fedorovich, V., Varfolomeev, S.D., Sizov, A. and Goryanin, I., 2009. Multi-electrode microbial fuel cell with horizontal liquid flow. *Water Science and Technology*, 60(2), pp.347–355.

Fedorovich, V., 2012. *Microbial fuel cell assembly*. EP 2225790 B1.

Feng, Y., He, W., Liu, J., Wang, X., Qu, Y. and Ren, N., 2014. A horizontal plug flow and stackable pilot microbial fuel cell for municipal wastewater treatment. *Bioresource Technology*, 156, pp.132–138.

Feng, Y., Wang, X., Logan, B.E. and Lee, H., 2008. Brewery wastewater treatment using air-cathode microbial fuel cells. *Applied Microbiology and Biotechnology*, 78, pp.873–880.

Feng, Y., Yang, Q., Wang, X. and Logan, B.E., 2010. Treatment of carbon fiber brush anodes for improving power generation in air-cathode microbial fuel cells. *Journal of Power Sources*, 195, pp.1841–1844.

Franks, A.E., Malvankar, N. and Nevin, K.P., 2010. Bacterial biofilms: the powerhouse of a microbial fuel cell. *Biofuels*, 1(4), pp.589–604.

Freguia, S., Rabaey, K., Yuan, Z. and Keller, J., 2007. Non-catalyzed cathodic oxygen reduction at graphite granules in microbial fuel cells. *Electrochimica Acta*, 53, pp.598–603.

Gajda, I., Greenman, J., Melhuish, C. and Ieropoulos, I., 2015. Self-sustainable electricity production from algae grown in a microbial fuel cell system. *Biomass and Bioenergy*, 82, pp.87–93.

Gálvez, A., Greenman, J. and Ieropoulos, I., 2009. Landfill leachate treatment with microbial fuel cells; scale-up through plurality. *Bioresource Technology*, 100, pp.5085–5091.

Gao, C., Wang, A., Wu, W.M., Yin, Y. and Zhao, Y.G., 2014. Enrichment of anodic biofilm inoculated with anaerobic or aerobic sludge in single chambered air-cathode microbial fuel cells. *Bioresource Technology*, 167, pp.124–132.

Ge, Z. and He, Z., 2016. Long-term Performance of a 200-Liter Modularized Microbial Fuel Cell System Treating Municipal Wastewater: Treatment, Energy, and Cost. *Environmental Science: Water Research and Technology*, 2, pp.274–281.

Ge, Z., Li, J., Xiao, L., Tong, Y. and He, Z., 2014. Recovery of Electrical Energy in Microbial Fuel Cells. *Environmental Science & Technology Letters*, 1, pp.137–141.

Ge, Z., Zhang, F., Grimaud, J., Hurst, J. and He, Z., 2013. Long-term investigation of microbial fuel cells treating primary sludge or digested sludge. *Bioresource Technology*, 136, pp.509–514.

Gerardi, M.H., 2003. *The Microbiology of Anaerobic Digesters*. *Vasa*. Willey.

Ghangrekar, M.M. and Shinde, V.B., 2007. Performance of membrane-less microbial fuel cell treating wastewater and effect of electrode distance and area on electricity production. *Bioresource Technology*, 98(15), pp.2879–2885.

Goodwin, J.A.S., Finlayson, J.M. and Low, E.W., 2001. A further study of the anaerobic biotreatment of malt whisky distillery pot ale using an UASB system. *Bioresource Technology*, 78(2), pp.155–160.

Goodwin, J.A.S. and Stuart, J.B., 1994. Anaerobic digestion of malt whisky distillery pot ale using upflow anaerobic sludge blanket reactors. *Bioresource Technology*, 49, pp.75–81.

Greenman, J., Gálvez, A., Giusti, L. and Ieropoulos, I., 2009. Electricity from landfill leachate using microbial fuel cells: Comparison with a biological aerated filter. *Enzyme and Microbial Technology*, 44(2), pp.112–119.

Gude, V.G., Kokabian, B. and Gadhamshetty, V., 2013. Beneficial bioelectrochemical systems for energy, water, and biomass production. *Journal of Microbial & Biochemical Technology*, S6(005), pp.1–14.

Gude, V.G., 2015. Energy and water autarky of wastewater treatment and power generation systems. *Renewable and Sustainable Energy Reviews*, 45, pp.52–68.

Gude, V.G., 2016. Wastewater treatment in microbial fuel cells - An overview. *Journal of Cleaner Production*, pp.1–21.

Ha, P.T., Lee, T.K., Rittmann, B.E., Park, J. and Chang, I.S., 2012. Treatment of Alcohol Distillery Wastewater Using a Bacteroidetes-Dominant Thermophilic Microbial Fuel Cell. *Environmental science & technology*, 45(5), pp.3022–3030.

Ha, P.T., Tae, B. and Chang, I.S., 2008. Performance and bacterial consortium of microbial fuel cell fed with formate. *Energy and Fuels*, 22, pp.164–168.

Habermann, W. and Pommer, E.H., 1991. Biological fuel cells with sulphide storage capacity. *Applied Microbiology and Biotechnology*, 35(1), pp.128–133.

HaoYu, E., Cheng, S., Scott, K. and Logan, B., 2007. Microbial fuel cell performance with non-Pt cathode catalysts. *Journal of Power Sources*, 171, pp.275–281.

He, Z., Minteer, S.D. and Angenent, L.T., 2005. Electricity generation from artificial wastewater using an upflow microbial fuel cell. *Environmental Science and Technology*, 39, pp.5262–5267.

He, Z., 2013. Microbial Fuel Cells: Now Let us Talk about Energy. *Environmental science & technology*, 47, pp.332–333.

Heidrich, E., Curtis, T. and Dolfing, J., 2015. Determination of the Internal Chemical Energy of Wastewater Determination of the Internal Chemical Energy of Wastewater. 45, pp.827–832.

Heidrich, E.S., Edwards, S.R., Dolfing, J., Cotterill, S.E. and Curtis, T.P., 2014. Performance of a pilot scale microbial electrolysis cell fed on domestic wastewater at ambient temperatures for a 12month period. *Bioresource Technology*, 173, pp.87–95.

ter Heijne, A., Hamelers, H.V.M., Saakes, M. and Buisman, C.J.N., 2008. Performance of non-porous graphite and titanium-based anodes in microbial fuel cells. *Electrochimica Acta*, 53, pp.5697–5703.

ter Heijne, A., Liu, F., Van Rijnsoever, L.S., Saakes, M., Hamelers, H.V.M. and Buisman, C.J.N., 2011. Performance of a scaled-up Microbial Fuel Cell with iron reduction as the cathode reaction. *Journal of Power Sources*, 196, pp.7572–7577.

Hernández-Fernández, F.J., Pérez De Los Ríos, A., Salar-García, M.J., Ortiz-Martínez, V.M., Lozano-Blanco, L.J., Godínez, C., Tomás-Alonso, F. and Quesada-Medina, J., 2015a. Recent progress and perspectives in microbial fuel cells for bioenergy generation and wastewater treatment. *Fuel Processing Technology*, 138, pp.284–297.

Hernández-Fernández, F.J., Pérez De Los Ríos, A., Salar-García, M.J., Ortiz-Martínez, V.M., Lozano-Blanco, L.J., Godínez, C., Tomás-Alonso, F. and Quesada-Medina, J., 2015b. Recent progress and perspectives in microbial fuel cells for bioenergy generation and wastewater treatment. *Fuel Processing Technology*, 138, pp.284–297.

Hiegemann, H., Herzer, D., Nettmann, E., Lübken, M., Schulte, P., Schmelz, K.-G., Gredigk-Hoffmann, S. and Wichern, M., 2016. An integrated 45L pilot microbial fuel cell system at a full-scale wastewater treatment plant. *Bioresource Technology*, 218, pp.115–122.

Hou, Q., Nie, C., Pei, H., Hu, W., Jiang, L. and Yang, Z., 2016. The effect of algae species on the bioelectricity and biodiesel generation through open-air cathode microbial fuel cell with kitchen waste anaerobically digested effluent as substrate. *Bioresource Technology*, 218, pp.902–908.

Hutchinson, A.J., Tokash, J.C. and Logan, B.E., 2011. Analysis of carbon fiber brush loading in anodes on startup and performance of microbial fuel cells. *Journal of Power Sources*, 196, pp.9213–9219.

Ieropoulos, I., Greenman, J., Melhuish, C. and Hart, J., 2005. Energy accumulation and improved performance in microbial fuel cells. *Journal of Power Sources*, 145, pp.253–256.

Jacobson, K.S., Kelly, P.T. and He, Z., 2015. Energy Balance Affected by Electrolyte Recirculation and Operating Modes in Microbial Fuel Cells. *Water Environment Research*, 87(3), pp.252–257.

Jadhav, G.S. and Ghangrekar, M.M., 2009. Performance of microbial fuel cell subjected to variation in pH, temperature, external load and substrate concentration. *Bioresource Technology*, 100, pp.717–723.

Janicek, A., Fan, Y. and Liu, H., 2014. Design of microbial fuel cells for practical application: a review and analysis of scale-up studies. *Biofuels*, 5(1), pp.79–92.

Jiang, D., Curtis, M., Troop, E., Scheible, K., McGrath, J., Hu, B., Suib, S., Raymond, D. and Li, B., 2011. A pilot-scale study on utilizing multi-anode/cathode microbial fuel cells (MAC MFCs) to enhance the power production in wastewater treatment. *International Journal of Hydrogen Energy*, 36, pp.876–884.

Jiang, D. and Li, B., 2009. Granular activated carbon single-chamber microbial fuel cells (GAC-SCMFCs): A design suitable for large-scale wastewater treatment processes. *Biochemical Engineering Journal*, 47, pp.31–37.

Kalathil, S., Lee, J. and Cho, M.H., 2011. Granular activated carbon based microbial fuel cell for simultaneous decolorization of real dye wastewater and electricity generation. *New Biotechnology*, 29(1), pp.32–37.

Kargi, F. and Eker, S., 2007. Electricity generation with simultaneous wastewater treatment by a microbial fuel cell (MFC) with Cu and Cu-Au electrodes. *Journal of Chemical Technology and Biotechnology*, 82, pp.658–662.

Karra, U., Troop, E., Curtis, M., Scheible, K., Tenaglier, C., Patel, N. and Li, B., 2013. Performance of plug flow microbial fuel cell (PF-MFC) and complete mixing microbial fuel cell (CM-MFC) for wastewater treatment and power generation. *International Journal of Hydrogen Energy*, 38, pp.5383–5388.

Kelly, P.T. and He, Z., 2014. Understanding the application niche of microbial fuel cells in a cheese wastewater treatment process. *Bioresource Technology*, 157, pp.154–160.

Kim, B.H., Park, H.S., Kim, H.J., Kim, G.T., Chang, I.S., Lee, J. and Phung, N.T., 2004. Enrichment of microbial community generating electricity using a fuel-cell-type electrochemical cell. *Applied Microbiology and Biotechnology*, 63, pp.672–681.

Kim, H.J., Hyun, M.S., Chang, I.S. and Kim, B.H., 1999. A microbial fuel cell type lactate biosensor using a metal-reducing bacterium, Shewanella putrefaciens. *Journal of Microbiology and Biotechnology*, 9(3), pp.365–367.

Kim, J.R., Kim, J.R., Cheng, S., Cheng, S., Oh, S.-E., Oh, S.-E., Logan, B.E. and Logan, B.E., 2007. Power generation using different cation, anion, and ultrafiltration membranes in microbial fuel cells. *Environmental Science and Technology*, 41(3), pp.1004–9.

Kim, T., An, J., Jang, J.K. and Chang, I.S., 2015. Coupling of anaerobic digester and microbial fuel cell for COD removal and ammonia recovery. *Bioresource Technology*, 195, pp.217–222.

Lanas, V., Ahn, Y. and Logan, B.E., 2014. Effects of carbon brush anode size and loading on microbial fuel cell performance in batch and continuous mode. *Journal of Power Sources*, 247, pp.228–234.

Lanas, V. and Logan, B.E., 2013. Evaluation of multi-brush anode systems in microbial fuel cells. *Bioresource Technology*, 148, pp.379–385.

Larminie, J. and Dicks, A., 2003. *Fuel cells systems explained*. 2nd ed. ed. Chichester: John Wiley & Sons Ltd.

Larrosa-Guerrero, A., Scott, K., Head, I.M., Mateo, F., Ginesta, A. and Godinez, C., 2010. Effect of temperature on the performance of microbial fuel cells. *Fuel*, 89, pp.3985–3994.

Lee, H.S., Parameswaran, P., Kato-Marcus, A., Torres, C.I. and Rittmann, B.E., 2008. Evaluation of energy-conversion efficiencies in microbial fuel cells (MFCs) utilizing fermentable and non-fermentable substrates. *Water Research*, 42, pp.1501–1510.

Leong, J.X., Daud, W.R.W., Ghasemi, M., Liew, K. Ben and Ismail, M., 2013. Ion exchange membranes as separators in microbial fuel cells for bioenergy conversion: A comprehensive review. *Renewable and Sustainable Energy Reviews*, 28, pp.575–587.

Li, Z., Yao, L., Kong, L. and Liu, H., 2008. Electricity generation using a baffled microbial fuel cell convenient for stacking. *Bioresource Technology*, 99(6), pp.1650–1655.

Liu, H., Cheng, S., Huang, L. and Logan, B.E., 2008. Scale-up of membrane-free single-chamber microbial fuel cells. *Journal of Power Sources*, 179, pp.274–279.

Liu, H., Cheng, S. and Logan, B.E., 2005. Power generation in fed-batch microbial fuel cells as a function of ionic strength, temperature, and reactor configuration. *Environmental Science and Technology*, 39, pp.5488–5493.

Liu, H., Grot, S. and Logan, B.E., 2005. Electrochemically assisted microbial production of hydrogen from acetate. *Environmental Science and Technology*, 39(11), pp.4317–4320.

Liu, H. and Logan, B.E., 2004. Electricity generation using an air-cathode single chamber microbial fuel cell in the presence and absence of a proton exchange membrane. *Environmental science & technology*, 38, pp.4040–4046.

Liu, H., Ramnarayanan, R. and Logan, B.E., 2004. Production of electricity during wastewater treatment using a single chamber microbial fuel cell. *Environmental science & technology*, 38, pp.2281–2285.

Logan, B.E., Cheng, S., Watson, V. and Estadt, G., 2007. Graphite Fiber Brush Anodes for Increased Power Production in Air-Cathode Microbial Fuel Cells. *Journal of Power Sources*, 41(9), pp.3341–3346.

Logan, B.E., Hamelers, B., Rozendal, R., Schr??der, U., Keller, J., Freguia, S., Aelterman, P., Verstraete, W. and Rabaey, K., 2006. Microbial fuel cells: Methodology and technology. *Environmental Science and Technology*, 40, pp.5181–5192.

Logan, B.E., Murano, C., Scott, K., Gray, N.D. and Head, I.M., 2005. Electricity generation from cysteine in a microbial fuel cell. *Water Research*, 39, pp.942–952.

Logan, B.E., Wallack, M.J., Kim, K., He, W., Feng, Y. and Saikaly, P.E., 2015. Assessment of Microbial Fuel Cell Connfigurations and Power Densities. *Environmental Science & Technology Letters*, 2, pp.206–214.

Logan, B.E., 2008. *Microbial Fuel Cells*. 1st ed. ed. New Jersey: Wiley & Sons, Inc.

Logan, B.E., 2010. Scaling up microbial fuel cells and other bioelectrochemical systems. *Applied Microbiology and Biotechnology*, 85, pp.1665–1671.

Logan, B.E., 2012. Essential data and techniques for conducting microbial fuel cell and other types of bioelectrochemical system experiments. *ChemSusChem*, 5(6), pp.988–994.

Lovley, D.R., 2006. Microbial fuel cells: novel microbial physiologies and engineering approaches. *Current Opinion in Biotechnology*, 17, pp.327–332.

Lu, L., Yazdi, H., Jin, S., Zuo, Y., Fallgren, P.H. and Ren, Z.J., 2014. Enhanced bioremediation of hydrocarbon-contaminated soil using pilot-scale bioelectrochemical systems. *Journal of Hazardous Materials*, 274, pp.8–15.

Mallick, P., Akunna, J.C. and Walker, G.M., 2010. Anaerobic digestion of distillery spent wash: Influence of enzymatic pre-treatment of intact yeast cells. *Bioresource Technology*, 101, pp.1681–1685.

Marcus, A.K., Torres, C.I. and Rittmann, B.., 2007. Conduction-based modelling of the biofilm anode of a microbial fuel cell. *Biotechnology and Bioengineering*, 98, pp.1171–1182.

Mardanpour, M.M., Esfahany, M.N., Behzad, T. and Sedaqatvand, R., 2012. Single chamber microbial fuel cell with spiral anode for dairy wastewater treatment. *Biosensors and Bioelectronics*, 38, pp.264–269.

McCarty, P.L., Bae, J. and Kim, J., 2011. Domestic wastewater treatment as a net energy producer - can this be achieved? *Environmental science & technology*, 45(17), pp.7100–7106.

Met Office, 2016. *Climate Summaries*. [online] Regional Values. Available at: <http://www.metoffice.gov.uk/climate/uk/summaries>.

Michie, I.S., Kim, J.R., Dinsdale, R.M., Guwy, A.J. and Premier, G.C., 2011. Operational temperature regulates anodic biofilm growth and the development of electrogenic activity. *Applied Microbiology and Biotechnology*, 92, pp.419–430.

Min, B., Cheng, S. and Logan, B.E., 2005. Electricity generation using membrane and salt bridge microbial fuel cells. *Water Research*, 39, pp.1675–1686.

Min, B., Román, Ó.B. and Angelidaki, I., 2008. Importance of temperature and anodic medium composition on microbial fuel cell (MFC) performance. *Biotechnology Letters*, 30, pp.1213–1218.

Mitchell, R. and Gu, J.D., 2010. *Low-energy wastewater treatment: strategies and technologies*. 2nd ed. *Environmental Microbiology*. New Jersey: Wiley-Blackwell.

Mohan, S.V., Raghavulu, S.V. and Sarma, P.N., 2008. Biochemical evaluation of bioelectricity production process from anaerobic wastewater treatment in a single chambered microbial fuel cell (MFC) employing glass wool membrane. *Biosensors and Bioelectronics*, 23(9), pp.1326–1332.

Mohana, S., Acharya, B.K. and Madamwar, D., 2009. Distillery spent wash: Treatment technologies and potential applications. *Journal of Hazardous Materials*, 163, pp.12–25.

Mustakeem, 2015. Electrode materials for microbial fuel cells: Nanomaterial approach. *Materials for Renewable and Sustainable Energy*, 4, pp.1–11.

Oliveira, V.B., Simoes, M., Melo, L.F. and Pinto, A.M.F.., 2013. A 1D mathematical model for a microbial fuel cell. *Energy*, 61, pp.463–471.

Ortiz-Martínez, V.M., Salar-García, M.J., de los Ríos, A.P., Hernández-Fernández, F.J., Egea, J.A. and Lozano, L.J., 2015. Developments in microbial fuel cell modeling. *Chemical Engineering Journal*, 271, pp.50–60.

Pant, D., Van Bogaert, G., Diels, L. and Vanbroekhoven, K., 2010. A review of the substrates used in microbial fuel cells (MFCs) for sustainable energy production. *Bioresource Technology*, 101, pp.1533–1543.

Parameswaran, P., Torres, C.I., Lee, H.S., Krajmalnik-Brown, R. and Rittmann, B.E., 2009. Syntrophic interactions among anode respiring bacteria (ARB) and Non-ARB in a biofilm anode: electron balances. *Biotechnology and Bioengineering*, 103(3), pp.513–523.

Park, D.H. and Zeikus, J.G., 2000. Electricity Generation in Microbial Fuel Cells Using Neutral Red as an Electronophore. *Applied and Environmental microbiology*, 66(4), pp.1292–1297.

Pham, T.H., Rabaey, K., Aelterman, P., Clauwaert, P., De Schamphelaire, L., Boon, N. and Verstraete, W., 2006. Microbial fuel cells in relation to conventional anaerobic digestion technology. *Engineering in Life Sciences*, 6(3), pp.285–292.

Picioreanu, C., Head, I.M., Katuri, K.P., van Loosdrecht, M.C.M. and Scott, K., 2007. A computational model for biofilm-based microbial fuel cells. *Water Research*, 41, pp.2921–2940.

Piggott, J.R. and Connor, J.M., 2003. Whisky, Whiskey and Bourbon: Products and Manufacture. In: B. Caballero, L.C. Trugo and P.. Finglas, eds., *Encyclopedia of Food Science and Nutrition*, 2nd editio. London: Academic Press, pp.6171–6177.

Potter, M.C., 1911. Electrical Effects Accompanying the Decomposition of Organic Compounds. *Proceedings of the Royal Society of London B: Biological Sciences*, 84(571), pp.260–276.

Premier, G.C., Kim, J.R., Massanet-Nicolau, J., Kyazze, G., Esteves, S.R.R., Penumathsa, B.K. V, Rodríguez, J., Maddy, J., Dinsdale, R.M. and Guwy, A.J., 2013. Integration of biohydrogen, biomethane and bioelectrochemical systems. *Renewable Energy*, 49, pp.188–192.

Rabaey, K., Angenent, L., Schroder, U. and Keller, J., 2009. *Bioelectrochemical Systems: From Extracellular Electron Transfer to Biotechnological Application*. 1st ed. ed. London: IWA Publishing.

Rabaey, K., Clauwaert, P., Aelterman, P. and Verstraete, W., 2005. Tubular microbial fuel cells for efficient electricity generation. *Environmental Science and Technology*, 39, pp.8077–8082.

Rabaey, K. and Verstraete, W., 2005. Microbial fuel cells: Novel biotechnology for energy generation. *Trends in Biotechnology*, 23, pp.291–298.

Ren, L., Ahn, Y., Hou, H., Zhang, F. and Logan, B.E., 2014. Electrochemical study of multi-electrode microbial fuel cells under fed-batch and continuous flow conditions. *Journal of Power Sources*, 257, pp.454–460.

Ren, L., Ahn, Y. and Logan, B.E., 2014. A Two-Stage Microbial Fuel Cell and Anaerobic Fluidized Bed Membrane Bioreactor (MFC-AFMBR) System for E ff ective Domestic Wastewater Treatment. *Environmental science & technology*, 48, pp.4199–4206.

Ringeisen, B.R., Henderson, E., Wu, P.K., Pietron, J., Ray, R., Little, B., Biffinger, J.C. and Jones-Meehan, J.M., 2006. High power density from a miniature microbial fuel cell using Shewanella oneidensis DSP10. *Environmental Science and Technology*, 40, pp.2629–2634.

Rismani-Yazdi, H., Carver, S.M., Christy, A.D. and Tuovinen, O.H., 2008. Cathodic limitations in microbial fuel cells: An overview. *Journal of Power Sources*, 180(2), pp.683–694.

Rittmann, B.E. and McCarty, P.L., 2001. *Environmental Biotechnology: Principles and Applications*. Boston: McGraw-Hill.

Rozendal, R. a., Hamelers, H.V.M. and Buisman, C.J.N., 2006. Effects of Membrane Cation Transport on pH and Microbial Fuel. *Environmental science & technology*, 40, pp.5206–5211.

Rozendal, R.A., Hamelers, H.V.M., Rabaey, K., Keller, J. and Buisman, C.J.N., 2008. Towards practical implementation of bioelectrochemical wastewater treatment. *Trends in Biotechnology*, 26(8), pp.450–459.

Saeed, H.M., Husseini, G.A., Yousef, S., Saif, J., Al-Asheh, S., Fara, A.A., Azzam, S., Khawaga, R. and Aidan, A., 2015. Microbial desalination cell technology: A review and a case study. *Desalination*, 359, pp.1–13.

Samsudeen, N., Sharma, A., Radhakrishnan, T.K. and Matheswaran, M., 2015. Performance investigation of multi-chamber microbial fuel cell: An alternative approach for scale up system. *Journal of Renewable and Sustainable Energy*, 7, pp.1–9.

Schroder, U., 2007. Anodic electron transfer mechanisms in microbial fuel cells and their energy efficiency. *Physical Chemistry Chemical Physics*, 9, pp.2619–2629.

Scotch Whisky Association, 2015. *Facts & figures*. [online] Available at: <http://www.scotch-whisky.org.uk/what-we-do/facts-figures/> [Accessed 4 Aug. 2016].

Scott, K., Cotlarciuc, I., Hall, D., Lakeman, J.B. and Browning, D., 2008. Power from marine sediment fuel cells: the influence of anode material. *Journal of Applied Electrochemistry*, 38, pp.1313–1319.

Scott, K. and Hao Yu, E., 2015. *Microbial Electrochemical and Fuel Cells; Fundamental and Applications*. 1st ed. *WP Woodhead Publishing*.

Scott, K., Murano, C. and Rimbu, G., 2007. A tubular microbial fuel cell. *Journal of Applied Electrochemistry*, 37, pp.1063–1068.

Scott, K., 2014. 10 - Microbial fuel cells: transformation of wastes into clean energy. In: *Membranes for Clean and Renewable Power Applications*. Woodhead Publishing Limited, pp.266–300.

Sharma, M., Bajracharya, S., Gildemyn, S., Patil, S.A., Alvarez-Gallego, Y., Pant, D., Rabaey, K. and Dominguez-Benetton, X., 2014. A critical revisit of the key parameters used to describe microbial electrochemical systems. *Electrochimica Acta*, 140, pp.191–208.

Sheets, J.P., Yang, L., Ge, X., Wang, Z. and Li, Y., 2015. Beyond land application: Emerging technologies for the treatment and reuse of anaerobically digested agricultural and food waste. *Waste Management*, 44, pp.94–115.

Shizas, I. and Bagley, D.M., 2004. Experimental Determination of Energy Content of Unknown Organics in Municipal Wastewater Streams. *Journal of Energy Engineering*, 130(2), pp.45–53.

von Sperling, M., 2007. *Biological Wastewater Treatment Vol.2: Basic principles of wastewater treatment*. 1st ed. London: IWA.

Sun, J., Hu, Y., Bi, Z. and Cao, Y., 2009. Improved performance of air-cathode single-chamber microbial fuel cell for wastewater treatment using microfiltration membranes and multiple sludge inoculation. *Journal of Power Sources*, 187(2), pp.471–479.

Sutton, P.M., Rittmann, B.E., Schraa, O.J., Banaszak, J.E. and Togna, A.P., 2011. Wastewater as a resource: a unique approach to achieving energy sustainability. *Water Science and Technology*, 63(9), pp.2004–2009.

Tran, H.T., Ryu, J.H., Jia, Y.H., Oh, S.J., Choi, J.Y., Park, D.H. and Ahn, D.H., 2010. Continuous bioelectricity production and sustainable wastewater treatment in a microbial fuel cell constructed with non-catalyzed granular graphite electrodes and permeable membrane. *Water Science & Technology*, 61(7), pp.1819–1827.

Tugtas, A.E., Cavdar, P. and Calli, B., 2013. Bio-electrochemical post-treatment of anaerobically treated landfill leachate. *Bioresource Technology*, 128, pp.266–272.

UN Water, 2015. *Wastewater management: A UN-Water Analytical Brief*. *UN Water*.

UNEP, 2016. *UNEP Frontiers 2016 Report: Emerging Issues of Environmental Concern*. Nairobi: United Nations Environment Programme.

Wang, D. Bin, Song, T.S., Guo, T., Zeng, Q. and Xie, J., 2014. Electricity generation from sediment microbial fuel cells with algae-assisted cathodes. *International Journal of Hydrogen Energy*, 39, pp.13224–13230.

Wang, X., Cheng, S., Feng, Y., Merrill, M.D., Saito, T. and Logan, B.E., 2009a. Use of carbon mesh anodes and the effect of different pretreatment methods on power production in microbial fuel cells. *Environmental Science and Technology*, 43, pp.6870–6874.

Wang, X., Feng, Y., Ren, N., Wang, H., Lee, H., Li, N. and Zhao, Q., 2009b. Accelerated start-up of two-chambered microbial fuel cells: Effect of anodic positive poised potential. *Electrochimica Acta*, 54, pp.1109–1114.

Wei, J., Liang, P. and Huang, X., 2011. Recent progress in electrodes for microbial fuel cells. *Bioresource Technology*, 102, pp.9335–9344.

Wen, Q., Wu, Y., Cao, D., Zhao, L. and Sun, Q., 2009. Electricity generation and modeling of microbial fuel cell from continuous beer brewery wastewater. *Bioresource Technology*, 100, pp.4171–4175.

Wilkinson, S., 2000. ``Gastrobots''---Benefits and Challenges of Microbial Fuel Cells in FoodPowered Robot Applications. *Autonomous Robots*, 9(2), pp.99–111.

Willey, J.M., Sherwood, L. and Woolverton, C.J., 2011. *Prescott's Microbiology*. 8th edit. ed. McGraw-Hill.

Winfield, J., Ieropoulos, I., Greenman, J. and Dennis, J., 2011. Investigating the effects of fluidic connection between microbial fuel cells. *Bioprocess and Biosystems Engineering*, 34, pp.477–484.

Wrap, 2016. *Mogden Formula Tool*. [online] Available at: <http://www.wrap.org.uk/content/mogden-formula-tool-0> [Accessed 5 Aug. 2016].

WWAP, 2014. *The United Nations World Water Development Report 2014: Water and Energy*.

Xiao, B., Han, Y., Liu, X. and Liu, J., 2014a. Relationship of methane and electricity production in two-chamber microbial fuel cell using sewage sludge as substrate. *International Journal of Hydrogen Energy*, 39, pp.16419–16425.

Xiao, L., Ge, Z., Kelly, P., Zhang, F. and He, Z., 2014b. Evaluation of normalized energy recovery (NER) in microbial fuel cells affected by reactor dimensions and substrates. *Bioresource Technology*, 157, pp.77–83.

Yong, Y.C., Dong, X.C., Chan-Park, M.B., Song, H. and Chen, P., 2012. Macroporous and monolithic anode based on polyaniline hybridized three-dimensional Graphene for high-performance microbial fuel cells. *ACS Nano*, 6(3), pp.2394–2400.

You, S., Zhao, Q., Zhang, J., Jiang, J., Wan, C., Du, M. and Zhao, S., 2007. A graphite-granule membrane-less tubular air-cathode microbial fuel cell for power generation under continuously operational conditions. *Journal of Power Sources*, 173, pp.172–177.

Yu, J., Seon, J., Park, Y., Cho, S. and Lee, T., 2012. Electricity generation and microbial community in a submerged-exchangeable microbial fuel cell system for low-strength domestic wastewater treatment. *Bioresource Technology*, 117, pp.172–179.

Yuan, H., Hou, Y., Abu-Reesh, I.M., Chen, J. and He, Z., 2016. Oxygen reduction reaction catalysts in microbial fuel cells for energy-efficient wastewater treatment : A review Materials Horizons. *Materials Horizon*.

Zeng, Y., Choo, Y.F., Kim, B.-H. and Wu, P., 2010. Modelling and simulation of two-chamber microbial fuel cell. *Journal of Power Sources*, 195, pp.79–89.

Zhang, F., Ge, Z., Grimaud, J., Hurst, J. and He, Z., 2013a. In situ investigation of tubular microbial fuel cells deployed in an aeration tank at a municipal wastewater treatment plant. *Bioresource Technology*, 136, pp.316–321.

Zhang, F., Ge, Z., Grimaud, J., Hurst, J. and He, Z., 2013b. Long-Term Performance of Liter-Scale Microbial Fuel Cells Treating Primary Effluent Installed in a Municipal Wastewater Treatment Facility. *Environmental Science & Technology*, 47, pp.4941–4948.

Zhang, X., Cheng, S., Liang, P., Huang, X. and Logan, B.E., 2011. Scalable air cathode microbial fuel cells using glass fiber separators, plastic mesh supporters, and graphite fiber brush anodes. *Bioresource Technology*, 102, pp.372–375.

Zhang, X., Pant, D., Zhang, F., Liu, J., He, W. and Logan, B.E., 2014. Long-Term Performance of Chemically and Physically Modified Activated Carbons in Air Cathodes of Microbial Fuel Cells. *ChemElectroChem*, 1, pp.1859–1866.

Zhang, X.C. and Halme, A., 1995. Modelling of a microbial fuel cell process. *Biotechnology Letters*, 17, pp.809–814.

Zhao, F., Harnisch, F., Schröder, U., Scholz, F., Bogdanoff, P. and Herrmann, I., 2005. Application of pyrolysed iron(II) phthalocyanine and CoTMPP based oxygen reduction catalysts as cathode materials in microbial fuel cells. *Electrochemistry Communications*, 7, pp.1405–1410.

Zhao, F., Harnisch, F., Schröder, U., Scholz, F., Bogdanoff, P. and Herrmann, I., 2006. Challenges and constraints of using oxygen cathodes in microbial fuel cells. *Environmental Science and Technology*, 40(17), pp.5193–5199.

Zhou, M., Wang, H., Hassett, D.J. and Gu, T., 2013. Recent advances in microbial fuel cells (MFCs) and microbial electrolysis cells (MECs) for wastewater treatment, bioenergy and bioproducts. *Journal of Chemical Technology and Biotechnology*, 88, pp.508–518.

Zhuang, L., Yuan, Y., Wang, Y. and Zhou, S., 2012a. Long-term evaluation of a 10-liter serpentine-type microbial fuel cell stack treating brewery wastewater. *Bioresource Technology*, 123, pp.406–412.

Zhuang, L., Zheng, Y., Zhou, S., Yuan, Y., Yuan, H. and Chen, Y., 2012b. Scalable microbial fuel cell (MFC) stack for continuous real wastewater treatment. *Bioresource Technology*, 106, pp.82–88.